The influence of genome size and limitation of nitrogen and phosphorus on photosynthesis efficiency

Sarah Seco Marques da Silva

School of Biological and Chemical Sciences,

Queen Mary University of London,

Mile End Road, London E1 4NS, UK.

Submitted in partial fulfilment of the requirements of the Degree of

Doctor of Philosophy

November 2017

Statement of originality

I, Sarah Seco Marques da Silva, confirm that the research included within this thesis is my own work or that where it has been carried out in collaboration with, or supported by others, that this is duly acknowledged below and my contribution indicated. Previously published material is also acknowledged below.

I attest that I have exercised reasonable care to ensure that the work is original, and does not to the best of my knowledge break any UK law, infringe any third party's copyright or other Intellectual Property Right, or contain any confidential material.

I accept that the College has the right to use plagiarism detection software to check the electronic version of the thesis.

I confirm that this thesis has not been previously submitted for the award of a degree by this or any other university.

Signature:

Date:

Acknowledgements

First, I thank my family and relatives, specially my parents for the everyday support and for always influencing me to the best.

I am immensely thankful to my ex-husband Julio for helping me since the beginning of my undergrad with my studies, and certainly, I wouldn't have tried a PhD abroad if it was not for his encouragement.

I am also really grateful to all my supervisors – Andrew Leitch, Ilia Leitch, Paula Rudall and Sasha Ruban – for the trust, the supervision, the fascinating opportunity to do this PhD with them and for believing in me, specially Andrew who was patient and supportive all the time. I also thank my panel member Mark Trimmer for suggestions and discussions and Richard Nichols for helping with statistics.

None of my experiments would succeed without the help of many. The technicians Monika Struebig, Phillip Howard, Petra Ungerer, Ian Sanders and Paul Fletcher, from Queen Mary and Maria Conejero and Chrissie Prychid from Kew Gardens. I am also thankful to Sasha's and Trimmer's group (students and post docs) and to my project students Thomaz Pinotti, Carlos Fantecelle, Claudia Batz and Joseph Wolfensohn.

I thank Erik Murchie, his group and the technician Phillip Davey for lending their equipment for photosynthetic measurements and for giving me support when I needed.

I thank Jaume Pellicer and Laura Kelly for the help with data and knowledge in *Fritillaria* and *Nymphaea*. Carlos Magdalena and other gardeners from Kew Gardens who gave me permission to work on those plants. Laurence Hill who lent me many *Fritillaria* plants to use in my analyses.

I am immensely grateful to have studied these last four years in the presence of such nice people of the 5th floor of Fogg building. Many thanks to Wencai Wang, Steven Dodsworth, Tiago Souto, Hernani Oliveira, Giacomo Vitali, Sally Faulkner, Leandro Santiago, Rodrigo Pracana and Emeline Favreau for backing me up, laughs and enjoyable moments. The friendship and support from Maïté Guignard, my dear friend, who helped me at every stage of my PhD.

I could not forget to thank the immense encouragement and friendship from my Brazilian friends Nanda, Yasmin, Mile, João and Augusto.

Finally, I acknowledge funding support from CAPES by Science without Borders scheme.

Abstract

Genome size varies 2,400-fold in angiosperms and is an important trait influencing cellular and physiological parameters. One of the major drivers of the astonishing genome size (GS) diversity in angiosperms is polyploidisation and most flowering plant lineages have undergone multiple rounds of polyploidy in their ancestry. Because of the frequency of ancestral polyploidy, one might expect angiosperm genomes to be larger than other eukaryotes, where polyploidy is less frequent. But this is not the case, where GS in angiosperms is skewed towards small genomes, suggesting that, following polyploidy, there is selection over time to reduce GS.

It is possible that one selection pressure that acts to reduce the size of the genome is the efficiency of photosynthesis, which may be enhanced in species with small genome sizes. This is because there is a positive correlation between the size of the nucleus and the guard cells across species, which can in turn influence the rate of gas exchange through stomata pores.

Photosynthesis may also be influenced by nitrogen (N) and phosphorus (P) availability. These macronutrients are limiting nutrients to plants and play an important role for them, because they are the main constituents of the nucleic acids and they play crucial role in photosynthesis in many processes. Nitrogen is needed to build photosynthetic proteins, but especially for the RuBisCO enzyme and chlorophylls, which are N demanding. Phosphorus is used as ATP and NADPH to give the chemical energy necessary for the fixation of CO_2. Both these N and P demands for photosynthesis may compete with the N and P demands of the nucleus, which may be higher in species with large genomes than species with smaller genomes. Thus in considering the selection constraints on genome size in plants it is necessary to consider the effects of GS and nutrient availability on photosynthesis.

The overall aim of this PhD project is to determine how GS and nutrient availability impacts photosynthesis. To do that three experimental systems are exploited. These are:

(1) The effects of GS on the efficiency of photosynthesis in plant genus *Fritillaria*, selected because it has particularly large genome sizes, and it has the largest range in genome size, all at the diploid level, for any genus (70 Gb/1C range). These materials enable determination of the impact of GS on cell size, gas exchange and light harvesting properties of photosynthesis. Surprisingly, no effect of GS on cell size

was observed, contrary to published expectation, but there was a significant correlation between GS and photosynthesis readings.

(2) The effects of GS on the efficiency of photosynthesis in plant genus *Nymphaea*, selected because it has small genome sizes and polyploidy variants. The polyploid variants enable the effect of step changes in GS associated with polyploidy to be determined. This enables the determination of the impact of polyploidy on photosynthesis and to determine the efficiency of photosynthesis across species in an aquatic plant genus. Exceptionally low non-photochemical quenching (NPQ) was observed in these species, indicative of highly efficient light energy use, perhaps associated with small genome sizes overall and an aquatic habit. There was a relationship between GS and cell size in this genus, despite the range of GS being smaller than for *Fritillaria*.

(3) The effect of nutrient availability and photosynthesis in wheat, selected because of its agricultural importance, its large genome size, and relatives at different ploidy levels with which the data could be compared in future studies. This material enables the effects of nutrient limitation on photosynthesis to be determined, and which components of photosynthesis are most impacted. The results revealed that some components of photosynthesis were significantly impacted by P alone (photochemical quenching (qP, negatively), non-photochemical quenching capacity (NPQ, positively)), others by N alone (maximum rate of carboxylation by RuBisCO (V_{cmax}, negatively)), whilst both N and P limitation and their interactions reduced biomass.

The data show that interactions between photosynthesis, N and P and GS play a role in influencing plant biomass. What we now need to know in future studies is if there are N and P trade-offs between the nucleic acid sink represented by the plant genome and proteins and pigments (chlorophyll) needed for photosynthesis. For example, RuBisCO, essential for the dark reaction of photosynthesis, is likely to compete with the nucleic acid sinks for N, whilst metabolic processes, which require for example ATP, NADPH or protein phosphorylation, are likely to compete with the nucleic acid sinks for P.

Contents

List of Figures

List of Supplementary Figures

List of Tables

List of abbreviations

A	CO_2 uptake
AL	Actinic light
A_{max}	Maximum CO_2 uptake
C	Carbon
C_c	CO_2 partial pressure at RuBisCO
C_i	Intracellular CO_2
E_k	Minimum saturating irradiance
ETR_{max}	Maximum electron transport rate
F_m'	Maximum fluorescence level under actinic light
F_o'	Minimum fluorescence without actinic light
F_s	Minimum fluorescence under actinic light
F_v/F_m	Maximum quantum efficiency of PSII photochemistry in dark-adapted tissues
GS	Genome size
g_s	Stomatal conductance
ILC	Induction light curve
IRGA	Infrared gas analysers
J_{max}	Maximum rate of electron transport used for regeneration of RuBP
K_c	Michaelis constant of RuBisCO for CO_2
K_o	Michaelis constant of RuBisCO for O_2
LM	Linear model
N	Nitrogen
NPQ	Non-photochemical quenching
O	Partial pressure of O_2 at RuBisCO

P	Phosphorus
P_i	Inorganic phosphorus
PICs	Phylogenetic independent contrasts
PSI	Photosystem I
PSII	Photosystem II
qP	Photochemical quenching
RC	Reaction centre
RCII	Reaction centre of photosystem II
R_d	Mitochondrial respiration rate
RLC	Rapid light curves
RuBisCO	Ribulose-1,5-bisphosphate carboxylase/oxygenase
RuBP	Ribulose-1,5-bisphosphate
TE	Transposable element
TEM	Transmission electron microscopy
V_{cmax}	Maximum rate of carboxylation of RuBisCO
WGD	Whole Genome Duplication
Γ^*	Photosynthetic compensation point

Chapter 1. General Introduction

Plant genome size

The distributions and ranges of genome sizes (GS) (i.e. amount of DNA in the unreplicated gametic nucleus (e.g. pollen or sperm) usually reported as picograms (pg) or base pairs (bp), where 1 pg ≈ 1 billion bp = 1000 Mb) vary considerably between the major groups of vascular plants (Leitch & Leitch, 2013). The lycophytes comprise c. 900 species and their GS varies 139-fold (1C = 0.086–11.97 pg). The monilophytes, comprise c. 11,000 species and their GS varies 196-fold (1C = 0.77–150.60 pg) (Leitch & Leitch, 2012; Hidalgo *et al.*, 2017). Gymnosperms have little GS variation (just 16-fold overall) compared with c. 2,400-fold variation in angiosperms, the largest range for any plant group (Pellicer *et al.*, 2010). The modal and mean GS are 1C = 0.6 and 5.9 pg in angiosperms, respectively, revealing that the distribution of GS is highly skewed (Figure 1.1). By contrast, the distribution of GS in the gymnosperms is less skewed, with higher mode and mean values (mode 1C = 10.0 pg, mean 1C = 18.8 pg), (Figure 1.1).

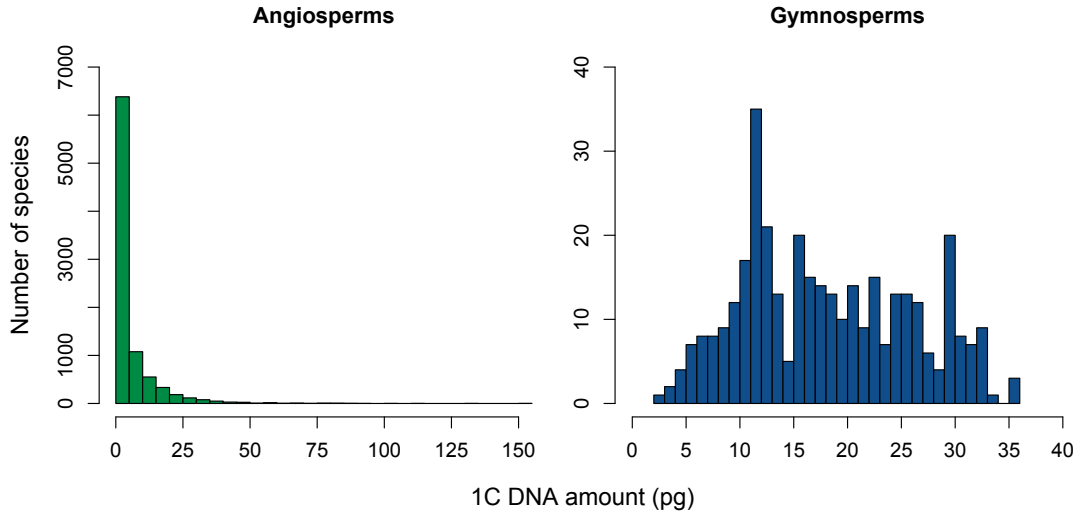

Figure 1.1. Histograms showing the distribution of genome sizes in two groups of vascular plants, angiosperms and gymnosperms. Data used from Bennett & Leitch (2012).

Variation in GS between species has implications at the chromosomal, cellular, physiological, organismal and ecological levels (Greilhuber & Leitch, 2013; Guignard *et al.*, 2016). One of the best known traits is the positive correlation between GS, nucleus size and cell size (Knight *et al.*, 2005). This may be because there is considered to be a constant ratio between the volume of the nucleus and cytoplasm in

animal and plant cells, which reflects the need to balance the nuclear and cytoplasmic processes. With a large genome there is more chromatin and a larger nuclear volume is therefore required to package it. This in turn may have consequences for the size of the cell itself. In animals, the size of red blood cells is correlated with GS (Gregory, 2005), while in plants, guard cell size has been shown to be broadly correlated with GS (Greilhuber & Leitch, 2013) although additional factors such as habitat type have also been shown to play a role in influencing the final size (Jordan *et al.*, 2015). In addition, GS has been shown to be positively correlated with the duration of cell cycle, probably because the increased packaging of DNA in species with large genomes leads to a longer DNA synthesis phase (Greilhuber & Leitch, 2013). Thus, species with large genomes tend to have large cells and slow cell division.

Gregory (2001) and Greilhuber & Leitch (2013) reviewed the theories that explain the evolution of GS. The theories diverge between selective and stochastic process. Variation in GS itself arises through two primary processes:

(1) The relative frequencies of accumulation and deletion of selfish genetic elements, i.e. transposable elements (TEs), which can trigger their own transmission and amplification within the genome (Ågren & Wright, 2015). These elements can also be deleted by the recombination machinery (Fedoroff, 2012), and the balance between rates of accumulation and deletion leads to changes in GS over time.

(2) Whole Genome Duplication (WGD) i.e. polyploidy, arising through mitotic or meiotic misdivision and which result, at least initially, in step-wise increases in GS (Soltis & Soltis, 2009), although the subsequent evolution of polyploid genomes can result in the elimination of DNA (i.e. genome downsizing) such that over time, polyploid genomes may not be significantly larger than their parental progenitors (Leitch & Bennett, 2004). Polyploidy is thought to account for 15% of speciation events in angiosperms and 30% of events in ferns (Wood *et al.*, 2009), and a WGD event is thought to have arisen frequently in the divergence of many angiosperm lineages (Jiao *et al.*, 2011; Van de Peer *et al.*, 2017).

Genomic plasticity

Approximately half a million species of vascular plants have been recognized and 94% of these are angiosperms (RBG Kew, 2016). The replacement of gymnosperms by angiosperms from the Cretaceous period onwards and the substantial difference in species numbers between these two groups have intrigued scientists and theories have been proposed to explain factors that may have contributed to the wide

diversification of angiosperm, these theories involve both ecological and genomic factors and their interaction in the generation of that diversity (Leitch & Leitch, 2012).

Because most flowering plant lineages are considered to have undergone multiple rounds of polyploidy in their ancestry (Jiao *et al.*, 2011; but see Ruprecht *et al.*, 2017, see Figure 1.2), and it is still taking place, coupled with shifting frequencies in TEs (Kejnovsky *et al.*, 2009), it suggests that angiosperm GS have been flexible and dynamic over evolutionary time scales. Because of the predicted frequency of ancestral polyploid events (Figure 1.2), one might expect that the genomes of extant angiosperm species would be larger than other eukaryotic groups, where polyploidy is less frequent. But this is not the case, suggesting that, following polyploidy, there is selection over time to reduce the size of the genome (Leitch & Bennett, 2004). Indeed, the GS in angiosperms is skewed towards small C-values (Figure 1.1), and this is a characteristic not observed in other vascular plant groups (Leitch & Leitch, 2012). These data suggest that there might be selection against large genomes. Knight et al. (2005) proposed the 'Large Genome Constraint Hypothesis', suggesting that species with large genomes pay a cost and may, under certain circumstances, be selected against. It has been observed that species with small genomes can adopt a wide range of life strategies, whereas, species with large genomes are more restricted to being obligate perennials. This could be because species with large genomes have slower cell divisions, and consequently cannot occupy an ephemeral niche (Greilhuber & Leitch, 2013).

Given that polyploidy has occurred iteratively in many angiosperm lineages and GS are typically small, it suggests that there are processes that delete DNA over time. Petrov (2002) suggested that the DNA amount of any organism reflected the dynamic balance between the loss of DNA with more frequent small deletions and the gain of DNA with more frequent long insertions, these being neutral processes that may be non-adaptive. However the analysis of GS in angiosperm polyploids indicate that this balance is operating predominantly in one direction, resulting in large-scale genome downsizing (Leitch & Bennett, 2004), and may argue that small GSs can have a selective advantage, at least in some circumstances. Potentially, with the accumulation of DNA, species with large genomes may have a higher demand for nutrients (nitrogen (N) and phosphorous (P)), because these nutrients are a substantial component of nucleic acids (14.5% N and 8.7% P by mass, assuming 1:1 ratio of purines and pyrimidines, (Sterner & Elser, 2002)) and on top of that the DNA needs to be packaged with proteins to make chromatin (e.g. histones, which are themselves rich in N). Plants that live in areas with limiting nutrients, may be selected against if they carry a large excess of non-coding DNA (Leitch & Leitch, 2008). Such a selection pressure may

explain why after polyploidy, genome downsizing in angiosperms is frequently observed (Leitch & Bennett, 2004).

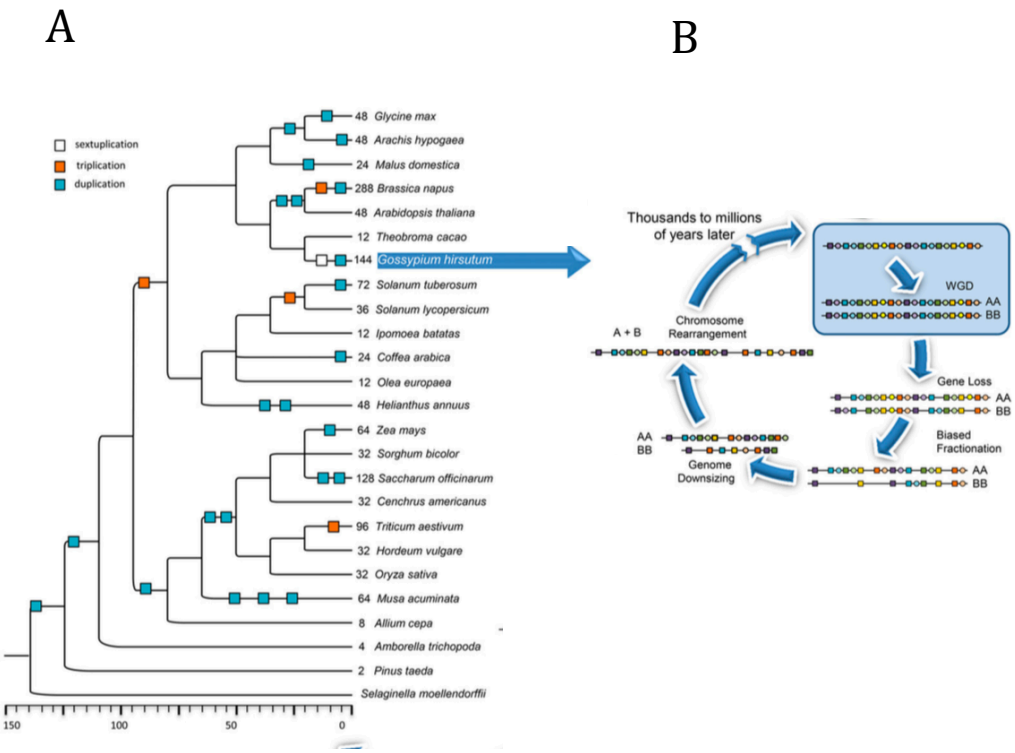

Figure 1.2. Mechanisms of polyploidy in plants, modified from Wendel (2015) showing: (A) Potential polyploidy events occurring with the divergence of angiosperms. The numbers at branch tips indicate the number of genome duplication that are predicted for each species. (B) Given that polyploidy or Whole Genome Duplication (WGD) recurs iteratively in most plant lineages, it is expected that most plant GS are large, yet most are in fact small. Thus it is hypothesised that after WGD there is gene loss, especially from one of the parental polyploid genomes (biased fractionation), leading to genome downsizing. Then with chromosomal rearrangements the genome returns over millions of years to a diploid like form in the “wondrous cycles of polyploidy”.

Photosynthesis

Given the large range in plant GS, and the fact that most plant species have small genomes, it is possible that there are selection pressures against species with large genomes because of the metabolic and resource costs of building and sustaining large genomes, which might compete for resources with those needed for photosynthesis and the generation of biomass (Knight *et al.*, 2005). In addition the scaling effects caused by increasing GS on cell size may negatively impact the flow of gases through

stomata, which again could impair photosynthesis. However, very few studies have tested these hypotheses, and that is one of the central aims of this thesis.

Plant metabolism drives plant growth through an interaction between environment and plant traits. Photosynthesis is a process transforming light energy into chemical energy to fix atmospheric CO_2. The mechanisms involved in photosynthesis are complex and can be divided into two main phases: the light phase and the dark phase.

The light phase of photosynthesis comprises a number of steps that are needed to enable the absorption of photons, the splitting of water for electron donation, and the transmission of the energy through an electron transport chain, leading to the chemical storage of energy in the form of ATP and NADPH (Ruban, 2013). The photosynthetic membranes, i.e. the thylakoid membranes in chloroplasts, is where everything begins. The photosynthetic membrane is composed of (Ruban, 2013):

- Lipids: these make up to 50% of the total membrane mass and are essential in shaping the protein complex structure to enable it to function;
- Pigments: chlorophylls and carotenoids play a key role in the process of photon absorption and/or electron transfer,
- Proteins and protein complexes: these make up to 80% of some membranes depending on the conditions, and they deal with the process of capturing light energy and converting the energy of excited electrons into chemical energy (i.e. NADPH and ATP) for the cell.

These components of the photosynthetic membrane interact to form photosynthetic complexes, which are: (i) the light harvesting antennae, (ii) photosystem II (PSII), (iii) cytochrome b6/f complex, (iv) photosystem I (PSI), and (v) ATPase. Figure 1.2, taken from Baker (2008), shows a schematic arrangement of these complexes. Each photosystem possesses its own light-harvesting antenna, an organised arrangement of pigments within the lipid membrane, which absorb photons and channels the energy to PSII or PSI. When the light is absorbed by a pigment molecule in the ground state (i.e. stable state), the electrons are lifted to an energy-rich excited state (Hall & Rao, 1999). The energy is then transferred to a reaction centre (RC) to initiate the electron transport chain but the energy can also be released as heat (non-photochemical quenching, NPQ) or fluorescence. After electron donation to the cytochrome b6/f complex, the RCII (i.e. reaction centre of PSII) acts as a strong oxidant that removes an electron from water, which is then used to replace electrons lost from chlorophyll *a* in the RCII once they have been donated to the electron chain. The electron transfer in PSII is linked to a proton discharge into the thylakoid lumen in a sequence of water

splitting reactions, which also generates O_2. The cytochrome b6/f complex transfers electrons to PSI, and the latter transfers the electrons to reduce NADP by forming NADPH. The accumulation of protons in lumen leads to the formation of a ∆-pH across the membrane and this electrochemical gradient is used by ATPase to form ATP from ADP and inorganic phosphate (Pi) (Ruban, 2013).

Two photons are the minimum quanta required to transfer one electron because. For each reduction of NADP two electrons are required, therefore 8 photons are necessary for the reduction of two molecules of NADP and the associated evolution of one molecule of O_2 or reduction of one molecule of CO_2. This is the quantum requirement of photosynthesis. The ratio of the absorbed quanta used in CO_2 assimilation to the total quanta absorbed is known as the quantum yield (Walker, 1992).

The balance in electron transfer between absorbed light and utilised light is disturbed at increasing high light. The RCs become progressively saturated, which leads to a reduction of energy used for photosynthesis and an increase in accumulation of unused, but potentially harmful, excitation energy in the photosynthetic membrane. This accumulation of energy can cause photoinhibition, and hence a decline in the photosynthetic efficiency associated with damage to RCII. A mechanism has evolved in plants to reduce the likelihood of photoinhibition and control the overproduction of ATP and NADPH and consequently the accumulation of protons in the lumen thylakoid caused by high light intensity. That mechanism is known as NPQ, and it functions in excess light by relieving PSII of excess energy. This process can be measured as a decline in chlorophyll fluorescence yield under conditions of high light (Ruban, 2013).

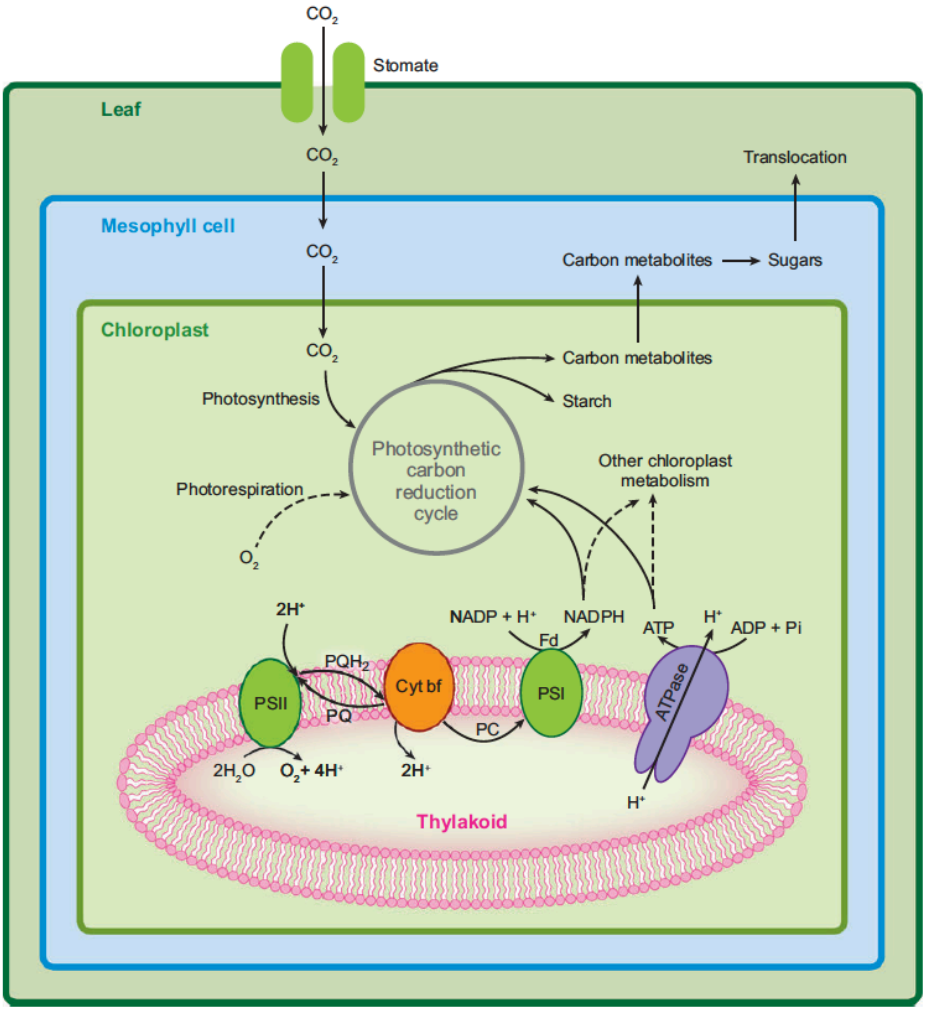

Figure 1.3. Relationship between the photosynthetic membrane complexes and CO_2 fixation (taken from Baker, 2008). Cyt bf, cytochrome b6/f complex; Fd, ferredoxin; PC, plastocyanin; PQ, plastoquinone; PQH_2, plastoquinol; PSI, photosystem I; PSII, photosystem II.

The main channels of de-excitation of PSII are photochemistry, heat and fluorescence. Fluorescence is a type of emission of light that takes place after absorption of a photon by a pigment molecule. It occurs when the electron of the molecule relaxes to its ground state from a higher quantum state (Hall & Rao, 1999). At ambient temperature the fluorescence emitted is mainly from PSII. The properties of chlorophyll fluorescence are now widely used to examine the state of photosynthetic machinery and its performance, and they have been used to predict the condition of the machinery in algae and higher plants (Baker, 2008). A pulse amplitude modulated (PAM) fluorimeter is used to register fluorescence induced by pulsed excitation light, generating information that can inform the activities of the electron transfer rate through the electron transport chain and other de-excitation channels (i.e. NPQ) (Ruban, 2013).

The dark phase of photosynthesis is the process by which CO_2 is fixed to form carbohydrates using the so called “assimilatory power” of NADPH and ATP produced in the light phase. The steps involved do not directly require light, and take place in the stroma of the chloroplasts. They can be divided in three phases: (i) carboxylation; (ii) reduction, and (iii) regeneration (Walker, 1992). There are three main pathways of carbon assimilation in plants, termed C3 and C4 photosynthesis and Crassulacean Acid Metabolism (CAM). The C3 pathway is described in greater detail here, because all the plants used for the experiments described in this thesis use that pathway.

The Calvin cycle is fundamental to carbon assimilation in all carbon assimilation pathways. It involves, in the first step, the addition of a CO_2 molecule to an acceptor. The acceptor is a sugar phosphate with five atoms of carbon (i.e. a pentose) and is called ribulose 1,5-bisphosphate (RuBP), the CO_2 is added to it to form two molecules of 3-phosphoglycerate (3-PGA, 3 carbon compound). This reaction is catalysed by the enzyme ribulose 1,5-bisphosphate carboxylase/oxygenase (RuBisCO) (Hall & Rao, 1999).

The 3-PGA molecules are then reduced, a step that requires NADPH and ATP. To reduce 3-PGA into a sugar requires the ATP-dependent phosphorylation of 3-PGA to form 1,3-biphosphogycerate (1,3-biPGA), and the subsequent reduction of 1,3-biPGA to glyceraldehyde 3-phosphate (G3P, triose P – a sugar phosphate with three atoms of carbon) by NADPH and release of Pi. Once the reduction of CO_2 into a sugar has been accomplished, the energy-conserving part of photosynthesis is complete (Hall & Rao, 1999).

The requirement at the last stage in the Calvin cycle is to regenerate the RuBP (i.e. the initial CO_2 acceptor), so the fixation of other molecules of CO_2 can continue. While some G3P are used to generate complex sugars, carbohydrates, fats, amino acids and organic acids, most of them are recycled for RuBP regeneration, which involves a complex series of reactions with 3-, 4-, 5-, 6- and 7-carbon sugar phosphates (Hall & Rao, 1999). The formation of these different products involves distinctive pathways that may be differentially impacted by light intensity, CO_2 and O_2 concentration. Three rounds of the Calvin cycle are necessary to make one molecule of triose (G3P), because each round fixes one molecule of CO_2 and the G3P requires 3 atoms of carbon (Walker, 1992).

The final equation of photosynthesis with the respective stoichiometries is:

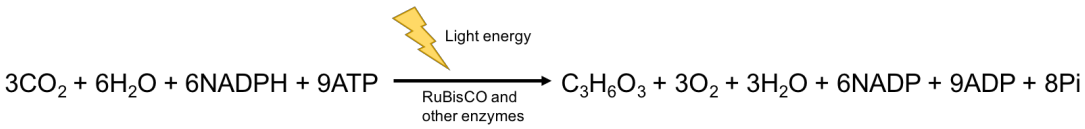

Today a range of infrared gas analysers (IRGA), as portable systems, are available to enable measurements of leaf photosynthetic CO_2 uptake (A), transpiration, stomatal conductance to vapour water (g_s) and intercellular CO_2 (Johnson & Murchie, 2011). This equipment enables assays of photosynthesis efficiency, which with modelling generates A/Ci curves, provides for calculations of RuBisCO activity and rate of RuBP regeneration. Photosynthesis is negatively impacted when RuBisCO catalyses the oxygenation of RuBP, resulting in O_2 fixation instead of CO_2 fixation, a process called photorespiration.

Nitrogen, phosphorus and fertilizers

Carbon (C), N and P are three of the main elements in the structure of organic molecules, despite this, N and P are not abundant in soil. The nucleic acids C:N:P ratio is 9.5:3.7:1 (Sterner & Elser, 2002). DNA and RNA molecules are rich in N and P, whilst histones and RuBisCO are rich in N and are the most abundant proteins in plant cells that are undergoing photosynthesis. The growth of cells via cell division is also expensive in terms of N and P since they are required for the synthesis of proteins and enzymes, cell membranes, pigments and nucleic acids. Inorganic phosphate (Pi) and organic phosphate esters are the forms in which P exists in plants and the largest organic P pool is found in nucleic acids (Veneklaas *et al.*, 2012).

In the soil, P is unavailable to the plant in the organic form and has to first be mineralised to its inorganic form before it can be taken up (Raghothama, 1999). On the other hand, N can be taken up as nitrate (NO_3^-) or ammonium (NH_4^+). Nitrate is mobile once taken up and can move easily through the xylem or be stored, but it cannot be used in organic synthesis as NO_3^-, and must first be converted to NH_3^- (Richardson *et al.*, 2009). Nitrate reduction reactions is an energy expensive process requiring NADH/NADPH as electron donors, therefore requiring P (Tischner, 2000). This demonstrates the complex interplay between N and P and how they interact within the plant.

Fertilisers play a vital role in improving biomass production in plants. There are year on year rises in fertiliser use globally (N, P and potassium (K)), with usage for agriculture expected to reach 200.5 million tonnes per annum by the end of 2018 (FAO, 2015). Global cereal production has increased by about 500 million tonnes in the last 10 years

(FAO, 2017), a consequence of higher inputs of fertilisers, increased irrigation, better pesticides and new crop varieties. These advances are fundamental if we are to sustain the human populations and prevent hunger especially as the human population is predicted to increase to 9 billion by 2050. Nevertheless, agriculture not only generates essential food but through the use of N and P, also impacts environments, degrading them through the excess run off of nutrients. Such impacts thus also have costs associated with them and these can be substantial (Carpenter *et al.*, 1998).

Over the last century, the increased application of N has resulted in increased atmospheric N deposition to terrestrial ecosystems, resulting in elevated N in soils relative to other elements. As a result, vegetation that used to be N-limited may now have sufficient availability of N, and plants may then become limited by P or other elements (Fenn *et al.*, 1998; Güsewell, 2004; Syers *et al.*, 2008). The shifting N:P stoichiometry can have profound effects on plant community structures (Crawley *et al.*, 2005). Thus it is essential that N and P are used efficiently, not only to reduce food costs but also to prevent contamination of the environment. It has been estimated that less than 50% of N and P fertilisers are taken up by crops in the year of its application (Tilman *et al.*, 2002). To improve the efficiency of fertiliser use for crop growth, much more research is needed into how N and P is metabolised and used by plants and the processes that lead to faster growth and/or better allocation of biomass to the product of the crop, e.g. in case of cereals, the seeds.

When excess fertiliser is added to the soil, a large proportion leaches into subsurface water. Excess irrigation or heavy rainfall also washes and releases P and residual N from the soil. The nutrient-rich water is then transported through streams and rivers to lakes. The slow moving water and high nutrient content in these large lake ecosystems provide a perfect environment for algae growth. Algal blooms reduce the dissolved oxygen content of the water, leading to death of fish and subsurface plants. Decomposition of the dead organic matter further reduces the dissolved oxygen content. Such eutrophication leads to loss of biodiversity, reduced quality of drinking water and of water for industry and agriculture. In addition the recreation-use of lakes is impaired (Carpenter *et al.*, 1998; Tilman *et al.*, 2002). Dodds *et al.* (2009) have estimated that these effects of eutrophication of freshwater systems cost approximately $2.2 billion annually in the United States. The cost increases still further if effects on terrestrial ecosystems are also considered, where excess fertilisers in the environment also leads to losses of biodiversity and ecosystem services that arise there too. In addition, an over-reliance on fertilisers, especially P, will be even more problematic in the future, because there are limits to global rock phosphate reserves. The mining of

phosphate rock and production of fertiliser is rising to match the increasing demand. Peak phosphorus is the point when production of phosphorous will begin to decline despite growing demand and the rock phosphate supplies are expected to reach peak productivity by 2050 (Cordell & White, 2011). Ridder *et al.* (2012) estimate that phosphate rock could be depleted within 50 to 100 years, however other reports suggests this is not the case, for example, the U.S. Geological Survey (2018) conclude that the world resources of phosphate rock are more than 300 billion tons and that there is no imminent depletion of it. There is therefore an urgent need to understand how N and P availability impacts photosynthesis and the generation of biomass, another central aim of this thesis.

Photosynthesis, genome size and N and P availability

It is possible that one of the selection pressures acting on plants to reduce the size of the genome is competition between resources needed for the nucleus and those needed for photosynthesis. Hence, to test that hypothesis, the correlation between GS and photosynthetic rates needs to be understood. Previous studies have shown that there is a scaling of the size of a guard cell and its nucleus leading to a positive correlation between stomatal size and plant GS (Beaulieu *et al.*, 2008; Knight & Beaulieu, 2008; Franks *et al.*, 2012a). Stomata are small pores distributed on the surface of leaves and consist of two guard cells bounded together. Stomatal size and density determine maximum leaf conductance of CO_2 and H_2O. The opening and closing system of stomata provide the leaf with the capacity to manage the partial pressure of CO_2 and the rate of transpiration. Changes in the rate of transpiration act to regulate temperature and water potential of the leaf. The rate of CO_2 assimilation can be limited by a number of factors, for example, light, temperature and water status. Both transpiration rate and rate of CO_2 assimilation depend also on stomatal conductance, which is a measure of the rate of diffusion of CO_2 and water through stomata (Farquhar & Sharkey, 1982). Franks & Beerling (2009) proposed from theoretical calculations that for the same total pore area, the conductance for H_2O or CO_2 is higher in smaller stomata than larger ones. Such a relationship has also been demonstrated experimentally (e.g. Franks & Farquhar (2001) and Drake *et al.* (2013)).

Throughout the history of land plants, the concentration of atmospheric CO_2 is estimated to have fluctuated from very high levels of ca. 4000 ppm (during the Devonian period) to as low as 180 ppm in the last glacial period (Franks *et al.*, 2012b). It is now approximately 400 ppm (NOAA, 2017). Studies of guard cell size in 211 fossil plant species over the last 400 Myr suggested that there had been coevolution between their

sizes and changes in CO_2 atmospheric concentration (Franks *et al.*, 2012a). Franks *et al.* (2012b) went on to suggest, after an experiment with angiosperms, a fern and a lycophyte grown under three different concentrations of CO_2, that the large changes in stomatal size over time had been accompanied by changes in plant GS, and that both stomatal size and plant GS co-evolved to track atmospheric CO_2 concentration.

Austin *et al.* (1982) compared metabolic rates across 15 genotypes of wheat with varying DNA contents. Their results showed a negative correlation between ploidy and photosynthetic rate. Other research has investigated the effects of within-species ploidy variation (i.e. cytotypes) on photosynthetic rate, and while some results showed a positive relationship (i.e. high ploidy levels had higher photosynthetic rates) (Randall *et al.*, 1977; Joseph *et al.*, 1981) others showed a negative correlation between these two factors (Garrett, 1978; Wullschleger *et al.*, 1996). In addition, Knight *et al.* (2005) showed in a meta-analysis of 24 species that GS was negatively correlated with maximum photosynthetic rate. Currently, the relationship between GS and photosynthesis parameters, if any, remains obscure, probably because the relationship between GS and photosynthesis can be impacted by leaf anatomical features and environmental adaptations. In addition, photosynthesis can be limited by a number of factors such as light intensity, CO_2 concentration, water availability, and temperature.

According to Franks *et al.* (2012b), changes in atmospheric CO_2 concentration may select for plants with optimal stomatal size to maximise stomatal conductance to CO_2 and photosynthesis efficiency, which may, in turn generate a selection pressure on GS. One problem in studying such correlations between species is that the plants under study are not completely independent and they share a common evolutionary history. Hence it is important to take into account phylogenetic relationships when analysing the impact of one trait on another. For example, Giussani *et al.* (2001) mentioned that the diversity of photosynthetic pathways (C3, C4) was as great within the genus *Panicum* as within the entire tribe. Thus, it would make little sense to compare species in this tribe without consideration of their phylogenetic relationships too, since closely related species are most likely to share similar characters (e.g. GS and photosynthetic characters), i.e. they have phylogenetic signal, which can, in analyses without phylogenetic consideration, lead to false impressions of character correlations.

Given the high demands for P and N in nucleic acids (Sterner & Elser, 2002) and the range of GSs in plants as noted above, it is important that we better understand how plant growth is impacted by interactions between GS and N and P availability. To date there are very few data on this subject, although two ecological studies suggest that N

and P limitation in the environment results in a plant community shift towards species with small GSs (Šmarda *et al.*, 2013; Guignard *et al.*, 2016). Potentially, the synthesis of DNA must compete for available N and P with the demands of photosynthesis, because of the requirement for RuBisCO (Evans, 1989; Makino, 2003; Parry *et al.*, 2008), requiring large numbers of N-rich amino acids and of nucleic acids requiring N and P to build the sugar phosphate backbone and nitrogenous bases of DNA and RNA. In a meta-analysis with 536 species Walker *et al.* (2014) found that leaf P was a determinant that modified the relationship between the maximum rate of RuBisCO activity and leaf N. Reich *et al.* (2009) found similar results in a global analysis of 314 species, showing that an increase in leaf P led to an increased sensitivity of the maximum rate of CO_2 uptake to leaf N. Further they showed that this relationship held across biomes with different N/P ratios. These results can be explained by the interaction between N and P through the need of P via ATP and NADPH for RuBP regeneration. Nevertheless, how GS also impacts these properties is poorly understood, and hence a core aim of the thesis is to address that deficiency.

Photosynthesis and ploidy

Photosynthetic rate can be influenced by several factors as mentioned in the previous section. However, another important factor that might impact photosynthesis is ploidy. Difference in ploidy can change photosynthetic rate by changes in cell volume, which can correlate with GS (as discussed earlier and which is further examined in Chapter 3), and by induced physiological changes (photosynthetic rate per cell is correlated with the amount of DNA per cell in polyploids (Warner & Edwards, 1993)).

Polyploidy can induce changes in anatomical properties of the plant and biochemical properties of the cell. Anatomical changes include variation in cell size, which affects mesophyll cell sizes, air spaces and numbers of organelles, which influence the rate of CO_2 diffusion for photosynthesis (Warner & Edwards, 1993). Biochemical changes are induced by variation induced in the transcriptome, likely caused through gene dosage effects and epigenetic silencing of duplicate alleles, influencing the production of proteins (Leitch & Leitch, 2008).

In a study of 15 genotypes of wheat and related species differing in ploidal level – diploids, tetraploids and hexaploids – Austin *et al.* (1982) analysed chlorophyll content, photosynthesis rate and leaf anatomy. Austin *et al.* (1982) revealed that polyploidy does influence photosynthesis, but the total impact on the whole plant remains unclear. They found that photosynthetic rates per unit leaf area were higher for the diploid species than the hexaploids, suggesting a negative correlation with ploidy. But this

trend may disappear if the leaf area of the entire plant is considered. Photosynthetic rates were positively correlated with stomatal density, and the latter being higher in diploids than in hexaploids. Leaf area and width were also negatively related to ploidy, while chlorophyll content was greater in hexaploids than diploids.

A recent study in diploids and tetraploids of *Fragaria* species (Gao *et al.*, 2017) was similar to that reported by Austin *et al.* (1982) and revealed that ploidy level is negatively associated with net photosynthetic rate, stomatal conductance and transpiration rate, indicating that increased ploidal level had a negative effect on photosynthetic capacity. In contrast, previous studies of tall fescue (*Festuca arundinacea* - Poaceae) have shown that an increase in ploidal levels from 4x-10x is associated with an increase in photosynthetic rate, which may be related to increased RuBisCO and chlorophyll concentrations (Randall *et al.*, 1977; Joseph *et al.*, 1981).

In other research in allopolyploids (i.e. hybridization followed by genome duplication) tetraploids of *Glycine dolichocarpa* and their diploids progenitors, Coate *et al.* (2012) found increases in guard cell length, in chloroplast number per palisade cell and maximum electron transport rate per cell with increased in ploidy level, although not the same was observed when analysed per unit leaf area basis, presumably because the tetraploids had fewer palisade cells per unit leaf area than the diploids.

In a study of leaf anatomical features in nine wheat genotypes with different ploidy and GS, Jellings & Leech (1984) found that photosynthetic capacity per unit leaf area is negatively related to mesophyll cell volume, with higher ploidal genotypes having larger mesophyll volumes. This study also discusses the importance of comparing photosynthetic measurements on a per cell basis, rather than on a per unit leaf area basis. Cell volume is thought to increase with ploidy. Thus, photosynthetic rate per cell may be greater in higher ploidy than lower ploidy genotypes if photosynthetic rate per unit leaf area is the same in both genotypes, because of the difference in the number of cells in the same leaf area.

These studies suggest that polyploidy may play an important role in the evolution of photosynthesis. Warner & Edwards (1993) suggest that the content of nuclear DNA, the relationship between cells and organelles, and the cellular structure of leaves should all be considered when making comparisons between photosynthesis and polyploidisation.

Aims

The overall aim of this PhD project is to investigate how photosynthetic efficiency is influenced by GS and how both are related to N and P availability. Chapter 2 examines the relationship between GS, photosynthetic rates and stomatal size and density in a plant genus with large GS, *Fritillaria* (Liliaceae), to test the hypothesis that there is a positive correlation between GS and cell size, which could have a detrimental effect on photosynthesis because of scaling effects (area/volume scaling) that may influence gas exchange or diffusion parameters of stomata. However, there were no effects of GS on cell size, contrary to published expectation, but there was a significant correlation between GS and photosynthesis measures. Chapter 3 analyses the relationship between GS and ploidy level, chlorophyll fluorescence parameters, stomatal size and density in water lilies (i.e. *Nymphaea,* Nymphaeaceae), to test the hypothesis that ploidy level influences photosynthesis in species that have small GSs (compared with *Fritillaria*). Exceptionally low NPQ was observed in these species, indicative of highly efficient light energy use, perhaps associated with small GS and an aquatic habit. There was a relationship between GS and cell size in this genus, despite the range of GS being smaller than for *Fritillaria*. Chapter 4, examines the relationship between photosynthesis efficiency and N and P availability in wheat to explore the impact of nutrient limitation and photosynthesis on biomass and seed production, to test the hypothesis that N and P stress influences photosynthesis. Some components of photosynthesis were found to be significantly impacted by P alone (photochemical quenching (qP, negatively), non-photochemical quenching capacity (NPQ, positively)), others by N alone (maximum rate of carboxylation by RuBisCO (V_{cmax}, negatively)), whilst both N and P limitation and their interactions reduced biomass. Such work is vital if we are to fully understand potential selection pressures in plant evolution and to improve our understanding of crops to maximise yield.

References

Ågren JA, Wright SI. **2015**. Selfish genetic elements and plant genome size evolution. *Trends in Plant Science* **20**: 195–6.

Austin RB, Morgan CL, Ford MA, Bhagwat SG. **1982**. Flag leaf photosynthesis of *Triticum aestivum* and related diploid and tetraploid species. *Annals of Botany* **49**: 177–189.

Baker NR. **2008**. Chlorophyll fluorescence: a probe of photosynthesis in vivo. *Annual Review of Plant Biolology* **59**: 89–113.

Beaulieu JM, Leitch IJ, Patel S, Pendharkar A, Knight CA. **2008**. Genome size is a strong predictor of cell size and stomatal density in angiosperms. *New Phytologist* **179**: 975–986.

Bennett MD, Leitch IJ. **2012**. Plant DNA C-values database (release 6.0, December 2012). <http://data.kew.org/cvalues/>.

Carpenter SR, Caraco NF, Correll DL, Howarth RW, Sharpley AN, Smith VH. **1998**. Nonpoint pollution of surface waters with phosphorus and nitrogen. *Ecological Applications* **8**: 559–568.

Coate JE, Luciano AK, Seralathan V, Minchew KJ, Owens TG, Doyle JJ. **2012**. Anatomical, biochemical, and photosynthetic responses to recent allopolyploidy in *Glycine dolichocarpa* (Fabaceae). *American Journal of Botany* **99**: 55–67.

Cordell D, White S. **2011**. Peak Phosphorus: clarifying the key issues of a vigorous debate about long-term phosphorus security. *Sustainability* **3**: 2027–2049.

Crawley MJ, Johnston AE, Silvertown J, Dodd M, Mazancourt C de, Heard MS, Henman DF, Edwards GR. **2005**. Determinants of species richness in the Park Grass Experiment. *The American Naturalist* **165**: 179–192.

Dodds WK, Bouska WW, Eitzmann JL, Pilger TJ, Pitts KL, Riley AJ, Schloesser JT, Thornbrugh DJ. **2009**. Eutrophication of U.S. freshwaters: analysis of potential economic damages. *Environmental Science & Technology* **43**: 12–19.

Drake PL, Froend RH, Franks PJ. **2013**. Smaller, faster stomata: Scaling of stomatal size, rate of response, and stomatal conductance. *Journal of Experimental Botany* **64**: 495–505.

Evans JR. **1989**. Photosynthesis and nitrogen relationships in leaves of C_3 plants.

Oecologia **78**: 9–19.

FAO. **2015**. World fertilizer trends and outlook to 2018. Food and Agriculture Organization of the United Nations.

FAO. **2017**. FAO Statistical databases. Food and Agriculture Organization of the United Nations. <http://www.fao.org/>.

Farquhar GD, Sharkey TD. **1982**. Stomatal conductance and photosynthesis. *Annual Review of Plant Physiology* **33**: 317–345.

Fedoroff N V. **2012**. Transposable elements, epigenetics, and genome evolution. *Science* **338**: 758–67.

Fenn ME, Poth MA, Aber JD, Baron JS, Bormann BT, Johnson DW, Lemly AD, Mcnulty SG, Ryan DF, Stottlemyer R. **1998**. Nitrogen excess in North American ecosystems: predisposing factors, ecosystem responses, and management strategies. *Ecological Applications* **8**: 706–733.

Franks PJ, Beerling DJ. **2009**. Maximum leaf conductance driven by CO_2 effects on stomatal size and density over geologic time. *Proceedings of the National Academy of Sciences* **106**: 10343–10347.

Franks PJ, Farquhar GD. **2001**. The effect of exogenous abscisic acid on stomatal development, stomatal mechanics, and leaf gas exchange in *Tradescantia virginiana*. *Plant Physiology* **125**: 935–42.

Franks PJ, Freckleton RP, Beaulieu JM, Leitch IJ, Beerling DJ. **2012a**. Megacycles of atmospheric carbon dioxide concentration correlate with fossil plant genome size. *Philosophical transactions of the Royal Society of London. Series B, Biological sciences* **367**: 556–564.

Franks PJ, Leitch IJ, Ruszala EM, Hetherington AM, Beerling DJ. **2012b**. Physiological framework for adaptation of stomata to CO_2 from glacial to future concentrations. *Philosophical Transactions of the Royal Society B: Biological Sciences* **367**: 537–546.

Gao S, Yan Q, Chen L, Song Y, Li J, Fu C, Dong M. **2017**. Effects of ploidy level and haplotype on variation of photosynthetic traits: Novel evidence from two *Fragaria* species (J Yang, Ed.). *PLOS ONE* **12**: e0179899.

Garrett MK. **1978**. Control of photorespiration at RuBP carboxylase/oxygenase level in ryegrass cultivars. *Nature* **274**: 913–915.

Giussani LM, Cota-Sánchez JH, Zuloaga FO, Kellogg EA. **2001**. A molecular phylogeny of the grass subfamily Panicoideae (Poaceae) shows multiple origins of C4 photosynthesis. *American Journal of Botany* **88**: 1993–2012.

Gregory TR. **2001**. Coincidence, coevolution, or causation? DNA content, cell size, and the C-value enigma. *Biological Reviews of the Cambridge Philosophical Society* **76**: 65–101.

Gregory T. **2005**. Genome size evolution in animals. In: Gregory T, ed. The evolution of the genome. San Diego: Elsevier, 3–87.

Greilhuber J, Leitch I. **2013**. Genome size and the phenotype. In: Greilhuber, J., Dolezel, J., Wendel JF, ed. Plant Genome Diversity Volume 2. Springer Vienna, 323–344.

Guignard MS, Nichols RA, Knell RJ, Macdonald A, Romila C-A, Trimmer M, Leitch IJ, Leitch AR. **2016**. Genome size and ploidy influence angiosperm species' biomass under nitrogen and phosphorus limitation. *New Phytologist* **210**: 1195–1206.

Güsewell S. **2004**. N : P ratios in terrestrial plants: variation and functional significance. *New Phytologist* **164**: 243–266.

Hall DO, Rao KK. **1999**. *Photosynthesis*. Cambridge University Press.

Hidalgo O, Pellicer J, Christenhusz M, Schneider H, Leitch AR, Leitch IJ. **2017**. Is there an upper limit to genome size? *Trends in Plant Science* **22**: 567–573.

Jellings AJ, Leech RM. **1984**. Anatomical variation in first leaves of nine *Triticum* genotypes, and its relationship to photosynthetic capacity. *New Phytologist* **96**: 371–382.

Jiao Y, Wickett NJ, Ayyampalayam S, Chanderbali AS, Landherr L, Ralph PE, Tomsho LP, Hu Y, Liang H, Soltis PS, *et al.* 2011. Ancestral polyploidy in seed plants and angiosperms. *Nature* **473**: 97–100.

Johnson G, Murchie E. **2011**. Gas exchange measurements for the determination of photosynthetic efficiency in *Arabidopsis* leaves. In: Jarvis R, ed. Chloroplast Research in Arabidopsis. Methods in Molecular Biology (Methods and Protocols). Humana Press, Totowa, NJ, 311–326.

Jordan GJ, Carpenter RJ, Koutoulis A, Price A, Brodribb TJ. **2015**. Environmental adaptation in stomatal size independent of the effects of genome size. *New Phytologist* **205**: 608–617.

Joseph MC, Randall DD, Nelson CJ. **1981**. Photosynthesis in polyploid tall fescue: II. photosynthesis and Ribulose-1,5-Bisphosphate Carboxylase of polyploid tall fescue. *Plant Physiology* **68**: 894–898.

Kejnovsky E, Leitch IJ, Leitch AR. **2009**. Contrasting evolutionary dynamics between angiosperm and mammalian genomes. *Trends in Ecology & Evolution* **24**: 572–582.

Knight CA, Beaulieu JM. **2008**. Genome size scaling through phenotype space. *Annals of Botany* **101**: 759–766.

Knight CA, Molinari NA, Petrov DA. **2005**. The large genome constraint hypothesis: evolution, ecology and phenotype. *Annals of Botany* **95**: 177–190.

Leitch IJ, Bennett MD. **2004**. Genome downsizing in polyploid plants. *Biological Journal of the Linnean Society* **82**: 651–663.

Leitch AR, Leitch IJ. **2008**. Genomic plasticity and the diversity of polyploid plants. *Science* **320**: 481–483.

Leitch AR, Leitch IJ. **2012**. Ecological and genetic factors linked to contrasting genome dynamics in seed plants. *New Phytologist* **194**: 629–646.

Leitch IJ, Leitch AL. **2013**. Genome size diversity and evolution in land plants. In: Greilhuber J., Dolezel J. WJ, ed. Plant Genome Diversity Volume 2. Vienna: Springer, 307–322.

Makino A. **2003**. Rubisco and nitrogen relationships in rice: leaf photosynthesis and plant growth. *Soil Science and Plant Nutrition* **49**: 319–327.

NOAA. **2017**. Global greenhouse gas reference network <https://www.esrl.noaa.gov/gmd/ccgg/trends/>. *National Oceanic and Atmospheric Administration*.

Parry MAJ, Keys AJ, Madgwick PJ, Carmo-Silva AE, Andralojc PJ. **2008**. Rubisco regulation: a role for inhibitors. *Journal of Experimental Botany* **59**: 1569–1580.

Van de Peer Y, Mizrachi E, Marchal K. **2017**. The evolutionary significance of polyploidy. *Nature Reviews Genetics* **18**: 411–424.

Pellicer J, Fay MF, Leitch IJ. **2010**. The largest eukaryotic genome of them all? *Botanical Journal of the Linnean Society* **164**: 10–15.

Petrov DA. **2002**. Mutational equilibrium model of genome size evolution. *Theoretical*

Population Biology **61**: 531–44.

Raghothama KG. **1999**. Phosphate acquisition. *Annual Review of Plant Physiology and Plant Molecular Biology* **50**: 665–693.

Randall DD, Nelson CJ, Asay KH. **1977**. Ribulose bisphosphate carboxylase: altered genetic expression in tall fescue. *Plant Physiology* **59**: 38–41.

RBG Kew. **2016**. *State of the World's Plants Report - 2016. Royal Botanic Gardens, Kew.*

Reich PB, Oleksyn J, Wright IJ. **2009**. Leaf phosphorus influences the photosynthesis-nitrogen relation: a cross-biome analysis of 314 species. *Oecologia* **160**: 207–212.

Richardson A, Barea J-M, McNeill A, Prigent-Combaret C. **2009**. Acquisition of phosphorus and nitrogen in the rhizosphere and plant growth promotion by microorganisms. *Plant and Soil* **321**: 305–339.

Ridder M, Jong S, Polchar J, Lingemann S. **2012**. Risks and opportunities in the global phosphate rock market. Robust strategies in times of uncertainty. *The Hague Centre for Strategic Studies (HCSS)*: 96.

Ruban A. **2013**. *The photosynthetic membrane: molecular mechanisms and biophysics of light harvesting*. United Kingdom: Wiley.

Ruprecht C, Lohaus R, Vanneste K, Mutwil M, Nikoloski Z, Van de Peer Y, Persson S. **2017**. Revisiting ancestral polyploidy in plants. *Science Advances* **3**: e1603195.

Šmarda P, Hejcman M, Březinová A, Horová L, Steigerová H, Zedek F, Bureš P, Hejcmanová P, Schellberg J. **2013**. Effect of phosphorus availability on the selection of species with different ploidy levels and genome sizes in a long-term grassland fertilization experiment. *New Phytologist* **200**: 911–921.

Soltis PS, Soltis DE. **2009**. The role of hybridization in plant speciation. *Annual Review of Plant Biology* **60**: 561–588.

Sterner RW, Elser JJ. **2002**. *Ecological Stoichiometry: The Biology of Elements from Molecules to the Biosphere*. Princeton University Press.

Syers J, Johnston A, Curtin D. **2008**. Efficiency of soil and fertilizer phosphorus use. *FAO Fertilizer and Plant Nutrition Bulletin no. 18*: 108.

Tilman D, Cassman KG, Matson PA, Naylor R, Polasky S. **2002**. Agricultural sustainability and intensive production practices. *Nature* **418**: 671–677.

Tischner R. **2000**. Nitrate uptake and reduction in higher and lower plants. *Plant, Cell and Environment* **23**: 1005–1024.

U.S. Geological Survey. **2018**. *Mineral commodity summaries 2018: U.S. Geological Survey*.

Veneklaas EJ, Lambers H, Bragg J, Finnegan PM, Lovelock CE, Plaxton WC, Price CA, Scheible W-R, Shane MW, White PJ, *et al.* 2012. Opportunities for improving phosphorus-use efficiency in crop plants. *New Phytologist* **195**: 306–320.

Walker DA. **1992**. *Energy, plants and man*. United Kingdom: Oxygraphics Limited.

Walker AP, Beckerman AP, Gu L, Kattge J, Cernusak LA, Domingues TF, Scales JC, Wohlfahrt G, Wullschleger SD, Woodward FI. **2014**. The relationship of leaf photosynthetic traits - V cmax and J max - to leaf nitrogen, leaf phosphorus, and specific leaf area: a meta-analysis and modeling study. *Ecology and evolution* **4**: 3218–35.

Warner DA, Edwards GE. **1993**. Effects of polyploidy on photosynthesis. *Photosynthesis Research* **35**: 135–147.

Wendel JF. **2015**. The wondrous cycles of polyploidy in plants. *American Journal of Botany* **102**: 1753–6.

Wood TE, Takebayashi N, Barker MS, Mayrose I, Greenspoon PB, Rieseberg LH. **2009**. The frequency of polyploid speciation in vascular plants. *Proceedings of the National Academy of Sciences* **106**: 13875–9.

Wullschleger SD, Sanderson MA, McLaughlin SB, Biradar DP, Rayburn AL. **1996**. Photosynthetic Rates and Ploidy Levels among Populations of Switchgrass. *Crop Science* **36**: 306–312.

Chapter 2. The influence of genome size on stomatal size and photosynthesis efficiency in *Fritillaria* (Liliaceae)

Summary

Introduction: The genus *Fritillaria* (Liliaceae), which comprises ca 140 species of bulbous perennial plants, includes species with the largest diploid genomes so far reported (1C-values ranging from 30.8pg to 100.4pg). This contrasts strikingly with the majority of angiosperms, which are characterized by much smaller genomes (data for >10,000 species show the modal 1C-value is 0.6 pg /1C, and mean = 5.1 pg/1C). While there is ongoing research into the molecular dynamics underpinning the origin and evolution of such large genomes, our understanding of how this impacts various physiological processes is more limited. This research aims to understand how photosynthesis is affected by genome size (GS) via its impact on stomatal size. Previous studies across a diverse range of plants have shown that there is a broad correlation between genome size and stomatal guard cell size, and that this may, in part be driven by changes in atmospheric CO_2 concentration over geological time. Given that guard cell size is likely to influence, for example, gas and water exchange dynamics needed for photosynthesis and hence potentially photosynthetic efficiency, we have probed this subject further by analyzing three different factors that contribute to photosynthetic efficiency in 16 species of *Fritillaria* and 3 species of Melanthiaceae that differ in genome size (1.68 – 152.2 pg/1C).

Methods: The approaches used were (i) infra-red gas analysis (IRGA) to investigate the rates of CO_2 uptake, (ii) pulse amplitude modulation (PAM) fluorometry to gain insights into the efficiency of light energy harvesting for photosynthesis, and (iii) stomatal measurements (size and density).

Results: An examination of *Fritillaria* species showed an inverse relationship between stomatal length and density. Adaxial, abaxial, juvenile and adult leaves differed in stomatal size and densities, with juvenile leaves showing distinct metabolic and photosynthetic properties compared with adult leaves. Surprisingly, despite the huge range in genome sizes observed in *Fritillaria*, there was no relationship between genome size and stomatal length or density. Several photosynthetic parameters (A_{max}, V_{cmax}, J_{max}, g_s, F_v/F_m and rETR) are significantly negatively correlated with genome size.

Discussion: The results shed light on how genome size interacts with other plant traits and abiotic factors to influence photosynthesis dynamics in these genome giants. Collectively these data suggest that for the species analysed here, stomatal size is

controlled by physiological processes and not by genome size alone, although it remains possible that genome size provides a minimum constraint on stomatal size and density. We recommend caution in interpreting fossil genome sizes from fossil stomatal data.

Introduction

The genome size variation in angiosperms (flowering plants), ranges 2,400-fold which is the largest range for any land plant group. Nevertheless, the mean and modal genome sizes for angiosperms are small at 1C = 5.9pg and 0.6pg, respectively (Leitch & Leitch, 2012). These characters contrast considerably with the other vascular plants, as seen in the General Introduction. Angiosperm species with very large (=giant) genomes (i.e. 1C > 35pg; Kelly & Leitch, 2011) are phylogenetically restricted to just five orders of angiosperms, Liliales, Asparagales, Commelinales, Ranunculales and Santalales (Leitch *et al.*, 2010). One of the major causes of genome size variation in angiosperms is polyploidisation (Soltis & Soltis, 2009; Wendel, 2015), with most or all angiosperms considered to have experienced at least one round of polyploidy in the history of their lineages (Jiao *et al.*, 2011; Van de Peer *et al.*, 2017). The other major process which contributes to genome size diversity is the amplification and deletion of repetitive DNA (Grover & Wendel, 2010; Kejnovsky *et al.*, 2012). Species with very large or giant genomes contrast strikingly with those of the model plant *Arabidopsis thaliana*, which has a very small genome (0.16pg/1C). This chapter aims to determine how genome size variation plays a role in influencing plant anatomy and photosynthesis.

The genus *Fritillaria* (Liliaceae) comprises *ca* 140 species of bulbous perennial plants, which are distributed across the temperate zones of the Northern Hemisphere. They are found in North America, Europe, the Mediterranean region and Central Asia, Japan and China (Rønsted *et al.*, 2005; Day *et al.*, 2014). Recent phylogenetic analyses of species relationships across the genus support its suggested division into the eight subgenera recognised by Rix (2001) based on morphological characters. The genus *Fritillaria* includes species with the largest range of diploid genome sizes so far reported, with 1C-values varying from 30.8pg to 100.4pg (Kelly *et al.* (2015) and J. Pellicer pers. comm.) (Figure 2.1), a range equivalent to 435 *A. thaliana* genomes. It includes *F. amabilis* from Japan which represents the species with the largest known diploid genome for any plant so far reported, with a 1C-value of 100.4pg (J. Pellicer pers. comm.). Most species (>95%) of *Fritillaria* have a genome that exceeds 35pg/1C, and these species are therefore considered to have 'giant' genomes (*sensu* Kelly & Leitch, 2011).

Because of the remarkable range of genome sizes at the diploid level, *Fritillaria* was selected in this study to determine the effects of genome size on stomatal size and on photosynthesis. Comparisons were also made between *Fritillaria* and three species

belonging to the monocot family Melanthiaceae, including the octoploid *Paris japonica* (152.2pg/1C) which has the largest known genome size for any eukaryote so far estimated using best practice techniques (Pellicer *et al.*, 2010; Hidalgo *et al.*, 2017).

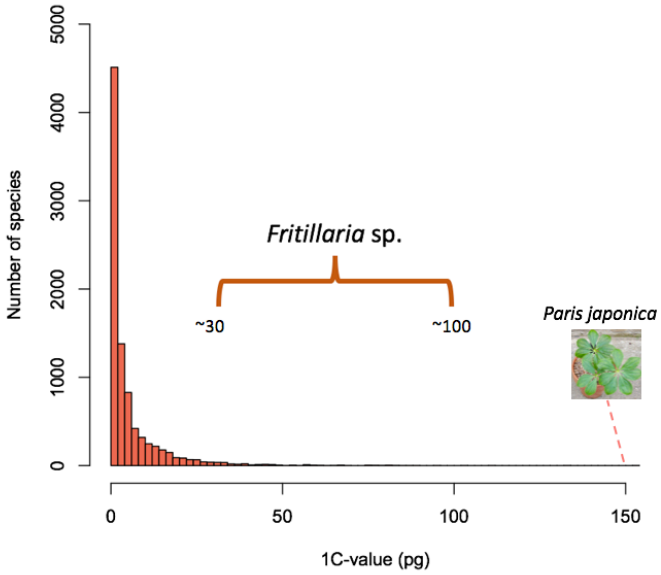

Figure 2.1. Range of C-values in 7542 angiosperm species highlighting the range in *Fritillaria* and the largest C-value of any plant which belongs to *Paris japonica* (data from Bennett & Leitch, 2012).

While there is ongoing research into the molecular dynamics underpinning the origin and evolution of such large genome sizes, our understanding of how genome size impacts physiological processes is more limited (e.g. Knight & Beaulieu (2008) and Símová & Herben (2012)).

Previous studies across a diverse range of plants have shown that there is a broad correlation between GS and stomatal guard cell size, potentially influencing gas exchange rates in the leaf (Beaulieu *et al.*, 2008; Knight & Beaulieu, 2008; Hodgson *et al.*, 2010, although see also Jordan *et al.* (2014)). Stomata are small pores distributed on the surface of leaves bordered by two specialized cells known as guard cells. They control gas exchange in plants, enabling CO_2 to enter and water and O_2 to exit the interior of the leaves (Hetherington & Woodward, 2003). Hence, plants use stomatal pores, and rates at which they open and close to minimize water loss and take up CO_2 to maximize photosynthetic efficiency, in terms of carbon assimilation (Lawson & Blatt, 2014). The architecture of the leaf (e.g. mesophyll cell size, mesophyll conductance) can also impact gas exchange in the leaf, which is considered in Chapter 4. Guard cell length is thought to be related to stomatal conductance (i.e. diffusion rate of CO_2 and

H_2O) (Fanourakis *et al.*, 2015). Stomatal conductance is higher for leaves with many small stomata (small pores) than for those with fewer but larger stomata (large pores). This means that higher photosynthesis efficiency is expected for leaves with a high density of small stomata (Franks & Beerling, 2009).

The work in this chapter exploits the huge range in GS found in *Fritillaria* species and compares data on stomatal size and photosynthetic efficiency for CO_2 uptake and fluorescence parameters with data from other species in Melanthiaceae. The advantage of focusing on *Fritillaria* is that there is a robust phylogenetic tree available (Day *et al.*, 2014) and the results can be examined in a phylogenetic context using only closely related species. This means that the results will not be confounded by anatomical, physiological or development features that may have evolved independently across widely divergent phylogenetic lineages. Here in *Fritillaria*, the analysis is restricted to herbaceous bulbous plants, and most species analysed are diploid (of the 16 *Fritillaria* species analysed, only two are triploid). Several approaches were adopted: infra-red gas analysis (IRGA) was used to investigate rates of CO_2 uptake and Rubisco activity; chlorophyll fluorescence was recorded using pulse amplitude modulation (PAM) fluorometry to provide information on the efficiency of the light energy harvesting machinery for photosynthesis, and; light microscopy was used to obtain stomatal measurements (length and density). The results were analysed using a range of approaches to see if there was any relation between genome size, stomatal size and density and photosynthesis rates.

The underlying hypothesis that is being tested in this study is as follows:

There is a correlation between GS and mesophyll and epidermal cells size. Potentially, increasing GS will have a detrimental effect on photosynthesis because of scaling effects on the cell (area/volume scaling) that may influence gas exchange or diffusion parameters of stomata. This hypothesis can be tested in *Fritillaria*, taking advantage of its enormous range in GS.

Material and methods

Plant material, experimental design and genome size

Data were collected from 16 species of *Fritillaria* including at least one species from each of the eight recognised subgenera to ensure the full phylogenetic diversity of the genus was covered. In addition, three species from the family Melanthiaceae were also

analysed (Table 2.1). The plant material used was either taken from the Living Collections at RBG Kew or from the personal collection of Laurence Hill (LH) (see http://www.fritillariaicones.com/), where they grow in an open area with a glass roof where temperature is not controlled (Figure 2.2,), but in the growing season it typically ranges for 0°C to 25 °C. Plants were grown in sand and an upper layer of gravel, in suitable sized pots to prevent them from being pot-bound ,and watered daily during spring growth, with weekly foliar fertilizers applied. Thereafter the bulbs were left to dry out. Measurements of photosynthesis and leaf sample for stomata assay were taken between 9 am and 5 pm in the spring of 2016 and 2017. Non-flowering plants were randomly selected for collection of data and only mature and fully expanded leaves were used for analyses with a minimum of two plants per species for stomatal analyses (Table 2.2) and at least three plants for photosynthetic analyses (Tables 2.3 and 2.4). Estimates of 1C DNA content were compiled either from the Plant DNA C-values database (Bennett and Leitch, 2012) or from unpublished data (J. Pellicer pers. comm.).

Figure 2.2. *Fritillaria* plants growing at the RBG Kew.

Photosynthetic measurements

Photosynthetic experiments were done in an unheated dark room in the Jodrell Laboratory (RBG Kew, London, UK). Plants were taken from the gardens to this room and manipulated indoors in the dark room with lights switched off when fluorescence

measurements were being taken place. The temperature in the IRGA chamber was taken at each measurement, and it varied between 19˚C and 23.5˚C.

Chlorophyll fluorescence

Chlorophyll *a* fluorescence measurements were performed on all plants using a Junior-PAM (Walz, Germany) a pulse-amplitude-modulated (PAM) photosynthesis yield analyser which generates actinic blue light (maximum wavelength 445nm) to excite chlorophyll. Prior to each measurement, plants were dark-adapted for 30 min. Both procedures described below were obtained using the WinControl-3.24 software that is supplied with the Junior-PAM. Figures 1S and 2S show example curves to guide with the following descriptions.

1. **Rapid light curves (RLC)**: These were measured using pre-installed software in Junior-PAM, where the actinic illumination was increased in intensity in eight steps from 0 to 65, 90, 125, 190, 285, 420, 625, 820 µmol photons $m^{-2}s^{-1}$ for a duration of 10 s (Ralph & Gademann 2005). Curve-fitting and the calculated parameters are given by the end of the procedure according to the methods given in Platt *et al.* (1980), which the following parameters:
   (i) rETR: relative ETR is an approximation of the rate of electron flow through PSII and is defined as the effective quantum yield of PSII (ϕPSII) multiplied by the photosynthetic activity radiation (PAR). It is an important parameter because it is related to the generation of ATP/NADPH (Walker, 1992). The pre-installed software in Junior-PAM fits a curve to the RLC using the following function, with an asymptotic maximum being the rETR value:

$$P = P_m(1 - e^{-\left(\frac{\alpha E_d}{P_m}\right)})$$

   where P_m is the photosynthetic capacity at saturating light, α is the initial slope of RLC and E_d is the irradiance.
   (ii) E_k is the minimum saturating irradiance and is calculated as ETR_{max}/α, where α is the initial slope of RLC;
   (iii) F_v/F_m, maximum quantum efficiency of photosystem II (PSII) photochemistry in dark-adapted tissues, derived from $(F_m-F_o)/F_m$ (Maxwell & Johnson, 2000), where F_m is the maximum fluorescence level after the first saturating light pulse, F_o is the basal in weak light (<1 µmol photons $m^{-2}s^{-1}$) fluorescence level and F_v is F_m-F_o. Note that in generating the Induction Light Curves (below), F_v/F_m is also obtained, and the value reported is the average of F_v/F_m obtained for both RLC and ILC.

2. Induction light curves (ILC): Further characterisation of the efficiency of photosynthesis can be determined by conducting ILCs, using a different portion of the same leaf used for RLC. This procedure is described in Murchie & Lawson (2013). ILCs are derived over a *c*. ~27 minute experiment that is divided into two cycles, each of which is itself divided into a light and a dark phase. In both cycles the leaf material is given a pulse of intense, saturating light. The ILC provides further information on PSII efficiency including F_v/F_m, which is normally 0.8 (Ruban, 2013). In generating the ILC over ~27 min, a pulse of light is given at the beginning of the experiment to determine the maximum fluorescence yield (i.e. F_v/F_m). Then actinic light (420 µmol photons m^{-2} s^{-1} intensity) was applied for 5 min and, during this light phase, 0.8 s of saturating light pulses (10,000 µmol photons $m^{-2}s^{-1}$) are applied every minute to determine the level of maximum fluorescence under actinic light (F_m'). The remaining part of the ILC is conducted without actinic light and saturating light pulses are applied every 2 minutes for about 7 minutes in total. After that phase, a second cycle is carried out of the same actinic light and then in the "dark" with saturating pulses of light . A weak light (<1 µmol photons $m^{-2}s^{-1}$) is always switched on in the "dark" periods to keep PSII reaction centres open, enabling observations of F_o levels. The following parameters were derived:

(i) NPQ, non-photochemical quenching, which is a measure of heat dissipation, and which causes a decline in fluorescence, calculated as $(F_m-F_m')/F_m$, where F_m' is the maximum fluorescence level under actinic light. NPQ values were taken from the last light pulse in the cycle of the ILC with actinic light;

(ii) qP, photochemical quenching, derived from $(F_m'-F_s)/(F_m'-F_o')$, where F_s is the minimum fluorescence under AL and F_o'. This is minimum fluorescence without actinic light (Rey, 1991; Ralph & Gademann, 2005; Ruban, 2013). qP values were taken from the last light pulse in the cycle of the ILC with actinic light.

A/Ci photosynthetic gas exchange

Photosynthetic measurements were taken on fully emerged and healthy leaves. Carbon dioxide uptake was measured using a CIRAS-1 gas exchange system (PP Systems, Amesbury, MA, USA) and a separated light source (Schott halogen cold light KL 1500) with a saturating irradiance of 1500 µmol $m^{-2}s^{-1}$, where the precise irradiance was measured with LI-190R (Li-Cor Biosciences, Lincoln, NE, USA). The intact leaf was clamped into an airtight 2.5 cm^2 cuvette at a vapour pressure deficit of 1.3 kPa and was acclimatized for 20-30 minutes at a CO_2 concentration of 400 µmol mol^{-1} until

a steady state of CO_2 uptake (A) was reached. Changing the CO_2 concentration in the cuvette is used to model photosynthesis parameters (Johnson & Murchie, 2011) and it was decreased in seven steps (300, 200, 120, 100, 80, 60 and 40 µmol mol^{-1}) before returning to the initial concentration, and then increased in five steps (600, 800, 1200, 2000 and 2200 µmol mol^{-1}) with around 5 minutes for acclimation at each step. The leaf area exposed was calculated for those samples where the leaf was smaller than the cuvette area using the image analysis software ImageJ (http://rsbweb.nih.gov/ij/index.html). Curve-fitting and modelling were performed in R (R Core Team, 2016) using the package Plantecophys (Duursma, 2015), which uses the model described by Farquhar *et al.* (1980) by *fitaci* function. A/C_i curves were generated to provide information on maximum CO_2 uptake (A_{max}) – which was taken from the CO_2 concentration 2000 µmol mol^{-1}, maximum rate of carboxylation (V_{cmax}) and maximum rate of electron transport used for regeneration of RuBisCO substrate (J_{max}). Further modelling was used to access information on mitochondrial respiration (R_d), it is the respiratory CO_2 release. Calculated parameters as the internal leaf CO_2 concentration (C_i), A and g_s (stomatal conductance, taken from CO_2 concentration 400 µmol mol^{-1}) are provided by the IRGA's software based on the biochemical model of photosynthesis (von Caemmerer & Farquhar, 1981). These parameters were chosen to find whether there is any impairment on photosynthesis (A_{max}, V_{cmax}, J_{max}, C_i), respiration (R_d) and conductance (g_s) depending on genome size and stomatal size.

The enzyme RuBisCO catalyses reactions for either fixation of CO_2 or O_2, according to the relative amount of these molecules in the chloroplast. Thus, CO_2 and O_2 are competitors because they compete for the same binding active site of RuBisCO. This is disadvantageous for CO_2 fixation and for photosynthesis and the modelling accounts for the possible fixation of O_2 (Farquhar *et al.*, 1980).

An example of what an A/Ci curve is shown in Figure 3S. The slope of the linear phase of the A/Ci curve is V_{cmax}, when A is limited by RuBisCO activity, and the response of A to CO_2 is given by (Farquhar *et al.*, 1980; Long & Bernacchi, 2003; Sharkey *et al.*, 2007; Johnson & Murchie, 2011):

$$A = V_{cmax}\left(\frac{C_c - \Gamma^*}{C_c + K_c(1 + O/K_o)}\right) - R_d$$

At higher CO_2 levels, A is increasingly limited by J_{max}, when A is limited by RuBisCO regeneration. The consequent response of A to CO_2 is:

$$A = J_{max}\left(\frac{C_c - \Gamma^*}{4C_c + 8\Gamma^*}\right) - R_d$$

Where C_c is the CO_2 partial pressure at RuBisCO, K_c is the Michaelis constant of RuBisCO for CO_2, O is the partial pressure of O_2 at RuBisCO, K_o is the Michaelis constant of RuBisCO for O_2, Γ^* is the photosynthetic compensation point – when CO_2 concentration at which the photorespiratory efflux of CO_2 equals the rate of photosynthetic CO_2 uptake. V_{cmax} is estimated as the slope and $-R_d$ is the intercept at curve-fitting.

Stomatal measurements

To estimate the stomatal density and length, the mid-section of mature, fully expanded leaves were analysed. For some plants the impression of the surface of the leaves were taken using the nail varnish method of Hilu & Randall (1984), and for other plants, a leaf peel was made by hand. For nail varnish impressions, leaf surfaces were covered in clear nail varnish. After drying, the surface was covered with clear tape and the leaf tissue removed, leaving the epidermis impression on the tape, which was transferred to a microscope slide and examined by microscopy. For leaf peels, leaf material stored in 70% ethanol were first fully hydrated in an ethanol series (2 min each in 70%, 50% 30% and water) and once hydrated, the leaf material was scraped with a razor blade in a drop of 70% bleach (Domestos®) in water until only the epidermis remained (= leaf peel). The leaf peel was rinsed in water and mounted on a microscope slides in a 1:1 (v/v) mixture of with glycerine/water). Abaxial (lower) and for some species the adaxial (upper) leaf surfaces were observed by light microscopy using a 20x objective lens. Photomicrographs were taken with a DFC365 FX camera mounted on a Leica DM6000 B microscope. Guard cell length was measured from at least 20 stomata from multiple areas from three leaves of different individuals (one leaf per plant) using the image analysis software ImageJ (http://rsbweb.nih.gov/ij/index.html). Stomatal density was calculated as the number of stomata per square millimetre of epidermis, measured in at least 20 different fields of the epidermis from three leaves taken from three different plants.

Constructing the phylogenetic tree

For all *Fritillaria* and Melanthiaceae species examined, a phylogenetic hypothesis of species relationships was reconstructed using nucleotide sequences for the plastid markers matK and rbcL that were obtained from Day *et al.* (2014) for *Fritillaria* species) and from Genbank (Benson *et al.*, 2013) for the Melanthiaceae species. Sequences were aligned in MEGA 7.0 (Kumar *et al.*, 2016) using Muscle (Edgar, 2004), the alignment checked visually, and sequences concatenated to a single contiguous sequence using Sea View (Gouy *et al.*, 2010). A maximum likelihood phylogenetic tree

was estimated (Figure 2.3) and verified for consistency using the phylogenetic tree given in Day *et al.* (2014).

Statistical analyses

Data were analysed by linear regression using linear models (LMs) carried out using R version 3.3.1 (R Core Team, 2016). When appropriate, data were transformed using the $\log_e$ or square root function. Phylogenetic independent contrasts (PICs) were used for each relationship investigated in order to take into account the expected covariance due to the shared phylogeny between the species being analysed. PICs for C-value as a function of leaf traits and photosynthetic parameters were conducted with the R package "ape" (Paradis *et al.*, 2004).

Leaf traits. Analysis of covariance was used in the models when guard cell length, developmental phase (juvenile and adult plants, Figure 2.4) and side (abaxial or adaxial) of the leaf were the explanatory variables compared with stomatal density, since they are continuous and categorical variables. Where both adult and juvenile phases of the life cycle were studied (i.e. for *Fritillaria eduardii*, *F. meleagris*, *F. persica* and *F. uva-vulpis*), the developmental phases were treated as categorical variables in the analyses. All the plants have stomata on the abaxial side, thus, for consistency, only the abaxial stomata were considered in the analyses for comparison with C-values. Photosynthetic efficiency was compared with the presence of stomata on the abaxial and adaxial surfaces of the leaf.

Photosynthetic parameters. Because measurements of *F. eduardii* and *F. persica* were taken from both juvenile and adult plants, and the data were found to be different between developmental phases, LMs were conducted, including both phases separately. The analyses were conducted to test whether (i) any of the photosynthetic parameters (V_{cmax}, J_{max}, A_{max}, g_s, C_i, R_d, qP, NPQ, rETR, F_v/F_m and E_k) were a function of stomatal density and size: (ii) there were differences in stomatal density and size, and photosynthetic parameters between adults and juveniles of *F. eduardii* and *F. persica*; (iii) photosynthetic parameters are a function of genome size.

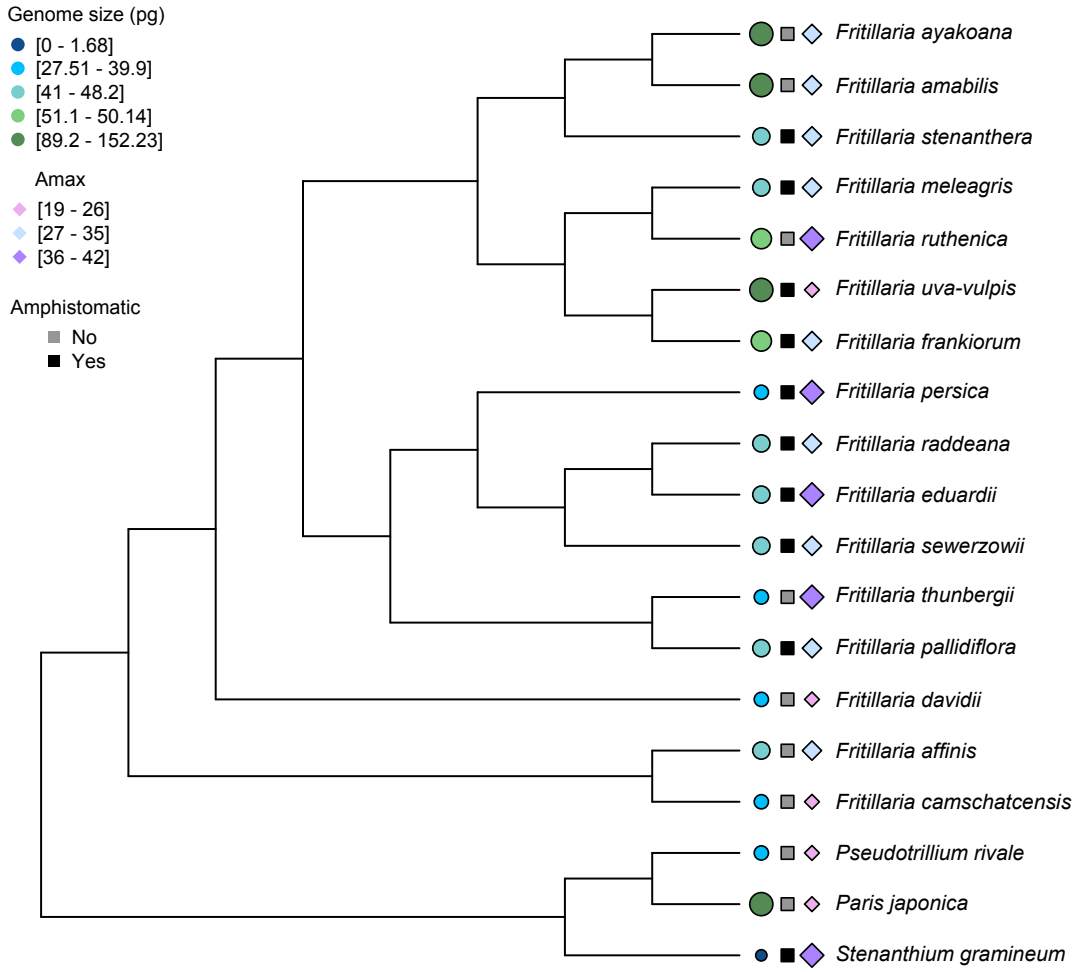

Figure 2.3. Phylogenetic tree of *Fritillaria* and the outgroup Melanthiaceae showing the distribution of genome sizes (C-values) and A_{max} variation among species and whether the species are amphistomatic.

A B C

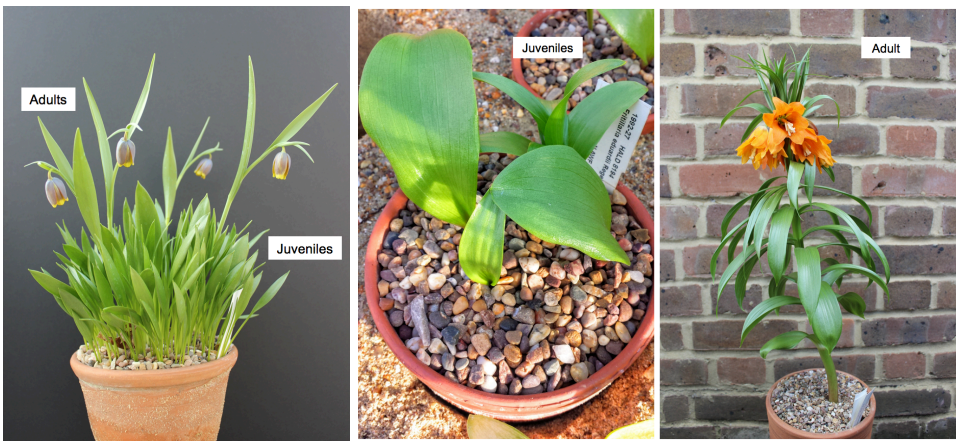

Figure 2.4. (A) Adult and juvenile plants of *Fritillaria uva-vulpis*. (B) Juvenile and (C) adult plants of *F. eduardii*.

Results

Stomatal length and density in Fritillaria

Stomatal lengths and densities were measured using light microscopy (Figure 2.5). Linear models (LM) were used to explore the relationships between stomatal length and density across *Fritillaria* species (Table 2.5 a-d). Overall, there was a big range in the stomatal lengths (44.55 to 105.38 µm) and densities (17.20 to 68.75 mm^2) between *Fritillaria* species when considering data from adaxial and abaxial leaf surfaces together (Table 2.2), with nine of the 16 *Fritillaria* species and one species of Melanthiaceae (i.e. *Stenanthium gramineum*) analysed observed to be amphistomatous (i.e. with stomata on both sides of the leaves). An examination of species in *Fritillaria* and Melanthiacae revealed that stomatal density was negatively associated with stomatal length (R^2 = 0.14, p <0.0001), especially on the abaxial surface of the leaf (R^2 = 0.47, p <0.0001; Figure 2.6).

An examination of just the *Fritillaria* species also showed a negative relationship between stomatal length and density (p <0.0001, Table 2.5a), with the adaxial surface having shorter stomata (p = 0.0329, Table 2.5b) at lower density (p <0.0001, Table 2.5a) than the abaxial surface. Plants with stomata on both sides of the leaf had lower stomatal densities than those with stomata on just the abaxial surface of the leaf (p <0.0001, Table 2.5a). For four species of *Fritillaria* with both adult and juvenile leaves,

the data revealed that juvenile leaves had a lower density of stomata (p = 0.0005, Table 2.5c) of larger stomata size (p = 0.0001, Table 2.5d).

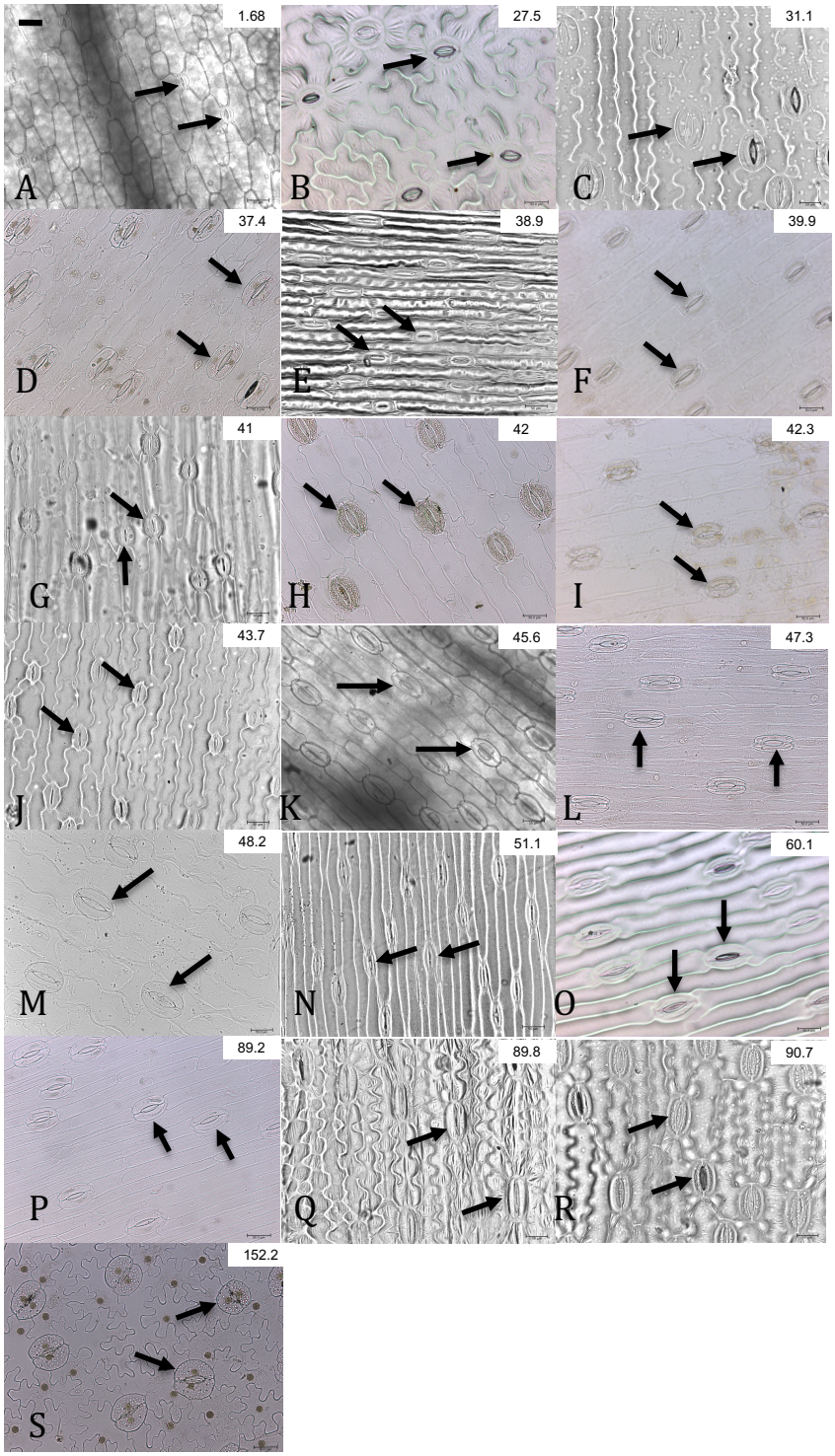

Figure 2.5. Photomicrographs of abaxial leaf surfaces of (A) *Stenanthium gramineum*, (B) *Pseudotrillium rivale*, (C) *Fritillaria davidii*, (D) *F. camschatcensis*, (E) *F. thunbergii*, (G) *F. persica*, (H) *F. eduardii*, (I) *F. raddeana*, (J) *F. sewerzowii*, (K) *F. pallidiflora*, (L)

F. affinis, (M) *F. meleagris*, (N) *F. stenanthera*, (O) *F. ruthenica*, (P) *F. frankiorum*, (Q) *F. uva-vulpis*, (R) *F. ayakoana*, (S) *F. amabilis*, (T) *Paris japonica.* Images are arranged in increasing genome size (1C-values in pg are given top right of each figure). A selection of stomata is arrowed. All species shown at the same magnification, black bar in (A) = 50μm.

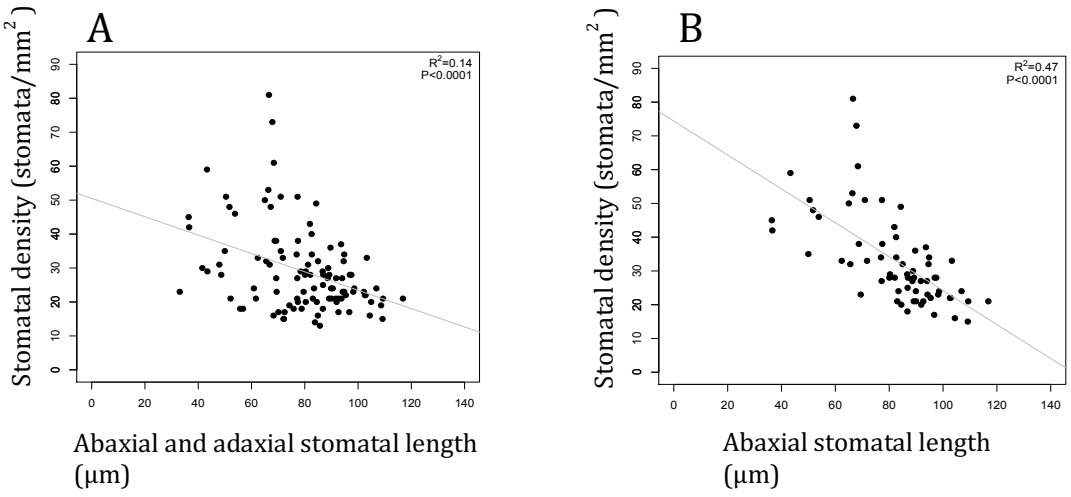

Figure 2.6. Plots showing a negative relationship between stomatal length and density across 16 species of *Fritillaria* and three species of Melanthiaceaee from juvenile and adult individuals. (A) Stomata analysed are from both the, abaxial and adaxial, leaf surfaces; (B) stomata analysed are from abaxial leaf surface only. Each point is a measurement from an individual plant (see also Table 2.3).

Genome size and stomatal length and density

Despite the huge range in genome sizes observed in the *Fritillaria* species studied (ranging from 1C = 31.1 to 1C = 90.7 pg, Table 2.1), there was no significant relationship between genome size (1C-value) and stomatal length or density (Table 2.6, Figure 2.7). An absence of any correlation was also apparent in the light microscopy images (Figure 2.5).

Photosynthesis efficiency and stomatal length and density

Statistical analyses of the *Fritillaria* data suggest that maximum net photosynthesis (A_{max}) and the maximum rate of RuBisCO regeneration (J_{max}) are both significantly correlated with stomatal density, but not stomatal length (Tables 2.7a-l, 2.8a, b). All other photosynthetic parameters measured showed no significant relationship in the analyses with stomatal length (A_{max}, J_{max}, V_{cmax}, g_s, C_i and R_d) or density (V_{cmax}, g_s, C_i

and R_d; Table 2.7). Nevertheless, some parameters (i.e. R_d, V_{cmax}) did have significantly more negative values in juvenile leaves, while g_s was significantly larger in juvenile leaves compared with adult leaves for the two *Fritillaria* species analysed (Table 2.7, Figure 2.8).

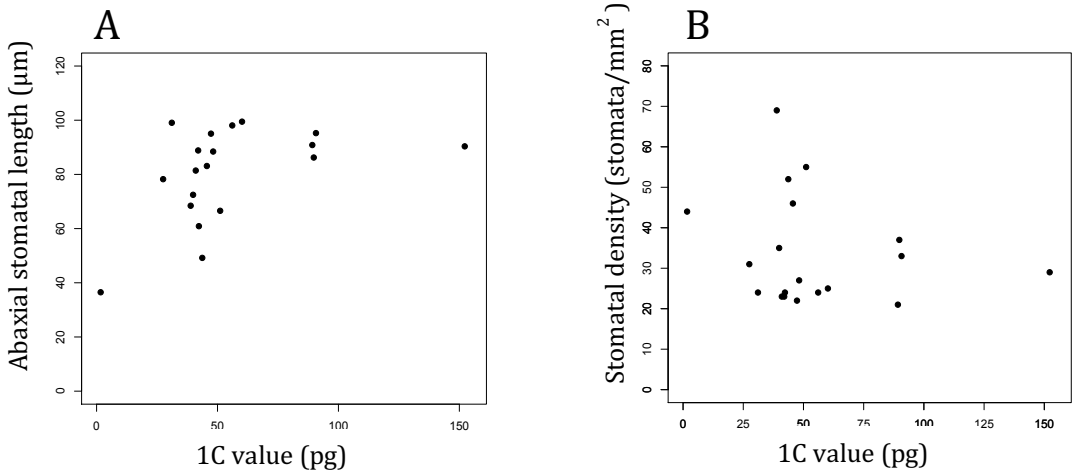

Figure 2.7. Plots showing the relationship between (A) 1C-values and stomatal length on abaxial side and (B) 1C-value and stomatal density on abaxial side in 16 species of *Fritillaria* and three species in Melanthiaceae. Each point is the mean value per species.

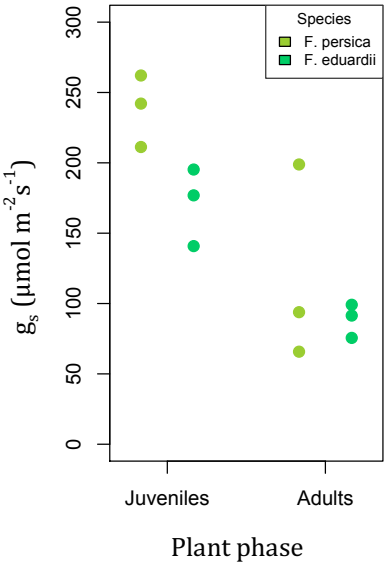

Figure 2.8. Stomatal conductance (g_s) at 400 µmol mol^{-1} of CO_2 for juvenile and adult leaves of *Fritillaria persica* and *F. eduardii*. Each point is an individual measurement.

Using LMs, no significant effects of stomatal size and density on the fluorescence parameters F_v/F_m, qP, NPQ, rETR, E_k (Table 2.9), were observed although a negative relationship in the juvenile leaves between both stomatal density and length and photochemical quenching (qP) (Table 2.7c,d). Nevertheless, PICs indicated a negative correlation between stomatal length and rETR (Table 2.8a). Table 2.10 summarise the main results.

Photosynthesis efficiency and genome size

LMs suggest that maximum net photosynthesis (A_{max}), maximum RuBisCO activity (V_{cmax}), maximum rate of RuBisCO regeneration (J_{max}) and stomatal conductance (g_s) are significantly and negatively correlated with genome size (Table 2.11, Figure 2.9). Mitochondria respiration (R_d) and intercellular CO_2 (C_i) are not correlated with genome size. In LMs analyses, F_v/F_m and rETR were also significantly negatively associated with genome size whilst NPQ was significantly positively correlated with genome size (Table 2.12). However, the relationship between NPQ and genome size was not recovered using PICs (Table 2.8). Table 2.13 shows the summary of the main statistical results.

Discussion

Different abaxial and adaxial stomatal densities

The negative relationship between stomatal length and density seen in previous studies (e.g. Beaulieu *et al.*, 2008; Franks & Beerling, 2009; Camargo & Marenco, 2011) is also found in this study of 16 *Fritillaria* species, and three Melanthiacaceae species, especially when analysing just the stomata from the abaxial side of *Fritillaria* leaves (Figure 2.6). In this analysis stomata were more abundant on the abaxial surface of the leaves than on the adaxial surface, and this too has been seen in other studies of amphistomatous species, i.e. those species with stomata on both leaf surfaces (Pereira & Kozlowski, 1977, Mott *et al.* 1982). In addition, in *Fritillaria* as well as some other species that have been analysed (e.g. Pereira & Kozlowski, 1977), those species with hypostomatic leaves (i.e. with stomata only on the abaxial surface of the leaf) had significant greater stomatal densities than any leaf surface of amphistomatous species, probably to compensate for the absence of stomata on the adaxial surface. A higher density of stomata on the abaxial leaf surface might be expected as it is not directly exposed to the sun and will be less prone to heat stress.

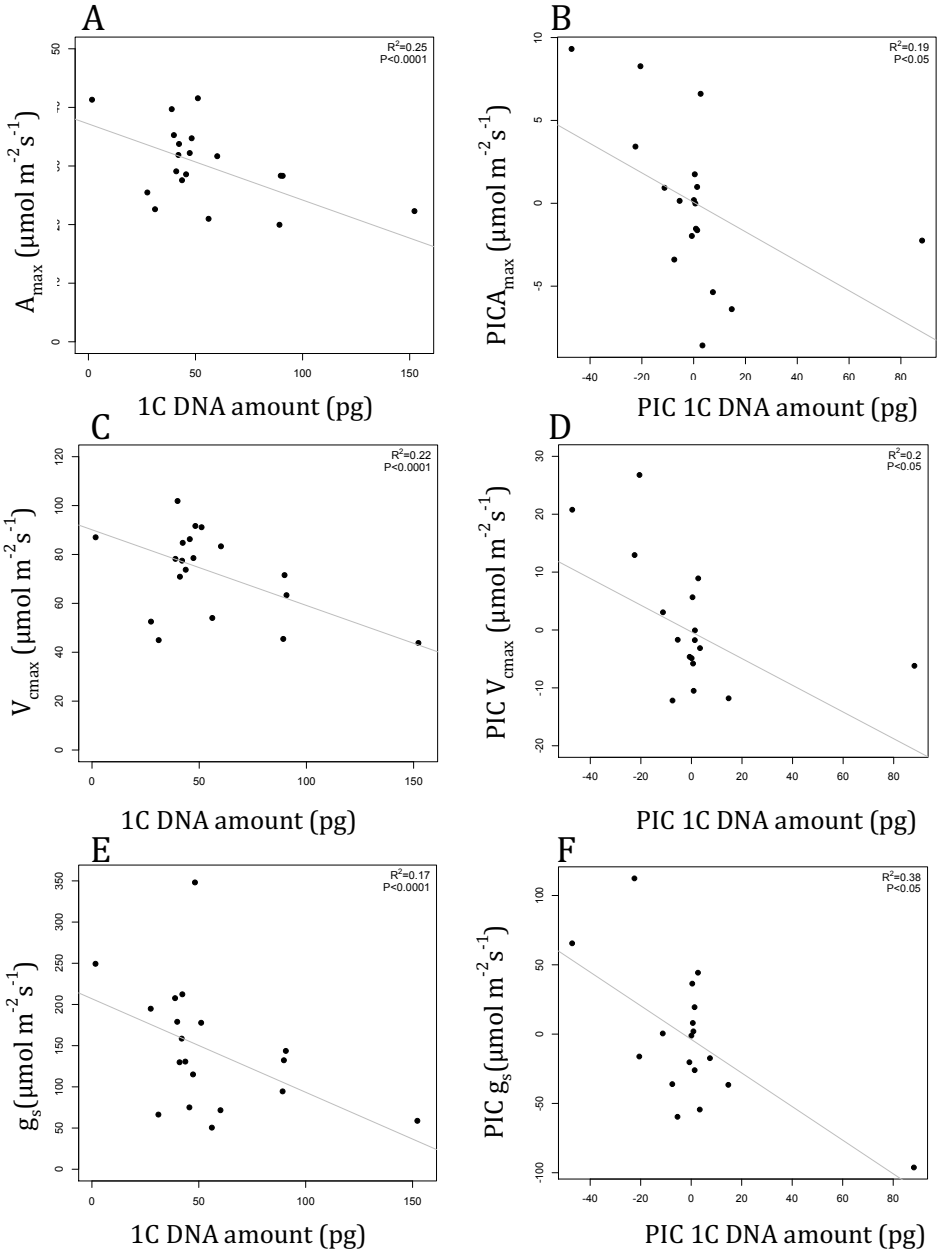

Figure 2.9. Scatter plots showing the relationships between metabolic rates and 1C-values with and without using phylogenetic independent contrasts (PIC).

Leaf characters at different developmental phases

Four species of *Fritillaria* where both juvenile and adult leaves were available for analysis (i.e. F*. eduardii, F. meleagris, F. persica* and *F. uva-vulpis*) revealed that their juvenile leaves had stomata that were larger and at a lower density than adult leaves on both adaxial and abaxial surfaces (Tables 2.5c,d and 2.3b). Associated with this, in two of these species of *Fritillaria* (*F. eduardii* and *F. persica*) juvenile leaves had

significantly lower RuBiSCO activity (V_{cmax}) and mitochondrial respiration rates (R_d) than adult leaves (Table 2.7 c,d,j,k), perhaps caused by leaf thickness or lower stomatal density. In addition, juvenile leaves had significantly larger g_s (stomatal conductance) than adult leaves, perhaps because the stomata are larger (Tables 2.7h and 2.5d, Figure 2.8). Yet this result is surprising since we might expect stomatal conductance (g_s), R_d and V_{cmax} to be closely linked to the gas exchange properties of the leaf, as suggested previously (Drake *et al.*, 2013; Raven, 2014). Potentially, the differences in leaf physiology and stomatal form are associated with the considerable leaf morphology and size differences between juvenile and adult leaves (as in *F. eduardii* and *F. uva-vulpis*, Figure 2.4). Indeed, in some species such as *F. uva-vulpis* the total surface area of a juvenile leaf (Figure 2.4b) is considerably greater than that of the adult leaves (Figure 2.4c) and this may also play a role in modifying the relationship between stomatal size and density and conductance as reported in some other species (Niklas *et al.*, 2007; Milla *et al.*, 2013).

Correlations between stomatal size and photosynthetic parameters

CO_2 uptake has been shown to be positively related to stomatal density and negatively related to guard cell length (Franks & Beerling, 2009). In the *Fritillaria* species examined, an analysis of the parameter A_{max} which measures the maximum CO_2 uptake, was significantly and positively correlated with stomatal density. This was expected, since past work has also revealed that leaves with smaller and more abundant stomata enhance or are associated with higher rates of gas exchange (Schlüter *et al.*, 2003; Xu & Zhou, 2008; Drake *et al.*, 2013; Lawson & Blatt, 2014). A study of stomatal density mutants of *Arabidopsis thaliana* showed that F_v/F_m and qP decreased in areas of leaves without stomata. The authors related this to a reduction of antenna complexes of photosystem II within the chloroplasts in these areas due to the decreased stomatal density (Büssis *et al.*, 2006). However these properties were not associated with stomatal length and density in the *Fritillaria* species studied here although a relationship between stomatal length and rETR (maximum relative electron transport rate) in *Fritillaria* (Table 2.10) was uncovered. Perhaps *Fritillaria* species with larger cells have larger antenna complexes and/or higher rates of electron transport. Clearly, further studies in a greater diversity of species across the phylogenetic tree of angiosperms are needed to unpick the relative contribution of evolutionary and ecological factors in influencing these photosynthetic traits.

An absence of correlation between genome size and stomatal size

Despite the enormous range in genome size observed in this study (i.e. 1C-values ranged from 31.1 - 90.71 pg in *Fritillaria* and 1.68 – 152.2 pg in Melanthiaceae), there was no clear correlation found between C-value and stomatal density or stomatal length (Figure 2.7). This was a surprise given the significant relationship between DNA amount and guard cell length and stomatal density reported previously (Beaulieu *et al.*, 2008; Hodgson *et al.*, 2010, Knight & Beaulieu 2008)). The lack of correlation between these characters for the plants analysed here may because of: (1) physiological differences between the ontological phase of the leaf, and on abaxial/adaxial leaf surfaces, impact stomatal size more than any effects of genome size, (2) the correlation between genome size and stomatal size is only apparent in species with small genome sizes (1C<3.5pg, Kelly & Leitch 2011)), and most data here (i.e. all but one outgroup species, *Stenanthium gramineum*, 1C=1.68pg) are from species with genomes greater than 27.51 pg/1C. It is possible that above a certain genome size threshold stomatal size does not scale proportionally with genome size because of selection pressures against very large pore sizes which can reduce gas diffusion parameters (Milla *et al.*, 2013). Assuming so, any increase in genome size must be accommodated for without necessarily an increase in cell size.

Associations between genome size and photosynthetic characters

Despite the lack of relationship between stomatal characters and genome size, some measures of photosynthesis (A_{max}, V_{cmax}, g_s, qP and rETR) are significantly, negatively correlated with genome size (Table 2.8c). Similar results were previously observed by Beaulieu *et al.* (2007) on a study done on 134 species across a broad phylogenetic divergence. These authors found a significant and negative association between A_{max} and R_d and genome size, however R_d was not found to be significantly associated with C-value in our study. Another study on 24 species revealed a significant negative correlation between genome size and photosynthetic rates (Knight *et al.*, 2005). This work builds on these previous works by considering also chlorophyll fluorescence parameters (qP, rETR).

All of these negative associations between genome size and photosynthetic processes support a hypothesis that metabolic demands of the nucleus compete with photosynthesis. A possible cause of that competition are resources for proteins, pigments and nucleic acids e.g. energy (ATP, NAPDH), nitrogen and phosphorus.

Conclusions

Franks *et al*. (2012a) has suggested that stomatal sizes measured from fossils correlate with paleo-CO_2 levels measured from geochemical data. The differences in stomatal size in *Fritillaria* leaves (e.g. adaxial/abaxial surface and development stage of the leaf (juvenile/adult)) do suggest that stomatal size has the potential to respond to physiological conditions, indeed this has been shown under different CO_2 levels (Franks et al. 2012b) and in different ecological conditions (Jordan et al. 2015). Franks *et al.* (2012a,b) and Lomax *et al* (2013) also suggest that a correlation between stomatal size and genome size in extant species can be used to predict genome sizes from fossils. Indeed, Franks *et al*. (2012a) argue that selection pressure on stomatal size by atmospheric CO_2 provides a selection pressure on the genome size itself, leading to correlations between paleo-genome sizes and paleo-CO_2 levels. However conclusions relating to a correlation between cell size and genome size are not supported by this work or previous studies by Jordan et al. (2015) in the family Proteaceae. However that association does exist for juvenile leaves, and it is possible that genome size sets a minimum cell size, and cell physiology may then act to increase cell size and influence the relationship. Whatever the reason for the lack of association between cell size and genome size, such observations mean that using fossil stomatal size to reconstruct fossil genome sizes (Franks et al. 2012, Lomax et al. 2013) must be interpreted with caution, perhaps particularly at the upper end of the range of genome sizes encountered in plants. More work is clearly needed on other plant groups, not only within angiosperms but in other land plant groups as well, since it is clear from the analyses presented here that there is also a phylogenetic component to the relationships between the various guard cell parameters, genome size and photosynthetic traits. It also emphasises the importance of analysing the data in a phylogenetic context, to model how genome size and plant physiology interact together in the control of stomatal size. Nevertheless while it is clear that genome size will determine the minimum size of guard cells (i.e. big genomes cannot fit inside small guard cells), and that this in turn will provide a selection pressure on density across all plants, additional genomic, physiological and ecological factors clearly may also play a role in causing stomatal size to vary from that minimum value set by genome size.

References

Beaulieu JM, Leitch IJ, Knight CA. **2007**. Genome size evolution in relation to leaf strategy and metabolic rates revisited. *Annals of Botany* **99**: 495–505.

Beaulieu JM, Leitch IJ, Patel S, Pendharkar A, Knight CA. **2008**. Genome size is a strong predictor of cell size and stomatal density in angiosperms. *New Phytologist* **179**: 975–986.

Bennett MD, Leitch IJ. **2012**. Plant DNA C-values database (release 6.0, December 2012). <http://data.kew.org/cvalues/>.

Benson DA, Cavanaugh M, Clark K, Karsch-Mizrachi I, Lipman DJ, Ostell J, Sayers EW. **2013**. GenBank. *Nucleic Acids Research* **41**: D36–D42.

Büssis D, von Groll U, Fisahn J, Altmann T. **2006**. Stomatal aperture can compensate altered stomatal density in *Arabidopsis thaliana* at growth light conditions. *Functional Plant Biology* **33**: 1037.

von Caemmerer S, Farquhar GD. **1981**. Some relationships between the biochemistry of photosynthesis and the gas exchange of leaves. *Planta* **153**: 376–387.

Camargo MAB, Marenco RA. **2011**. Density, size and distribution of stomata in 35 rainforest tree species in Central Amazonia. *Acta Amazonica* **41**: 205–212.

Day PD, Berger M, Hill L, Fay MF, Leitch AR, Leitch IJ, Kelly LJ. **2014**. Evolutionary relationships in the medicinally important genus *Fritillaria* L. (Liliaceae). *Molecular Phylogenetics and Evolution* **80**: 11–19.

Drake PL, Froend RH, Franks PJ. **2013**. Smaller, faster stomata: Scaling of stomatal size, rate of response, and stomatal conductance. *Journal of Experimental Botany* **64**: 495–505.

Duursma RA. **2015**. Plantecophys - An R Package for Analysing and Modelling Leaf Gas Exchange Data. *PLoS ONE* **10**: e0143346.

Edgar RC. **2004**. MUSCLE: multiple sequence alignment with high accuracy and high throughput. *Nucleic acids research* **32**: 1792–7.

Fanourakis D, Giday H, Milla R, Pieruschka R, Kjaer KH, Bolger M, Vasilevski A, Nunes-Nesi A, Fiorani F, Ottosen C-O. **2015**. Pore size regulates operating stomatal conductance, while stomatal densities drive the partitioning of conductance between leaf sides. *Annals of Botany* **115**: 555–65.

Farquhar GD, von Caemmerer S, Berry JA. **1980**. A biochemical model of photosynthetic CO_2 assimilation in leaves of C3 species. *Planta* **149**: 78–90.

Franks PJ, Beerling DJ. **2009a**. Maximum leaf conductance driven by CO_2 effects on stomatal size and density over geologic time. *Proceedings of the National Academy of Sciences* **106**: 10343–10347.

Franks PJ, Beerling DJ. **2009b**. Maximum leaf conductance driven by CO_2 effects on stomatal size and density over geologic time. *Proceedings of the National Academy of Sciences* **106**: 10343–10347.

Franks PJ, Freckleton RP, Beaulieu JM, Leitch IJ, Beerling DJ. **2012**. Megacycles of atmospheric carbon dioxide concentration correlate with fossil plant genome size. *Philosophical transactions of the Royal Society of London. Series B, Biological sciences* **367**: 556–564.

Gouy M, Guindon S, Gascuel O. **2010**. SeaView version 4: a multiplatform graphical user interface for sequence alignment and phylogenetic tree building. *Molecular Biology and Evolution* **27**: 221–224.

Grover CE, Wendel JF. **2010**. Recent insights into mechanisms of genome size change in plants. *Journal of Botany* **2010**: 1–8.

Hetherington AM, Woodward FI. **2003**. The role of stomata in sensing and driving environmental change. *Nature* **424**: 901–908.

Hidalgo O, Pellicer J, Christenhusz M, Schneider H, Leitch AR, Leitch IJ. **2017**. Is there an upper limit to genome size? *Trends in Plant Science* **22**: 567–573.

Hilu KW, Randall JL. **1984**. Convenient method for studying grass leaf epidermis. *Taxon* **33**: 413.

Hodgson JG, Sharafi M, Jalili A, Díaz S, Montserrat-Martí G, Palmer C, Cerabolini B, Pierce S, Hamzehee B, Asri Y, *et al.* 2010. Stomatal vs. genome size in angiosperms: the somatic tail wagging the genomic dog? *Annals of Botany* **105**: 573–584.

Jiao Y, Wickett NJ, Ayyampalayam S, Chanderbali AS, Landherr L, Ralph PE, Tomsho LP, Hu Y, Liang H, Soltis PS, *et al.* 2011. Ancestral polyploidy in seed plants and angiosperms. *Nature* **473**: 97–100.

Johnson G, Murchie E. **2011**. Gas exchange measurements for the determination of photosynthetic efficiency in *Arabidopsis* leaves. In: Jarvis R, ed. Chloroplast Research

in Arabidopsis. Methods in Molecular Biology (Methods and Protocols). Humana Press, Totowa, NJ, 311–326.

Jordan GJ, Carpenter RJ, Koutoulis A, Price A, Brodribb TJ. **2015**. Environmental adaptation in stomatal size independent of the effects of genome size. *New Phytologist* **205**: 608–617.

Kejnovsky E, Hawkins JS, Feschotte C. **2012**. Plant transposable elements: biology and evolution. In: Wendel J,, In: Greilhuber J,, In: Doležel J,, In: Leitch I, eds. Plant Genome Diversity Volume 1. Vienna: Springer Vienna, 17–34.

Kelly L, Leitch I. **2011**. Exploring giant plant genomes with next-generation sequencing technology. *Chromosome Research* **19**: 939–953.

Kelly LJ, Renny-Byfield S, Pellicer J, Macas J, Novák P, Neumann P, Lysak MA, Day PD, Berger M, Fay MF, *et al.* 2015. Analysis of the giant genomes of *Fritillaria* (Liliaceae) indicates that a lack of DNA removal characterizes extreme expansions in genome size. *New Phytologist* **208**: 596–607.

Knight CA, Beaulieu JM. **2008**. Genome size scaling through phenotype space. *Annals of Botany* **101**: 759–766.

Knight CA, Molinari NA, Petrov DA. **2005**. The large genome constraint hypothesis: evolution, ecology and phenotype. *Annals of Botany* **95**: 177–190.

Kumar S, Stecher G, Tamura K. **2016**. MEGA7: Molecular evolutionary genetics analysis version 7.0 for bigger datasets. *Molecular Biology and Evolution* **33**: 1870–1874.

Lawson T, Blatt MR. **2014**. Stomatal size, speed, and responsiveness impact on photosynthesis and water use efficiency. *Plant Physiology* **164**: 1556–1570.

Leitch IJ, Beaulieu JM, Chase MW, Leitch AR, Fay MF. **2010**. Genome size dynamics and evolution in monocots. *Journal of Botany* **2010**: 1–18.

Leitch IJ, Beaulieu JM, Cheung K, Hanson L, Lysak MA, Fay MF. **2007**. Punctuated genome size evolution in Liliaceae. *Journal of Evolutionary Biology* **20**: 2296–2308.

Leitch AR, Leitch IJ. **2012**. Ecological and genetic factors linked to contrasting genome dynamics in seed plants. *New Phytologist* **194**: 629–646.

Long SP, Bernacchi CJ. **2003**. Gas exchange measurements, what can they tell us about the underlying limitations to photosynthesis? Procedures and sources of error. *J Exp Bot* **54**: 2393–2401.

Maxwell K, Johnson GN. **2000**. Chlorophyll fluorescence - a practical guide. *Journal of Experimental Botany* **51**: 659–668.

Milla R, de Diego-Vico N, Martín-Robles N. **2013**. Shifts in stomatal traits following the domestication of plant species. *Journal of Experimental Botany* **64**: 3137–3146.

Mott KA, Gibson AC, O'Leary JW. **1982**. The adaptive significance of amphistomatic leaves. *Plant, Cell & Environment* **5**: 455–460.

Murchie EH, Lawson T. **2013**. Chlorophyll fluorescence analysis: a guide to good practice and understanding some new applications. *Journal of Experimental Botany* **64**: 3983–3998.

Niklas KJ, Cobb ED, Niinemets U, Reich PB, Sellin A, Shipley B, Wright IJ. **2007**. 'Diminishing returns' in the scaling of functional leaf traits across and within species groups. *PNAS* **104**: 8891–6.

Paradis E, Claude J, Strimmer K. **2004**. APE: analyses of phylogenetics and evolution in R language. *Bioinformatics* **20**: 289–290.

Van de Peer Y, Mizrachi E, Marchal K. **2017**. The evolutionary significance of polyploidy. *Nature Reviews Genetics* **18**: 411–424.

Pellicer J, Fay MF, Leitch IJ. **2010**. The largest eukaryotic genome of them all? *Botanical Journal of the Linnean Society* **164**: 10–15.

Pereira JS, Kozlowski TT. **1977**. Variations among woody angiosperms in response to flooding. *Physiologia Plantarum* **41**: 184–192.

Platt T, Gallegos CL, Harrison WG. **1980**. Photoinhibition of photosynthesis in natural assemblages of marine phytoplankton. *Journal of Marine Research* **38**: 687–701.

R Core Team. **2016**. R: A language and environment for statistical computing. R Foundation for Statistical Computing.

Ralph PJ, Gademann R. **2005**. Rapid light curves: a powerful tool to assess photosynthetic activity. *Aquatic Botany* **82**: 222–237.

Raven JA. **2014**. Speedy small stomata? *Journal of Experimental Botany* **65**: 1415–1424.

Rey F. **1991**. Photosynthesis-irradiance relationships in natural phytoplankton populations of the Barents Sea. *Polar Research* **10**: 105–116.

Rix M. **2001**. *Fritillaria*: a revised classification together with an updated list of species.

The Fritillaria group of the Alpine Garden Society.

Rønsted N, Law S, Thornton H, Fay MF, Chase MW. **2005**. Molecular phylogenetic evidence for the monophyly of *Fritillaria* and *Lilium* (Liliaceae; Liliales) and the infrageneric classification of *Fritillaria*. *Molecular Phylogenetics and Evolution* **35**: 509–527.

Ruban A. **2013**. *The photosynthetic membrane: molecular mechanisms and biophysics of light harvesting*. United Kingdom: Wiley.

Schlüter U, Muschak M, Berger D, Altmann T. **2003**. Photosynthetic performance of an *Arabidopsis* mutant with elevated stomatal density (sdd1-1) under different light regimes. *Journal of Experimental Botany* **54**: 867–874.

Sharkey TD, Bernacchi CJ, Farquhar GD, Singsaas EL. **2007**. Fitting photosynthetic carbon dioxide response curves for C_3 leaves. *Plant, Cell & Environment* **30**: 1035–1040.

Símová I, Herben T. **2012**. Geometrical constraints in the scaling relationships between genome size, cell size and cell cycle length in herbaceous plants. *Proceedings of the Royal Society B: Biological Sciences* **279**: 867–875.

Soltis PS, Soltis DE. **2009**. The role of hybridization in plant speciation. *Annual Review of Plant Biology* **60**: 561–588.

Walker DA. **1992**. *Energy, plants and man*. United Kingdom: Oxygraphics Limited.

Wendel JF. **2015**. The wondrous cycles of polyploidy in plants. *American Journal of Botany* **102**: 1753–6.

Xu Z, Zhou G. **2008**. Responses of leaf stomatal density to water status and its relationship with photosynthesis in a grass. *Journal of Experimental Botany* **59**: 3317–3325.

Tables

Table 2.1. Plant material analysed in the current work

Species	Accession number	Family	1C-value (pg)	Stage of the plant material used for analyses of: Stomata	CO_2	Origin*
FAMILY LILIACEAE						
Fritillaria* subgenus *Fritillaria						
F. frankiorum	LH 091	Liliaceae	60.14	Juvenile	Juvenile	LH
F. meleagris	2008-1307; MYF1 2013	Liliaceae	47.3	Juvenile and adult	Juvenile	RBG, Kew
F. pallidiflora	LH 452	Liliaceae	43.7	Juvenile	Juvenile	LH
F. ruthenica	2004-3479	Liliaceae	51.1	Juvenile	Juvenile	RBG, Kew
F. thunbergii	2002-141	Liliaceae	38.9	Juvenile	Juvenile	RBG, Kew
F. uva-vulpis	1958-42603	Liliaceae	89.2	Juvenile and adult	Juvenile	RBG, Kew
Fritillaria* subgenus *Japonica						
F. amabilis	LH 855	Liliaceae	90.71	Juvenile	Juvenile	LH
F. ayakoana	LH 784	Liliaceae	89.8	Juvenile	Juvenile	LH
Fritillaria* subgenus *Rhinopetalum						
F. stenanthera	1995-4414	Liliaceae	48.2	Juvenile	Juvenile	RBG, Kew
Fritllaria* subgenus *Petilium						
F. eduardii	Juvenile:1992-27 Adult: 2008-1309	Liliaceae	41	Juvenile and adult	Juvenile and adult	RBG, Kew
F. raddeana	RAD; 2012	Liliaceae	45.55	Adult	Adult	RBG, Kew
Fritillaria* subgenus *Korolkovia						
F. sewerzowii	2004-3480	Liliaceae	42.3	Juvenile	Juvenile	RBG, Kew
Fritillaria* subgenus *Theresia						
F. persica	Juvenile: 2008-793 Adult: PERA	Liliaceae	39.9	Juvenile and adult	Juvenile and adult	RBG, Kew
Fritillaria* subgenus *Davidii						
F. davidii	LH 044	Liliaceae	31.1	Juvenile	Juvenile	LH
Fritillaria* subgenus *Liliorhiza						
F. affinis	2014-1439	Liliaceae	45.6	Juvenile	Juvenile	RBG, Kew
F. camschatcensis	LH 617	Liliaceae	37.41	Juvenile	Juvenile	LH
FAMILY MELANTHIACEAE						
Paris japonica	1981-518	Melanthiaceae	152.2	Adult	Adult	RBG, Kew

Pseudotrillium rivale	1991-518	Melanthiaceae	27.51	Adult	Adult	RBG, Kew
Stenanthium gramineum	2010-1005	Melanthiaceae	1.68	Adult	Adult	RBG, Kew

* LH = Laurence Hill; RBG, Kew = Royal Botanic Gardens, Kew

Table 2.2. Average and standard deviation (SD) of stomatal length and density for all species of *Fritillaria* and Melanthiaceae analysed (AB = abaxial side; AD = adaxial side; n = number of specimens).

		Stomatal length (μ m)		Stomatal density (stomata/mm^2)	
Species	n	AB	AD	AB	AD
F. affinis	2	83.10±4.44	-	46±3.00	-
F. amabilis	3	95.24±6.01	-	33.33±2.87	-
F. ayakoana	3	86.20±8.66	-	37.33±9.74	-
F. camschatcensis	3	98.07±8.20	-	24.40±8.71	-
F. davidii	3	99.06±5.16	-	23.67±2.36	-
F. eduardii juvenile	3	81.42±11.40	68.60±4.92	23.33±6.18	17.00±2.83
F. eduardii adult	3	54.69±5.50	51.93±3.19	38.67±6.65	23.33±5.56
F. frankiorum	3	99.47±6.49	89.35±4.00	25.34±7.01	18.78±3.70
F. meleagris juvenile	3	95.04±2.34	80.63±3.61	22.27±0.90	17.20±2.97
F. meleagris adult	3	85.73±4.00	70.59±2.60	27.12±2.10	20.32±4.72
F. pallidiflora	3	49.19±4.38	44.55±2.99	52.00±5.35	29.00±0.82
F. persica juvenile	3	105.38±11.32	97.35±11.70	20.91±0.27	24.34±5.24
F. persica adult	3	72.47±3.39	72.21±4.66	35.13±1.83	37.09±8.02
F. raddeana	3	88.84±8.43	76.20±4.00	22.98±1.77	18.40±1.08
F. ruthenica	3	66.57±1.38	-	54.67±4.64	-
F. sewerzowii	2	69.43±5.35	60.89±4.88	23.00±4.52	24.00±3.10
F. stenantera	3	88.44±6.02	97.83±6.17	27.42±0.46	21.27±1.24

F. thunbergii	3	68.44±2.27	-	68.75±12.70	-
F. uva-vulpis juvenile	4	90.84±8.12	80.68±7.96	20.67±3.15	18.3±3.09
F. uva-vulpis adult	3	87.36±6.74	71.87±5.52	33.93±5.17	30.71±6.10
Paris japonica	3	90.35±5.25	-	28.95±2.20	-
Pseudotrillium rivale	3	78.24±1.6	-	31.05±4.81	-
Stenanthium gramineum	2	36.50±0.10	44.94±11.86	43.50±1.50	20.50±2.50

Table 2.3 Average and standard deviation of photosynthetic parameters for all species of *Fritillaria* and Melanthiaceae analysed (n = number of specimens).

Species	n	Phase	A_{max}	V_{cmax}	J_{max}	g_s	C_i	R_d
F. affinis	5	Juvenile	28.6±1.2	86.3±8.1	169.7±6.4	75.1±15.9	174.2±20.4	3.7±0.4
F. amabilis	5	Juvenile	28.3±1.9	63.3±2.8	156.8±15.0	143.6±43.1	242.6±22.8	2.1±0.6
F. ayakoana	3	Juvenile	28.3±1.9	71.5±16.3	141.9±21.3	132.3±40.3	219.1±41.6	1.3±0.8
F. camschatcensis	5	Juvenile	21.0±2.3	54.0±12.1	110.5±14.3	50.5±11.7	1870.3±30.5	2.3±1.2
F. davidii	5	Juvenile	22.6±1.6	44.9±3.3	118.2±7.7	66.4±15.4	222.1±23.8	1.9±0.4
F. eduardii	3	Juvenile	35.9±4.2	83.0±6.8	183.8±28.3	171.0±24.8	229.0±17.5	1.6±0.6
F. eduardii	3	Adult	22.3±2.5	58.8±7.4	118.6±11.3	88.7±10.7	210.1±19.3	1.7±0.1
F. frankiorum	3	Juvenile	31.7±1.3	83.3±2.8	178.6±15.3	71.6±22.3	163.1±24.1	2.9±0.5
F. meleagris	6	Juvenile	32.2±3.5	78.5±7.3	174.7±21.3	115.1±26.8	201.8±27.1	2.4±0.4
F. pallidiflora	5	Juvenile	27.6±2.7	73.8±12.9	155.2±25.2	130.7±30.9	218.9±21.2	2.8±1.4
F. persica	3	Juvenile	29.8±0.6	62.9±7.1	168.5±17.1	238.5±22.9	295.7±11.7	2.4±0.6

F. persica	3	Adult	40.7±7.8	140.8±40.1	235.4±50.9	99.6±57.1	164.4±28.3	3.3±0.7
F. raddeana	3	Adult	31.9±3.4	77.5±13.4	173.3±21.8	158.6±38.2	237.4±36.3	2.0±0.5
F. ruthenica	4	Juvenile	41.6±5.9	91.1±11.3	212.4±31.6	177.8±31.5	221.3±17.5	1.5±0.8
F. sewerzowii	5	Juvenile	33.8±1.9	84.8±4.5	187.0±8.8	212.3±51.4	242.2±20.2	1.8±0.5
F. stenantera	3	Juvenile	34.7±2.7	91.7±2.2	182.3±18.7	348.1±24.8	270.6±7.4	0.8±0.7
F. thunbergii	3	Juvenile	39.7±2.5	78.2±7.1	214.9±20.4	207.6±14.5	251.5±9.5	1.1±0.7
F. uva-vulpis	6	Juvenile	20.0±2.5	45.5±5.3	105.3±15.0	94.5±21.8	240.1±18.0	1.9±0.4
Paris japonica	5	Adult	22.31.8	43.8±3.3	117.4±7.1	58.8±10.4	218.1±26.1	2.1±0.5
Pseudotrillium rivale	3	Adult	25.5±3.6	52.5±4.5	133.7±20.8	194.9±61.7	284.5±15.2	1.5±0.4
Stenanthium gramineum	7	Adult	41.3±7.7	87.0±6.7	181.8±12.1	249.4±58.0	246.4±20.4	1.7±1.0

Table 2.4 Average and standard deviation of fluorescence parameters for all species of *Fritillaria* and Melanthiaceae analysed (n = number of specimens).

Species	n	Phase	Fv/Fm	qP	NPQ	rETR	Ek
F. affinis	5	Juvenile	0.802±0.010	0.641±0.040	1.523±0.135	24.95±4.13	251.90±35.44
F. amabilis	5	Juvenile	0.776±0.006	0.654±0.034	1.862±0.272	29.09±4.11	276.49±22.08
F. ayakoana	3	Juvenile	0.788±0.014	0.641±0.074	1.762±0.136	25.55±7.59	246.32±89.99
F. camschatcensis	5	Juvenile	0.748±0.023	0.509±0.035	1.453±0.195	21.03±2.15	280.85±22.51
F. davidii	4	Juvenile	0.785±0.004	0.383±0.063	1.201±0.316	24.65±2.71	246.06±10.52
F. eduardii	3	Juvenile	0.785±0.014	0.640±0.030	2.244±0.512	30.03±1.04	278.54±17.02
F. eduardii	3	Adult	0.746±0.019	0.633±0.065	2.026±0.441	25.16±5.06	238.63±41.08
F. frankiorum	3	Juvenile	0.795±0.004	0.517±0.025	1.489±0.231	24.93±3.59	291.75±54.43
F. meleagris	5	Juvenile	0.797±0.004	0.599±0.038	1.655±0.116	33.66±3.29	295.61±21.52
F. pallidiflora	5	Juvenile	0.784±0.015	0.680±0.057	1.741±0.194	26.79±4.39	270.71±24.75
F. persica	3	Juvenile	0.774±0.011	0.480±0.097	2.234±0.338	16.13±2.30	251.52±38.04
F. persica	3	Adult	0.777±0.006	0.707±0.015	1.348±0.227	39.22±3.44	391.87±5.86

F. raddeana	3	Adult	0.778±0.006	0.720±0.024	1.875±0.173	21.43±1.51	212.61±14.95
F. ruthenica	3	Juvenile	0.785±0.012	0.556±0.016	1.400±0.129	30.43±3.53	260.03±17.06
F. sewerzowii	5	Juvenile	0.796±0.018	0.611±0.030	1.884±0.224	34.79±4.75	376.12±51.19
F. stenantera	3	Juvenile	0.768±0.005	0.608±0.014	1.358±0.121	45.15±6.16	536.41±55.47
F. thunbergii	3	Juvenile	0.776±0.008	0.659±0.024	1.791±0.124	24.13±1.01	234.86±2.68
F. uva-vulpis	6	Juvenile	0.742±0.040	0.496±0.116	2.261±0.540	17.91±2.82	276.62±32.96
Paris japonica	5	Adult	0.784±0.019	0.459±0.042	1.954±0.387	14.42±3.89	288.50±57.10
Pseudotrillium rivale	3	Adult	0.715±0.028	0.586±0.031	2.087±0.127	14.00±0.98	226.64±7.24
Stenanthium gramineum	6	Adult	0.816±0.007	0.651±0.026	1.632±0.150	53.52±13.25	454.96±51.70

Table 2.5. Output of linear models used to explore the relationships between stomatal density, length, side of leaf (i.e. adaxial/abaxial) and phase of growth (i.e. juvenile/adult) in 16 species of *Fritillaria.*

(a) density ~ length + side + both sides of leaf

	Estimate	Std. Error	t-value	Pr(<|t|)
(Intercept)	77.682	5.0466	15.393	<0.0001
Stomatal length	-0.4315	0.0546	-7.901	<0.0001
Adaxial	-9.3349	2.0325	-4.593	<0.0001
Stomata on both sides	-13.0944	2.3912	-5.476	<0.0001

(b) length ~ side + both sides of leaf

	Estimate	Std. Error	t-value	Pr(<|t|)
(Intercept)	85.349	3.67	23.259	<0.0001
Adaxial	-8.155	3.765	-2.166	0.0329
Stomata on both sides	-2.274	4.533	-0.502	0.6172

(c) density ~ length + side + phase

	Estimate	Std. Error	t-value	Pr(<|t|)
(Intercept)	41.9163	5.8729	7.137	<0.0001
Stomatal length	-0.1192	0.0747	-1.596	0.1178
Adaxial	-5.2737	2.0126	-2.62	0.0121
Juvenile	-8.4679	2.2325	-3.793	0.0005

(d) length ~ side + phase

	Estimate	Std. Error	t-value	Pr(<|t|)
(Intercept)	75.606	3.261	23.187	<0.0001
Adaxial	-9.496	3.802	-2.498	0.0163
Juvenile	16.12	3.795	4.247	0.0001

Table 2.6. Linear models exploring the relationships between genome size (C-value), stomatal density and length and phase of leaf growth (juvenile and adult) in *Fritillaria.* (significant values are given in bold).

(a) log(density) ~ C-value + phase

	Estimate	Std. Error	t-value	Pr(<|t|)
(Intercept)	3.3783	0.12230	27.617	<0.0001
C-value	-0.0001	0.00200	-0.058	0.9540
Juvenile	-0.1377	0.08197	-1.680	0.0963

(b) log(length) ~ C-value + phase

	Estimate	Std. Error	t-value	Pr(<|t|)
(Intercept)	4.1202	0.0669	67.659	<0.0001
C-value	0.0017	0.0010	1.624	0.1080
Juvenile	0.2437	0.0408	5.973	**<0.0001**

Table 2.7. Linear models exploring the relationships between photosynthetic parameters (A_{max}, J_{max}, V_{cmax}, g_s, C_i and R_d) and stomatal characters in *Fritillaria* (significant values are highlighted in bold).

(a) A_{max} ~ stomatal density

	Estimate	Std. Error	t-value	Pr(<|t|)
(Intercept)	27.1671	1.8178	14.95	<0.0001
density	0.1242	0.0567	2.19	**0.0313**

(b) A_{max} ~ stomatal length

	Estimate	Std. Error	t-value	Pr(<|t|)
(Intercept)	33.031	3.67400	8.990	<0.0001
length	-0.028	0.00446	-0.627	0.5330

(c) V_{cmax} ~ stomatal density + phase

	Estimate	Std. Error	t-value	Pr(<|t|)
(Intercept)	76.4564	8.1282	9.406	<0.0001
density	0.3867	0.2003	1.931	0.0570
Juvenile	-15.1712	5.9609	-2.545	**0.0128**

(d) V_{cmax} ~ stomatal length + phase

	Estimate	Std. Error	t-value	Pr(<|t|)
(Intercept)	89.6864	13.4260	6.680	<0.0001
length	-0.0132	0.1950	-0.068	0.9462
Juvenile	-16.4631	7.5726	-2.174	**0.0326**

(e) J_{max} ~ stomatal density

	Estimate	Std. Error	t-value	Pr(<|t|)
(Intercept)	147.0503	10.7242	13.712	<0.0001
density	0.7011	0.3347	2.095	0**.0393**

(f) J_{max} ~ stomatal length

	Estimate	Std. Error	t-value	Pr(<|t|)
(Intercept)	181.2	21.6196	8.382	<0.0001
length	-0.171	0.2623	-0.652	0.5160

(g) g_s ~ stomatal density + phase

	Estimate	Std. Error	t-value	Pr(<|t|)
(Intercept)	113.6509	26.7476	4.249	<0.0001
density	0.2978	0.659	0.452	0.6525
Juvenile	35.7593	19.6155	1.772	0.0802

(h) g_s ~ stomatal length + phase

	Estimate	Std. Error	t-value	Pr(<|t|)
(Intercept)	140.7910	43.2022	3.259	<0.0001
length	-0.2760	0.6267	-0.440	0.6610
Juvenile	40.0036	24.3672	1.642	**0.01045**

(i) C_i ~ stomatal density + phase

	Estimate	Std. Error	t-value	Pr(<|t|)
(Intercept)	211.0140	14.1954	14.865	<0.0001
density	-0.0600	0.349	-0.181	0.8567
Juvenile	19.2291	10.41	1.847	0.0684

(j) C_i ~ stomatal length + phase

	Estimate	Std. Error	t-value	Pr(<|t|)
(Intercept)	212.5600	22.9273	9.271	<0.0001
length	-0.0561	0.333	-0.169	0.866
Juvenile	20.8084	12.9316	1.609	0.111

(k) R_d ~ stomatal density + phase

	Estimate	Std. Error	t-value	Pr(<|t|)
(Intercept)	2.5760	0.3228	7.980	<0.0001
density	-0.0022	0.0080	-0.275	0.7840
Juvenile	-0.5877	0.2370	-2.482	**0.0151**

(l) R_d ~ stomatal length + phase

	Estimate	Std. Error	t-value	Pr(<|t|)
(Intercept)	1.8267	0.5152	3.545	0.0006
length	0.0106	0.0075	1.426	0.1576
Juvenile	-0.828	0.2906	-2.852	**0.0060**

Table 2.8. Phylogenetic independent contrasts estimates with (A) stomatal length, (B) stomatal density, and (C) genome size as a function of the trait shown (significant values are highlighted in bold).

A. Stomatal length

	A_{max}	V_{cmax}	J_{max}	R_d	C_i	g_s	qP	NPQ	rETR	E_k
Slope	-0.159	-0.411	-0.502	0.005	-0.492	-1.720	-0.002	0.001	-0.327	-1.405
R^2	0.086	0.091	-0.005	-0.047	0.002	0.102	0.075	-0.060	0.281	0.032
p	0.119	0.112	0.355	0.673	0.325	0.099	0.135	0.900	**0.011**	0.224

B. Stomatal density

	Stomatal length	A_{max}	V_{cmax}	J_{max}	R_d	C_i	g_s	qP	NPQ	rETR	E_k
Slope	-0.427	0.3493	0.5965	0.201	-0.015	0.526	1.758	0.002	-0.002	0.099	-1.106
R^2	0.260	0.3649	0.1320	0.295	0.001	-0.017	0.042	0.026	-0.046	-0.040	-0.025
p	**0.015**	**0.0036**	0.0701	**0.009**	0.328	0.415	0.198	0.239	0.651	0.586	0.464

C. Genome size

	Stomatal length	Stomatal density	A_{max}	V_{cmax}	J_{max}	R_d	C_i	g_s	qP	NPQ	rETR	E_k
Slope	0.175	-0.053	-0.090	-0.231	-0.409	0.003	-0.291	-1.215	-0.001	0.002	-0.117	-0.328
R^2	0.120	-0.030	0.190	0.200	0.136	-0.040	0.056	0.380	0.254	0.007	0.180	-0.032
p	0.082	0.517	**0.036**	**0.031**	0.067	0.587	0.167	**0.003**	**0.016**	0.304	**0.040**	0.514

Table 2.9. Linear models exploring the relationships between chlorophyll fluorescence parameters (F_v/F_m, qP, NPQ, rETR, E_k) and stomatal characters in *Fritillaria,* (significant values are highlighted in bold).

(a) F_v/F_m~ stomatal density + phase

	Estimate	Std. Error	t-value	Pr(<|t|)
(Intercept)	0.7676	0.0063	121.72	<0.0001
density	0.0001	0.0002	0.828	0.41
Juvenile	0.0077	0.0047	1.649	0.103

(b) F_v/F_m ~ stomatal length + phase

	Estimate	Std. Error	t-value	Pr(<|t|)
(Intercept)	0.77	0.001	73.886	<0.0001
length	$-4.4x10^{-5}$	1.5×10^{-4}	-0.292	0.771
Juvenile	0.008	$5.7x10^{-3}$	1.44	0.154

(c) qP ~ stomatal density + phase

	Estimate	Std. Error	t-value	Pr(<|t|)
(Intercept)	0.648	0.029	22.26	<0.0001
density	0.0014	0.0007	1.934	0.0566
Juvenile	-0.128	0.0214	-6	**<0.0001**

(d) qP ~ stomatal length + phase

	Estimate	Std. Error	t-value	Pr(<|t|)
(Intercept)	0.726	0.048	15.154	<0.0001
length	-0.0005	0.0007	-0.762	0.448
Juvenile	-0.121	0.027	-4.492	**<0.0001**

(e) NPQ ~ stomatal density

	Estimate	Std. Error	t-value	Pr(<|t|)
(Intercept)	1.96	0.116	16.918	<0.0001
density	-0.007	0.004	-1.648	0.103

(f) NPQ ~ stomatal length + phase

	Estimate	Std. Error	t-value	Pr(<|t|)
(Intercept)	2.099	0.2412	8.703	<0.0001
length	-0.005	0.0035	-1.446	0.152
Juvenile	0.128	0.136	0.942	0.349

(g) rETR ~ stomatal density

	Estimate	Std. Error	t-value	Pr(<|t|)
(Intercept)	26.197	2.288	11.45	<0.0001
density	0.046	0.072	0.63	0.53

(h) rETR ~ stomatal length + phase

	Estimate	Std. Error	t-value	Pr(<|t|)
(Intercept)	31.958	4.924	6.491	<0.0001
length	-0.053	0.07	-0.759	0.45
Juvenile	-0.209	2.63	-0.079	0.937

(i) E_k ~ stomatal density

	Estimate	Std. Error	t-value	Pr(<|t|)

(Intercept)	319.16	22.73	14.04	<0.0001
density	-0.85	0.72	-1.188	0.238

(j) E_k ~ stomatal length

	Estimate	Std. Error	t-value	Pr(<|t|)
(Intercept)	239.7	47.02	5.097	<0.0001
length	0.6745	0.56	1.193	0.237

Table 2.10. Summary of the statistical significant results relating stomatal measurements and photosynthetic parameters after PIC analyses.

Stomatal length		Stomatal density	
	rETR	A_{max}	J_{max}
Slope	-0.327	0.3493	0.201
R^2	0.281	0.3649	0.295
p	**0.011**	**0.0036**	**0.009**

Table 2.11. Linear models exploring the relationships between photosynthetic parameters (A_{max}, J_{max}, V_{cmax}, g_s, C_i and R_d) and genome size (1C-value) in *Fritillaria.* (Significant values are highlighted in bold).

(a) $\log(A_{max})$ ~ 1C-value + phase

	Estimate	Std. Error	t-value	Pr(<|t|)
(Intercept)	3.594	0.062	56.029	<0.0001
1C-value	-0.0051	0.0012	-4.4	**<0.0001**
Juvenile	0.0578	0.0498	1.162	0.248

(b) $\log(V_{cmax})$ ~ 1C-value+ phase

	Estimate	Std. Error	t-value	Pr(<|t|)
(Intercept)	4.6121	0.0812	56.788	<0.0001
1C-value	-0.0054	0.0015	-3.649	**0.0004**
Juvenile	-0.0771	0.063	-1.224	0.22

(c) $\log(J_{max})$ ~ 1C-value

	Estimate	Std. Error	t-value	Pr(<|t|)
(Intercept)	5.334	0.0659	80.964	<0.0001
1C-value	-0.0052	0.0012	-4.355	**<0.0001**

(d) g_s ~ 1C-value + phase

	Estimate	Std. Error	t-value	Pr(<|t|)
(Intercept)	158.2	21.8283	7.248	<0.0001
1C-value	-0.887	0.3977	-2.23	**0.027**
Juvenile	38.2744	16.9379	2.26	**0.026**

(e) C_i ~ 1C-value + phase

	Estimate	Std. Error	t-value	Pr(<|t|)
(Intercept)	203.0644	11.6219	17.473	<0.0001
1C-value	0.1488	0.2118	0.703	0.484
Juvenile	14.0052	9.0182	1.553	0.123

(f) R_d ~ 1C-value + phase

	Estimate	Std. Error	t-value	Pr(<|t|)
(Intercept)	2.6054	0.2686	9.699	<0.0001
1C-value	-0.0024	0.0049	-0.502	0.6168
Juvenile	-0.442	0.208	-2.119	**0.0363**

Table 2.12. Linear models exploring relationships between chlorophyll fluorescence parameters (F_v/F_m, qP, NPQ, rETR, E_k) and genome size in *Fritillaria*. (Significant values are highlighted in bold).

(a) F_v/F_m~ 1C value + phase

	Estimate	Std. Error	t-value	Pr(<|t|)
(Intercept)	0.792	0.007	112.293	<0.0001
1C value	-0.0004	0.0001	-3.65	**0.0004**
Juvenile	0.012	0.006	2.161	**0.033**

(b) qP ~ 1C value + phase

	Estimate	Std. Error	t-value	Pr(<|t|)
(Intercept)	0.69	0.025	27.053	<0.0001
1C value	-2.5×10^{-5}	4.6×10^{-4}	-0.055	0.956
Juvenile	-0.12	0.02	-5.91	**<0.0001**

(c) NPQ ~ 1C value

	Estimate	Std. Error	t-value	Pr(<|t|)
(Intercept)	1.44	0.116	12.427	<0.0001
1C value	0.007	0.002	3.123	**0.0023**

(d) rETR ~ 1C value

	Estimate	Std. Error	t-value	Pr(<|t|)
(Intercept)	33.71	2.29	14.731	<0.0001
1C value	-0.117	0.041	-2.818	**0.0058**

(e) E_k ~ 1C value + phase

	Estimate	Std. Error	t-value	Pr(<|t|)
(Intercept)	303.46	24.02	12.64	<0.0001
1C value	-0.6124	0.43	-1.41	0.16
Juvenile	33.18	18.94	1.752	0.083

Table 2.13. Summary of the statistical significant results relating genome size and photosynthetic parameters after PIC analyses.

Genome size					
	A_{max}	V_{cmax}	g_s	qP	rETR
Slope	-0.090	-0.231	-1.215	-0.001	-0.117
R^2	0.190	0.200	0.380	0.254	0.180
p	**0.036**	**0.031**	**0.003**	**0.016**	**0.040**

Chapter 3. The influence of genome size and ploidy level on stomatal size and chlorophyll fluorescence in *Nymphaea* (water lilies)

Summary

Introduction: Nymphaeales is an early diverging angiosperm group representing the water lily lineage and comprises three families, Hydatellaceae, Cabombaceae and Nymphaeaceae. Nymphaeaceae is the most species-rich family in the order, with five genera; *Nymphaea* is the most diverse genus, containing 54 species and five subgenera. *Nymphaea* includes the species with the smallest genome sizes and the highest chromosome range amongst Nymphaeaceae, in which the ploidy level varies from 2n=2x to 2n=16x (Pellicer *et al.*, 2013). This chapter aims to determine if there is a relationship between genome size (GS) and/or ploidy level and stomatal size and photosynthetic measures. It has been proposed that polyploidy can impact photosynthesis because polyploidy may influence the anatomical properties of the leaf through cell size scaling or though intracellular aspects.

Methods: The approaches used were (i) pulse amplitude modulation (PAM) fluorometry to gain insights into the efficiency of light energy harvesting for photosynthesis, (ii) stomatal measurements (size and density), and (iii) length of palisade cells, number of chloroplasts and length of chloroplasts.

Results: Linear modelling revealed significant ($p<0.05$) positive relationships between GS and ploidy level and guard cell length, although stomatal density was not significantly related to GS or ploidy. Maximum relative electron transport rate (rETR) was negatively associated to ploidy and stomatal length, while maximum quantum efficiency of photosystem II (F_v/F_m) was positively related to ploidy and stomatal length. Non-photochemical quenching (NPQ) was positively related to stomatal density. Chlorophyll fluorescence parameters were not significantly related to GS. The number of chloroplasts significantly increased in higher ploidy level cells and in longer cells, and the length of palisade cells is positively related to ploidy. rETR is significantly negatively associated with length of palisade cells and number of chloroplasts.

Discussion: Stomatal length and GS and stomatal length and ploidy level have positive strong relationships, reflecting the influence of GS on cell size. The negative relationship between rETR and ploidy level may reflects the association between rETR and cell size, since rETR is also negatively related to guard cell length, ploidy and palisade cell length, and guard cell length is strongly related to rETR and ploidy. F_v/F_m

is positively associated with ploidy and guard cell length, which indicates a higher efficient of photochemical conversions in higher ploidy levels and in plants with longer guard cells.

Introduction

Nymphaeales (i.e. the water lily lineage) is an early diverging angiosperm group comprising three families Hydatellaceae, Cabombaceae and Nymphaeaceae and ~80 species. Nymphaeaceae is the most species-rich family in the order, with five genera, these being; *Nymphaea* (= the most diverse genus, containing 54 species and five subgenera), *Nuphar* (= 8 species), *Barclaya* (4 species), *Victoria* (2 species) and *Euryale* (1 species) (Qiu *et al.*, 2010). *Nymphaea* includes the species with the smallest GS and has the highest chromosome number range amongst Nymphaeaceae, with ploidy levels ranging from 2n=2x to 2n=16x (Pellicer *et al.*, 2013).

This chapter aims to determine if there is a relationship between GS and/or ploidy level and stomatal size and photosynthetic measures, to build on Chapter 2's analysis of these relationships in *Fritillaria* and Melanthiaceae. *Nymphaea* species were chosen for comparison because: (1) they are from a lineage that diverged from the remaining angiosperms in the late Jurassic (ca. 140 Mya, The Angiopserm Phylogeny Group, 2016), presenting us with data that can be used to make evolutionary inferences relating to photosynthesis and genome size; (2) species in Nymphaeaceae have a range of ploidy levels, enabling determination of the effect of polyploidy (i.e. genome doubling) on these measures; (3) all species have similar life strategies, all being aquatic and are grown under similar conditions (light, water, nutrients etc.). It is known that *Nymphaea* is a sun-loving plant genus capable of maintaining high rates of photosynthesis in high irradiance (Ritchie, 2012) and their leaves float on the surface of water, whilst the stem and rhizome are below water. These leaves have a large aerenchyma (open spaces between cells), which makes them float (Ritchie, 2012). The adaxial surface of the leaf has many stomata, meaning that there is gas exchange with the air.

It has been proposed that polyploidy may impact photosynthesis because polyploidy can influence the anatomical properties of the leaf through cell size scaling, which in turn may influence biochemical and physiological properties of the leaf, for example, through different rates of CO_2 diffusion (Dornhoff & Shibles, 1976; Warner & Edwards, 1993; Romero-Aranda *et al.*, 1997). Polyploidy may also impact photosynthetic capacity through intracellular effects (e.g. size and number of chloroplasts) (Jellings & Leech, 1984). Polyploidy may alter photosynthetic capacity if it results in altered resistance to CO_2 diffusion (e.g. cell size) or cell biochemistry (Warner & Edwards, 1993).

Previous studies of tall fescue (*Festuca arundinacea* - Poaceae) have shown that an

increase in ploidy levels from 4x-10x is associated with an increase in CO_2 exchange rate, which may be related to increased RuBisCO and chlorophyll concentrations (Randall *et al.*, 1977; Joseph *et al.*, 1981). In contrast, recent studies in *Fragaria* species have revealed that increased ploidal level is associated with a decrease in CO_2 uptake (Gao *et al.*, 2017). Photosynthetic capacity is negatively related to mesophyll cell volume in genotypes of wheat that differ in ploidy level (and genome size), with higher ploidal genotypes having larger mesophyll volumes (Jellings & Leech, 1984). These data are in line with the negative relationship observed between genome size and photosynthetic characters in *Fritillaria* and species in Melanthiaceae, particularly A_{max}, V_{cmax}, g_s, F_v/F_m and ETR_{max} (Chapter 2).

There are not many studies that have analysed the relationship between ploidy level and chlorophyll fluorescence parameters, although Greer *et al.* (2017) suggested quantum efficiency may be reduced in diploids compared with triploids of quaking aspen (*Populus tremuloides*), whereas no significant increase in electron transport rate was observed. To build on these data, the approach taken in this study was to investigate fluorescence characters of photosynthesis using pulse amplitude modulation (PAM) fluorometry, and to compare the data with measures of stomatal length and density, measures of genome size and ploidy level, and measures of palisade cells and chloroplasts. Nine species of *Nymphaea* were studied, together with *Victoria cruziana* (Nymphaeaceae) (which together with *Euryale* comprise the sister lineage to *Nymphaea*), with the largest 1C-value in this study (1C=4.1pg), and *Brasenia schreberi* (Cabombaceae) was included as an outgroup.

Material and methods

Plant material, genome size and ploidy

Data were collected from nine species of *Nymphaea* (including representatives from each of the five subgenera), *Victoria cruziana* and *Brasenia schreberi* (Table 3.1). The material studied was obtained from the RBG Kew Living Collections. Photosynthetic measurements were taken during July, November and December of 2015 and 2016, between 8 and 12 pm (Table 3.1). A minimum of 3 replicates per species was used for collection of photosynthetic data (Table 3.4). All plants were grown in a glass house under natural light supplemented with artificial light (Figure 3.1) in tanks with filtered water. The artificial light was automatically switched on and off between 6 am and 7 pm depending on the intensity of the natural light and temperature kept at 30˚C inside water and 25˚C outside. The irradiance of the light was measured with LI-190R (Li-Cor Biosciences, Lincoln, NE, USA) at the start of the experiment.

Estimates of 1C-value and ploidy level were compiled from published data (Pellicer *et al.* (2013), see Table 3.1). Nine out of the 11 species studied in this work were based on the same accessions as used to estimate GS and ploidal level.

Chlorophyll fluorescence

Chlorophyll fluorescence data were collected as described in Chapter 2. This required developing Junior-PAM methods for aquatics. A floating foam box was used over a floating sheet of foam and the water -lily leaf and the Junior-PAM placed between the two (Fig. 3.1). The box covered the leaf and the Junior-PAM while chlorophyll fluorescence readings were obtained. Leaves were dark-adapted for 30 minutes before measurements with the box on top of them.

Figure 3.1. Water lilies leaves in a tank at RBG Kew. Fluorescence measurements are being conducted on one of the leaves.

Stomatal measurements

Stomatal density and length were determined by measuring stomata from the centre of the leaf adjacent to the central vein form the adaxial surface, since these species have stomata only on this surface. Leaf peels and impressions derived using nail varnish (Hilu & Randall, 1984) were made as described in Chapter 2. The number of individuals analysed per species is given in Table 3.2.

Ultrastructure of chloroplasts and length of palisade cells

The same region of the leaf as for “Stomatal measurements” was used for length of palisade cells, number of chloroplasts in the palisade cells and length of chloroplasts. An area of leaf about 0.5 cm^2 in size was kept in Formalin-Acetic-Alcohol (FAA) and left for up to one month at 4 °C. Fixed samples were dehydrated through graded ethanol series and then into a series of ethanol:resin solutions before being placed into 100% resin. Specimens were transferred into gelatine capsules for polymerisation. The resin was polymerised, between 58-60°C at 440mmHg, for 18 to 24 hours. Ultrathin sections were made with a Reichert-Jung Ultracut E ultramicrotome (Leica, Vienna, Austria) and stained with aqueous solution of uranyl acetate for 30 min and lead citrate for 5 min. A H-7650 transmission electron microscope (TEM, Hitachi H-7650) was used to image chloroplasts in the sectioned material. At least 30 measurements of each character were taken from three sections of the same leaf. The figures are 2D images of transverse sections of the leaf. The number of chloroplasts in each cell was counted from these images, the number reflecting only those chloroplasts that fall in the section, as previously reported for chloroplast numbers in mesophyll cells (Dong *et al.*, 2017).

Phylogenetic tree and statistical analyses

A phylogenetic tree of Nymphaeales using DNA sequence data taken from Pellicer *et al.* (2013) was modified to account for species representation here (Figure 3.2). The data were statistically analysed in R with linear models (LMs) as explained in the previous chapter. LMs use individual values for analyses, whilst PICs use the average values per species. Light intensities at the start of the experiment and the date of collection (called “season” in the analyses) were considered in the models as fixed effects, but light intensities had no influence on the results, while season had some effect in some LMs.

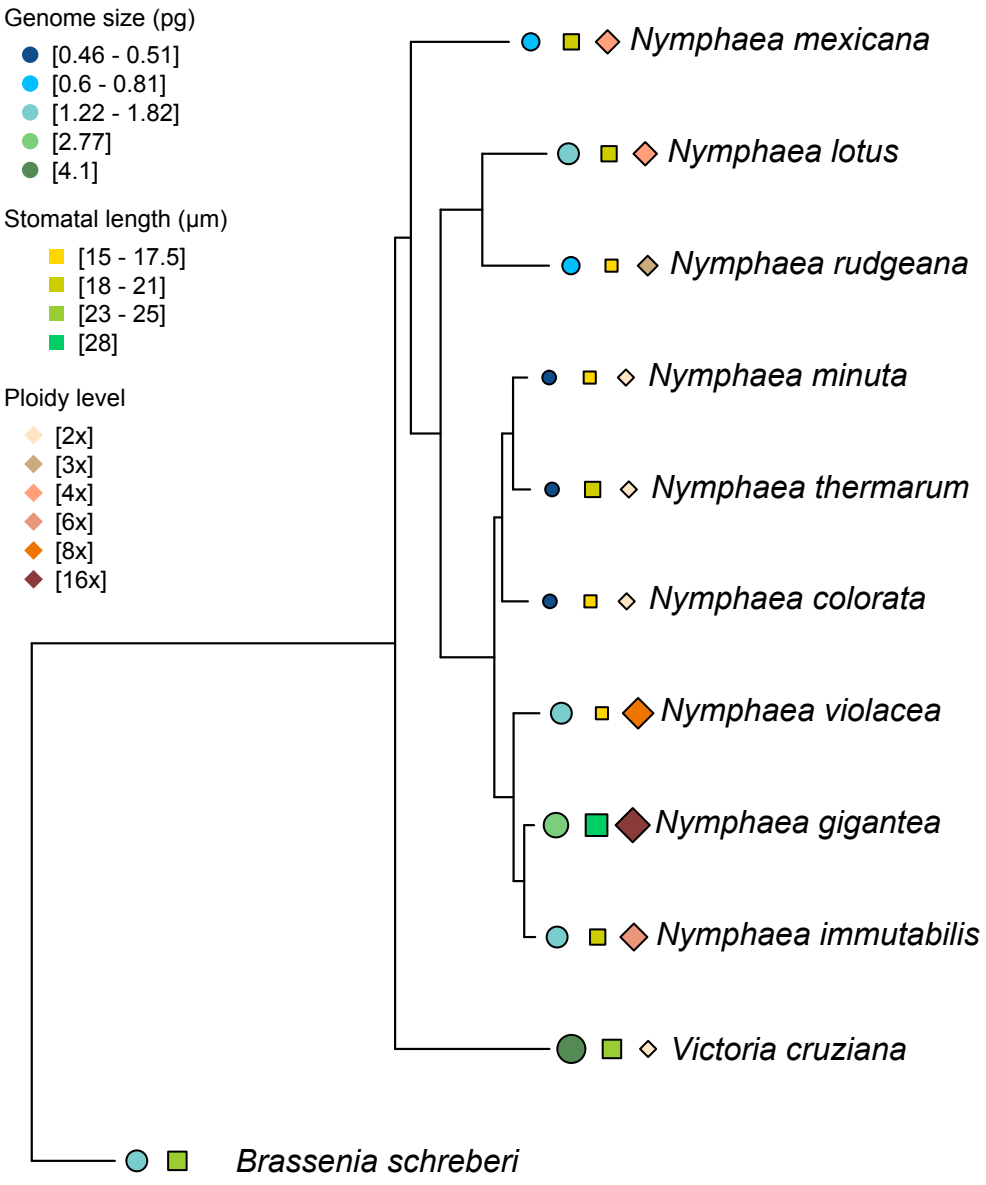

Figure 3.2. Phylogenetic tree of Nymphaeaceae and the outgroup *Brasenia schreberi* showing the distribution of genome sizes (C-values), stomatal length and ploidy level variation among species.

Results

Stomatal length and density in Nymphaea

Figure 3.3 shows the range in lengths and densities of stomata across the studied species. Stomatal lengths for *Nymphaea* species ranged from 15 to 28 µm (Table 3.2, Figure 3.3), while the stomatal density varied from 339 stomata/mm^2 in *N. thermarum* to 944 stomata/mm^2 in *N. minuta* (Table 3.2, Figure 3.3), which is an almost 3-fold range. Plotting stomatal length against stomatal density suggests there is a negative relationship, but when considering phylogenetic relationships (phylogenetic independent contrasts - PICs) between species, that relationship was shown to be non-significant (Tables 3.3a, 4b, Figures 3.4A, B).

Genome size, ploidy and stomatal length and density

There was a 6-fold range in genome size in *Nymphaea* species studied (0.46 pg/1C-to 2.77 pg/1C-value) and an 8-fold range in ploidy level (2n=2x to 2n=16x). There was a significant positive relationship between genome size and stomatal length, including when phylogenetic relationships were considered ($p<0.001$, $R^2=0.41$, Tables 3.3B, 4A Figures 3.4C, D). Stomatal lengths were similarly positively correlated with ploidy level ($p<0.0001$, $R^2=0.56$, Tables 3.3c, 4b, Figures 3.4E, F), probably because ploidy is strongly significantly correlated with genome size ($p<0.05$, $R^2=0.59$, Tables 3.3f, 4a, Figure 3.5). Stomatal density was negatively correlated with genome size and ploidal level, although the relationship was not significant.

Chlorophyll fluorescence characteristics

Figure 3.6 shows the RLCs for all species with rETR dependent on PAR (i.e. light intensities). rETR values varied between 29.3 electrons $m^{-2}s^{-1}$ in *Nymphaea gigantea* and 53.1 electrons $m^{-2}s^{-1}$ in *N. colorata* in *Nymphaea* group (Table 3.6). *Brasenia schreberi* had the highest average value of rETR (=73.8 electrons $m^{-2}s^{-1}$) and *Victoria cruziana* the second highest one (=61.7 electrons $m^{-2}s^{-1}$) (Table 3.6). Only rETR of *N. lotus* reached a plateau. Interestingly, *N. lotus* had the lowest values of NPQ with average of 0.319, while all the other species had mean values of NPQ above 0.7, with the highest value being 1.211 in *N. minuta* (Figure 3.7, Table 3.6).

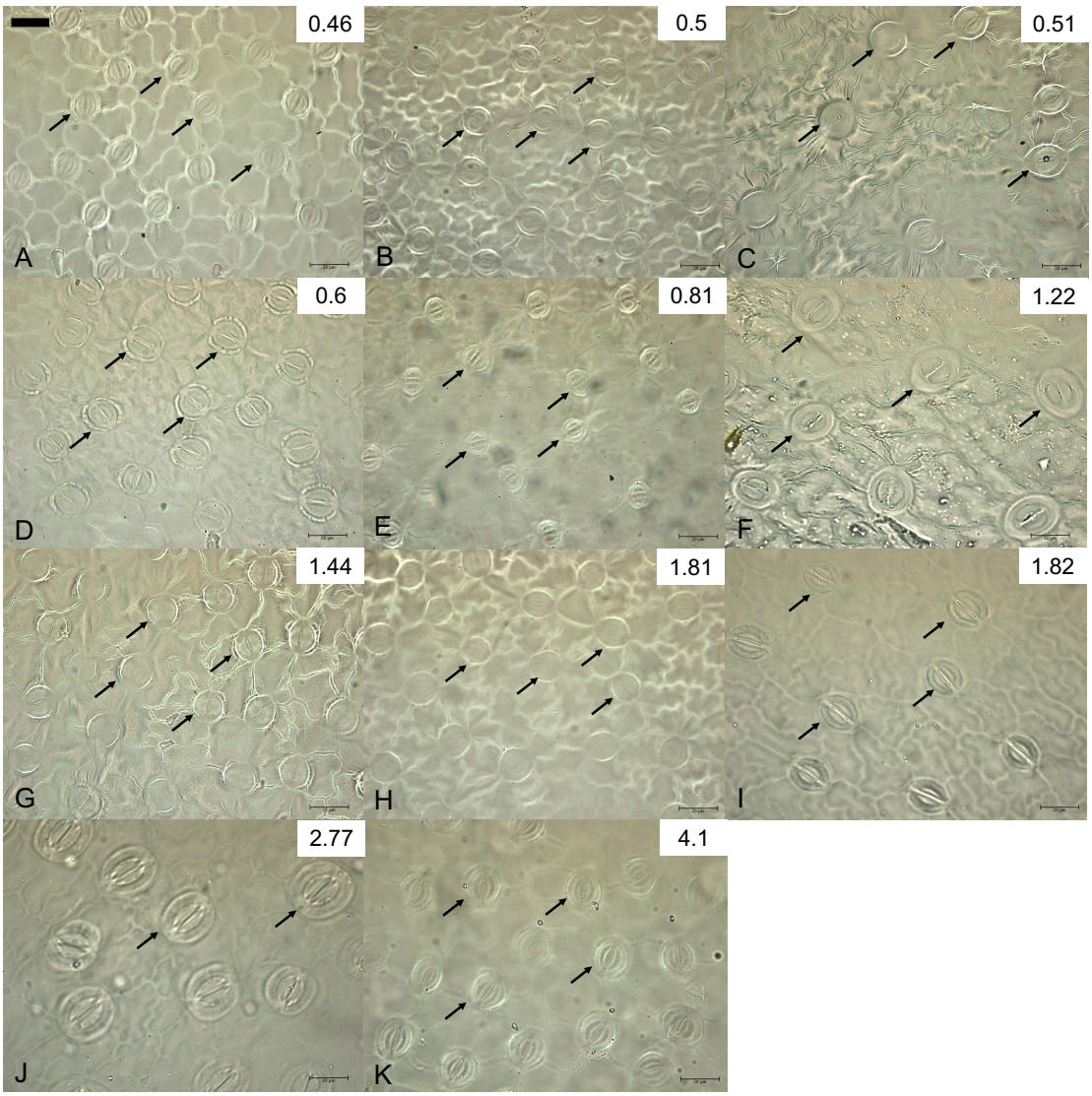

Figure 3.3. Adaxial leaf surfaces with evident stomata of (A) *Nymphaea minuta*, (B) *N. colorata*, (C) *N. thermarum*, (D) *N. mexicana*, (E) *N. rudgeana*, (F) *Brasenia schreberi*, (G) *N. immutabilis*, (H) *N. violaceae*, (I) *N. lotus* var. *dentata*, (J) *N. gigantea* and (K) *Victoria cruziana* arranged in increasing 1C genome size (given top right in each figure). All species shown at the same magnification, black bar in (A) = 20 μm. A selection of stomata is arrowed.

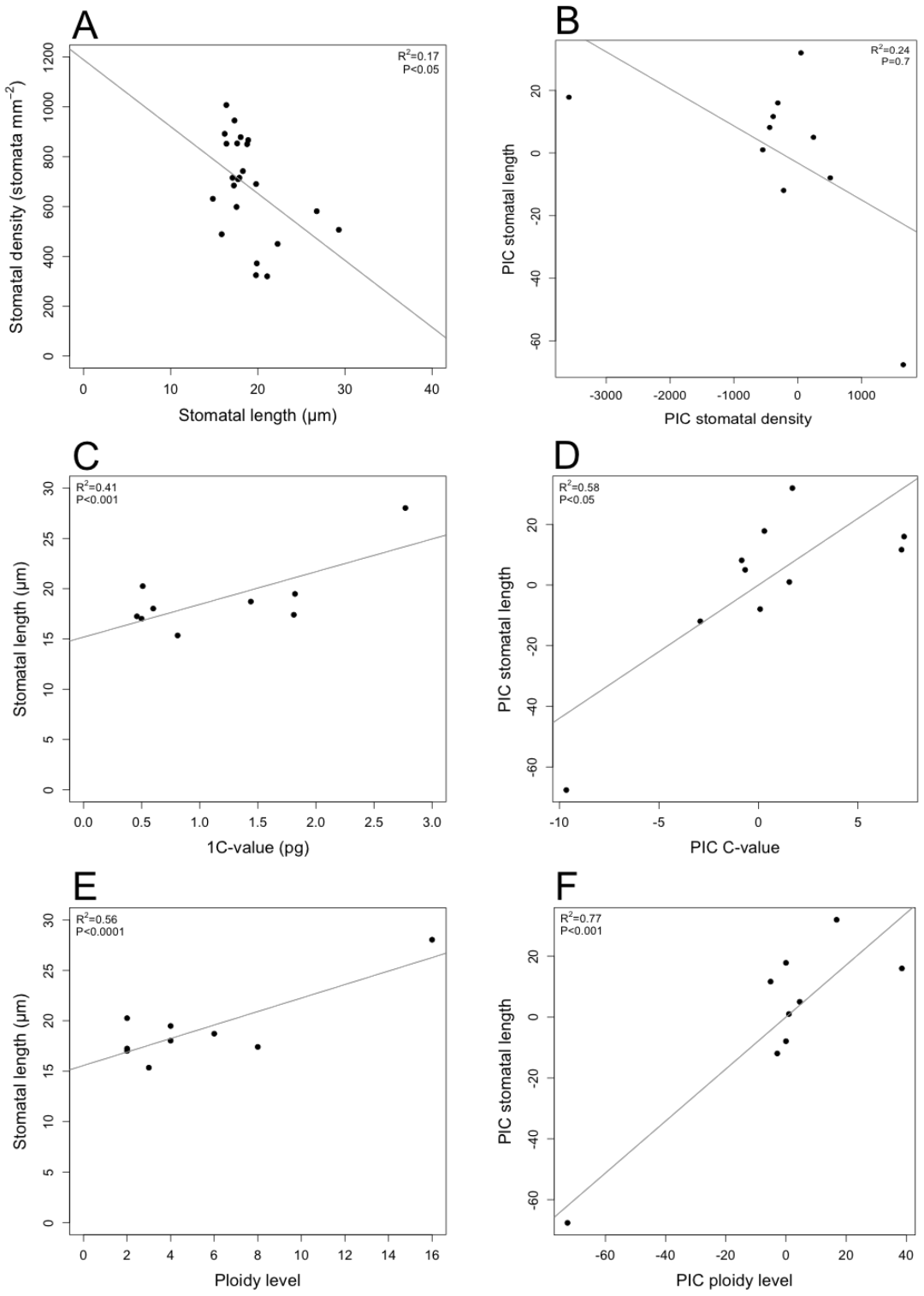

Figure 3.4. Scatter plots showing the relationships between stomata characters and genome size and ploidy level and their respective phylogenetic independent contrasts (PIC). (A) Stomatal length and density of all individuals of *Nymphaea*, each point is an individual measure; (B) PICs of genome size and stomatal length correlated; (C) GS and average values of stomatal length in *Nymphaea*; (D) PICs of (C); (E) ploidy level and average values of stomatal length in *Nymphaea*, and (F) PICs of (E).

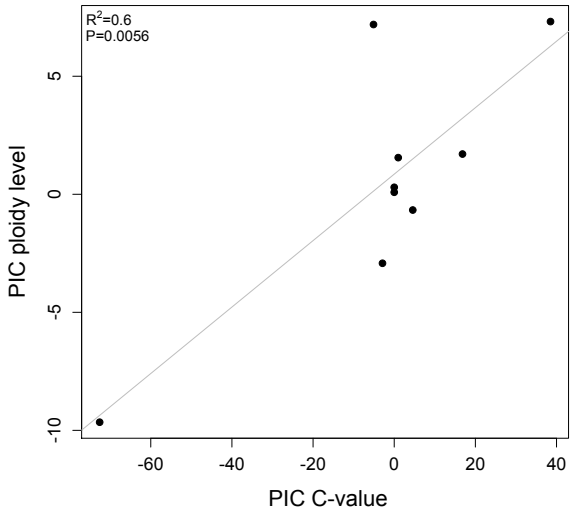

Figure 3.5. Scatter plot showing the phylogenetic independent contrasts (PIC) relationship between genome size (C-value) and ploidy level.

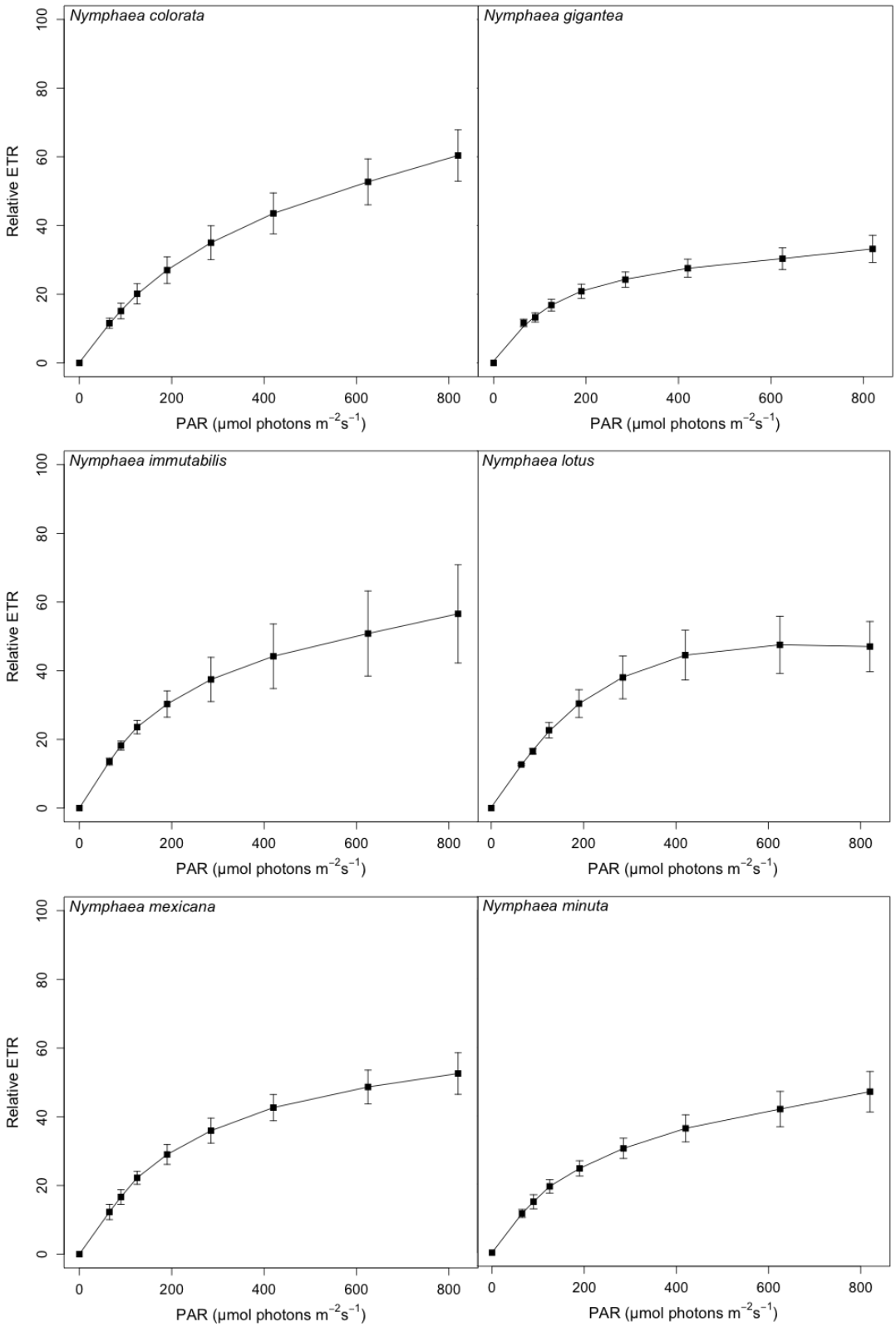

Figure 3.6. Rapid light curves showing rETR dependent on PAR for all species studied. Each point is a mean and the error bars are the standard deviation (SD).

Figure 3.6. (continued)

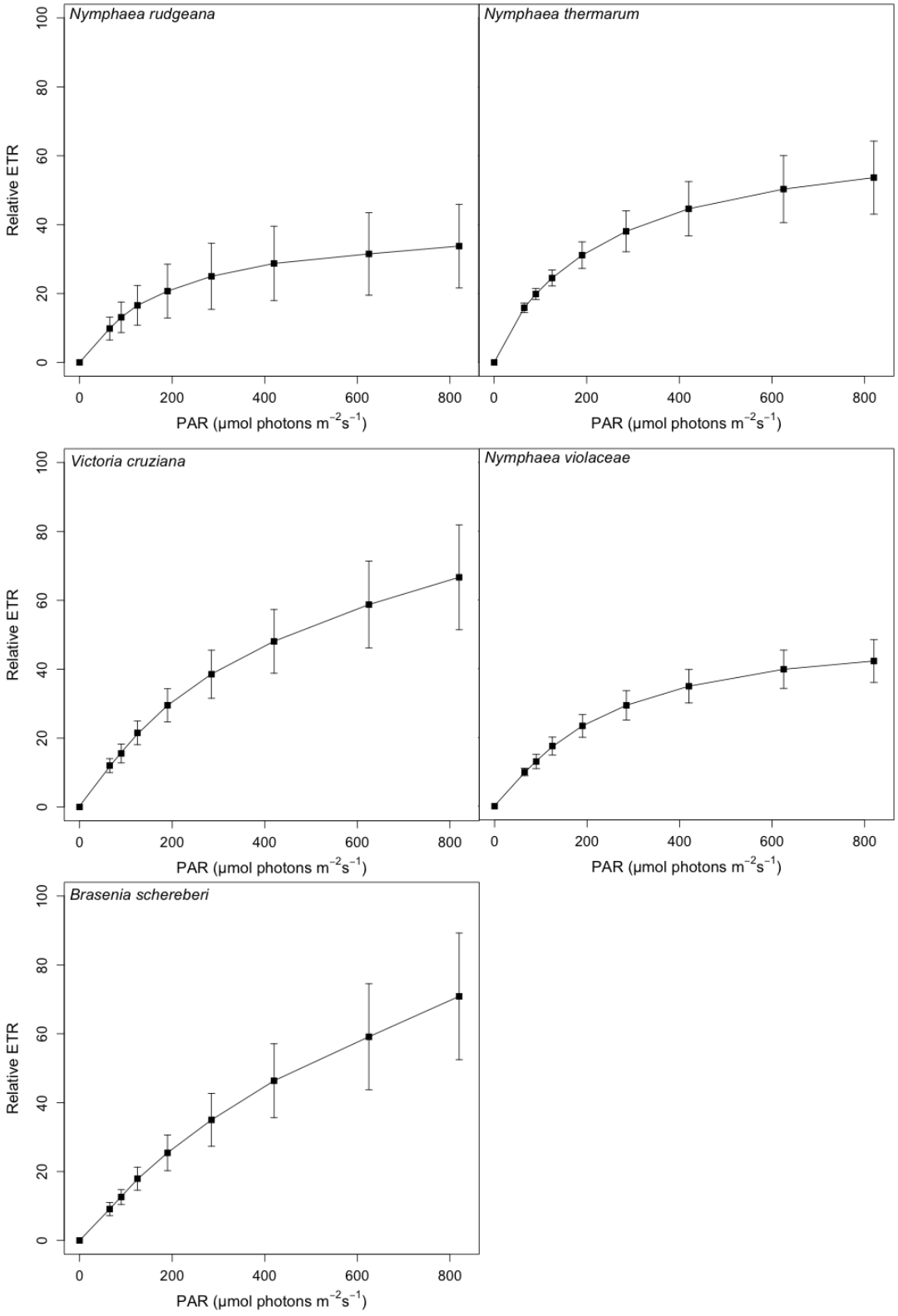

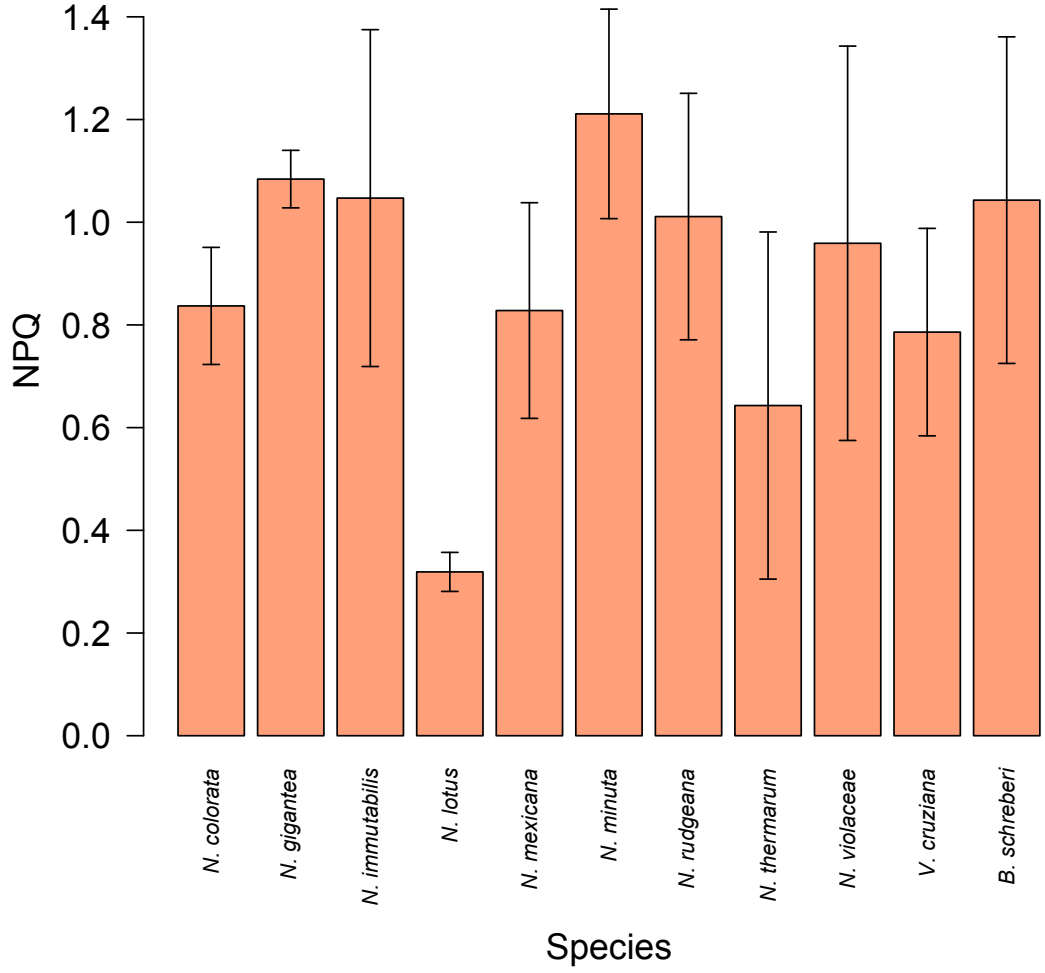

Figure 3.7. NPQ for all species analysed. Averages and standard deviations are given.

Chlorophyll fluorescence and stomatal length and density

Chlorophyll fluorescence parameters were compared with stomatal lengths and densities using PICs (Table 3.4) and LMs (Table 3.5). Using PICs, the results showed there was a positive relationship between stomatal length and F_v/F_m ($p<0.05$, $R^2=0.45$, Table 3.4c) and a negative relationship between stomatal length and rETR ($p<0.05$, $R^2=0.38$, Table 3.4c). Stomatal density and NPQ are significantly and positively related to each other ($p<0.05$, $R^2=0.34$, Table 3.4d). The measure qP is not significantly related with stomatal length or stomatal density, although both are related to E_k using LM (Table 3.5), a correlation that is lost when factoring in phylogenetic relationships using PICs (Table 3.4). Using PICs, stomatal density is close to being significantly negatively correlated with F_v/F_m ($p=0.0504$, $R^2=0.29$, Table 3.4d).

Chlorophyll fluorescence, genome size and ploidy

Average and standard deviation for all chlorophyll fluorescence parameters are presented in Table 3.6 for the species studied. PICs analyses showed a significant negative relationship between rETR and ploidy level ($p<0.05$, $R^2=0.68$, Tables 3.7h, 4b, Figure 3.8), while F_v/F_m was found to be significantly and positive related to ploidy level ($p<0.05$, $R^2=0.45$, Table 3.4b). Despite a relationship between genome size and ploidy level and between ploidy level and chlorophyll fluorescence parameters (see above), none of the chlorophyll parameters were statistically significant in relation to genome size.

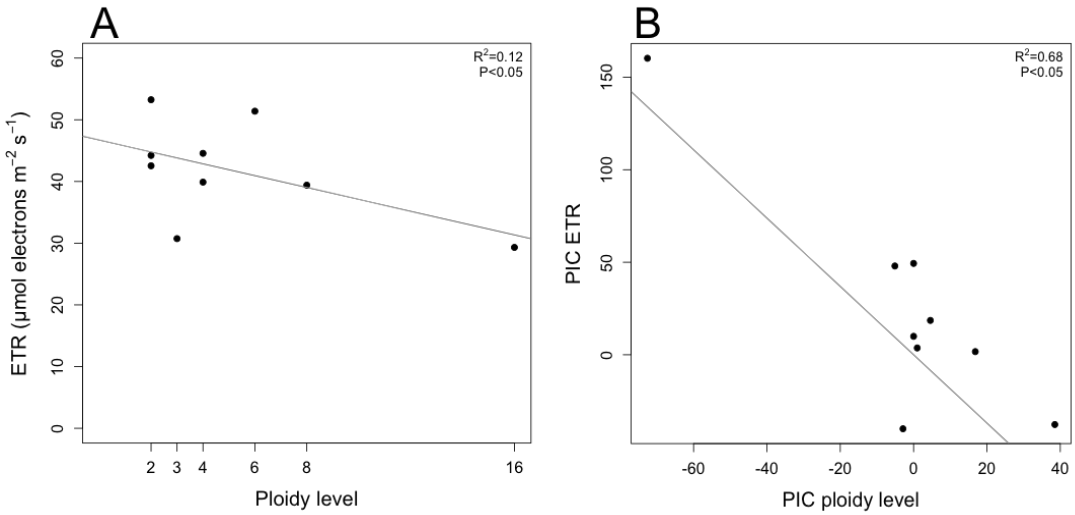

Figure 3.8. Scatter plots showing maximum relative electron transport (ETR) and ploidy level relationships. (A) The average values of Nymphaea and (B) the phylogenetic independent contrasts (PIC) are given.

Analyses of palisade cells and chloroplasts

The ultrastructure of leaf material from all species except *Brasenia schreberi* were compared (i.e. length of palisade cells, number of chloroplasts in the palisade cells and length of chloroplasts) and the data presented (Table 3.8, Figure 3.9). Genome size and ploidy level were analysed as functions of microscopy anatomy parameters (Tables 3.9 a-f, 3.10 a-b), while the latter were analysed as functions of chlorophyll fluorescence parameters (Tables 3.9 g-u, 3.10 c-g). Ploidy level is positively and significantly correlated with length of palisade cells and number of chloroplasts in the cells (Tables 3.9d-e, 3.10b). The relationship between genome size and palisade cells or number of chloroplasts in the cells appeared significant in LMs (Table 3.9a-b) but was not significant when incorporating phylogeny to the analyses (Table 3.10a). Analyses with chlorophyll fluorescence revealed significant and negative between ETR_{max} and

length of palisade cells or number of chloroplasts (Table 3.10c), and between E_k and length of palisade cells (Table 3.10d). While F_v/F_m, qP and NPQ are not significant to any of the microscopy anatomy parameters when analysing with PICs. Using PICs, the analysis of the relationship between number of chloroplasts and length of palisade cells shows to be significant and positive (Table 3.10h).

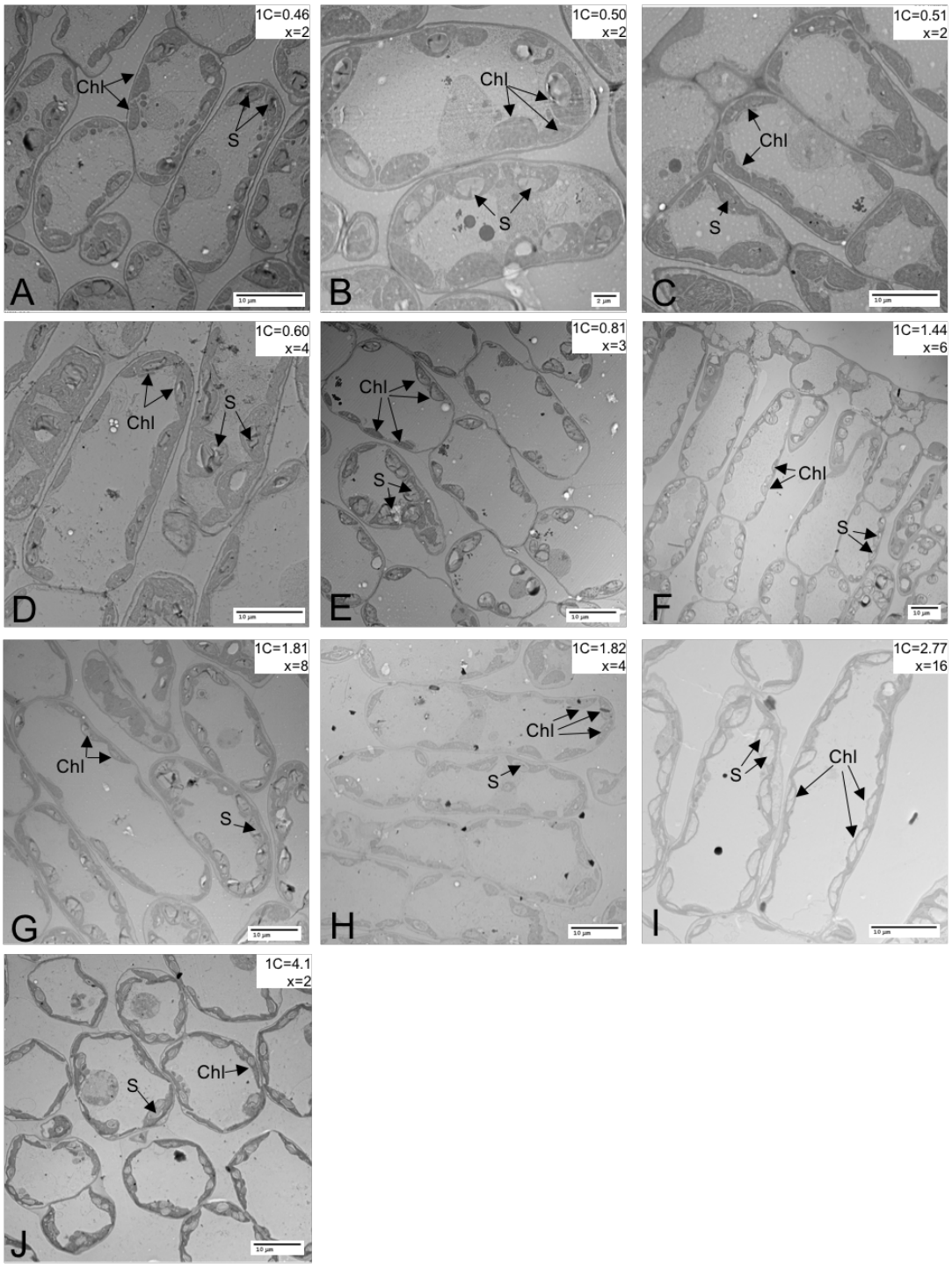

Figure 3.9. Transmission electron transmission microscopy showing the mesophyll palisade cells with chloroplasts of (A) *Nymphaea minuta*, (B) *N. colorata*, (C) *N. thermarum*, (D) *N.*

mexicana, (E) *N. rudgeana*, (F) *N. immutabilis*, (G) *N. violaceae*, (H) *N. lotus* var. *dentata*, (I) *N. gigantea* and (J) *Victoria cruziana* arranged in increasing 1C genome size (given top right in each figure). A selection of some chloroplasts and grains of starch are evidenced with black arrows. Chl=chloroplast; S=starch grain; x=ploidy level.

Discussion

It has been suggested that allopolyploidy (i.e. resulting from polyploidy in association with interspecific hybridization) may improve photosynthetic efficiency compared with autopolyploidy (i.e. genome doubling that arises within a species) (Warner & Edwards, 1993), perhaps because of advantages arising through fixed heterozygozity (hybrid vigour) (Chen, 2010). All the polyploid species analysed here are likely to be autopolyploids, or derived from allopolyploidy between closely related populations, which reduces the opportunity of benefits arising through hybrid vigour.

Stomatal size and density and genome size

There was an insignificant, but negative relationship between stomatal length and density amongst the water lilies and their relatives studied here. Previously, a significant negative correlation was reported across multiple plant groups (Beaulieu *et al.*, 2008; Franks & Beerling, 2009; Camargo & Marenco, 2011), and was found in Chapter 2's analysis of *Fritillaria* and Melanthiaceae species. Nonetheless, in support of previous studies (Beaulieu *et al.*, 2008; Greilhuber & Leitch, 2013), but contrasting with data in Chapter 2, there was a significant positive relationship between stomatal length and genome size and stomatal length and ploidy level. These data probably reflect the influence of genome size/ploidy level on cell size, as reported previously in, for example, Cactaceae (Negrón-Ortiz, 2007) and reviewed in Greilhuber & Leitch (2013). Stomatal density in *Nymphaea* was high compared with *Fritillaria*. *Nymphaea minuta* had the highest stomatal density within the group, with values comparable to rice, which has stomata on both sides of the leaf (Ohsumi *et al.*, 2007). However, all stomata are on the adaxial surface in *Nymphaea*, whilst for rice there are stomata on both surfaces. Thus if the adaxial surface only is considered in these two species, *Nymphaea minuta* has about double the density for rice. Such an adaptation in *Nymphaea* may also provide a selection pressure in these species for small genome sizes (1C= 0.5-2.77 pg, Table 3.1) compared to other angiosperms (median GS is 1C = 6 pg), given that genome may correlate with guard cell size (but see Chapter 2).

In species of *Fritillaria* and Melanthiaceae, and as reported elsewhere for other plant groups (Chapter 2), genome size does not always correlate with stomatal size. However, this correlation does frequently occur (Greilhuber & Leitch, 2013), as found here in water lilies.

Potentially, genome size is a predictor of the “minimum functional size” of a cell (Gregory, 2001; Beaulieu *et al.*, 2008), but the actual size of the cell is influenced by physiological factors that can cause enlargement of the cell from that minimum. The significant correlation between genome size and stomatal size in water lilies could have arisen because of a correlation with a minimum functional size, coupled with similar physiologies between species, all of which are aquatics growing in similar media and temperatures, with similar habits and leaf morphologies, the latter with stomata only on adaxial side of the leaf.

Correlations with ploidy level and ultrastructure characters

In the analysis here a positive correlation between ploidy level and length of palisade cells and number of chloroplasts was observed, the latter previously reported between diploids and tetraploids of *Chrysanthemum*, with reports of ~8 and ~13 chloroplasts per cell respectively (Dong *et al.*, 2017). These numbers are similar to those for *Nymphaea*. There was also an observed positive relationship between number of chloroplasts and length of palisade cells in *Nymphaea*. It is likely that higher ploidy level cells are larger because the nucleus is bigger and that the larger cells can support greater numbers of chloroplasts.

Correlations with chlorophyll fluorescence

Previous studies have found an influence of ploidy and genome size on photosynthetic capacity (Randall *et al.*, 1977; Joseph *et al.*, 1981; Warner & Edwards, 1993; Nasiri *et al.*, 2015; Gao *et al.*, 2017; Dong *et al.*, 2017), however it is noticeable that not many studies have included chlorophyll fluorescence measures to their correlations as is done here. Previous studies have noted that despite a relationship between ploidy level and photosynthetic capacity, there was either no effect, or only a small effect of genome size on photosynthesis (DeMaggio *et al.*, 1971). Two chlorophyll fluorescence measures are important here (1) F_v/F_m determines the maximum photochemical efficiency of photosystem II (PSII) and (2) rETR, which measures the electron transport rate through PSII reaction centres, which generates ATP. In water lilies, there is no effect of genome size on rETR and F_v/F_m, although there is a negative relationship between rETR and ploidy level and a positive relationship with F_v/F_m.

The negative association between rETR and ploidy level may reflect the scaling effects of ploidy on cell size and number of chloroplasts, since the latter are also negatively associated with rETR. However, it would be expected that more chloroplasts would lead to higher rETR. rETR is measured over a unit leaf area, and not on a per cell basis. Potentially larger cells with more chloroplasts may actually have fewer numbers of chloroplasts per unit area of leaf because of fewer, larger cells. Future work, needs to estimate the numbers of chloroplasts and cells per unit area measured for rETR estimates.

Greer *et al.* (2017) and Coate *et al.* (2012), in contrast to the work here, did not find any significant relationship between ploidy level and rETR, although Coate *et al*. found a significant and positive relationship between ploidy and rETR in allopolyploids of *Glycine* sp. when the estimation was per cell. Jellings & Leech (1984) discussed how a positive relationship between photosynthetic rate and ploidy level when measured per cell, could be negative when measured per unit leaf area. They argued that the relationship can change in a per cell to a per tissue analysis because of surface area to volume ratio scaling effects with increasing cell size and because larger cells have larger airspaces, allowing for faster movement of gases.

The ratio F_v/F_m is typically ~0.8 across plants, reflecting an efficient light energy conversion into the energy of electrons moving into the electron transport chain (Demmig & Björkman, 1987; Ruban, 2013). A decline in F_v/F_m is a sensitive indicator of change in photosynthesis and in the physiology of the plant in general, resulting from any type of stress (Murchie & Lawson, 2013). F_v/F_m is positively associated with ploidy and stomatal length in this study, which indicates a higher efficiency of photochemical conversions in higher ploidy levels and in plants with higher stomatal length. This could be related to a higher number of chloroplasts in the cells of plants with larger cells (DeMaggio *et al.*, 1971; Warner & Edwards, 1993; Dong *et al.*, 2017), however there was no association between F_v/F_m and those ultrastructure characteristics studies here, potentially because the number of cells measured is unknown, as discussed for rETR above.

Non-photochemical quenching (NPQ)

Non-photochemical quenching is the heat dissipation of chlorophyll excitation energy and it is a photoprotective process that reduces excess excitation energy within chlorophyll pigments and prevents damage of antenna complexes in PSII (Murchie & Lawson, 2013; Ruban, 2013). There was a surprisingly small NPQ signature for most of these plants analysed. NPQ was lower than 1 for six out of the eleven species studied and *N. lotus* had an extreme low NPQ, suggesting that most of the energy provided by the PAM fluorometer was used by PSII for photochemistry. This suggestion is supported by the observation that for nine of the eleven species studied the qP (photochemical quenching) greater than 0.5 for 9. Indeed, these water lilies had a much lower NPQ compared with the *Fritillaria* and Melanthiaceae species studied on Chapter 2 (where all of them had NPQ values greater than 1.2), and with *Arabidopsis thaliana* in a study done with the same type of ILC as used here, but with the application of different actinic light intensities (Johnson *et al.*, 2008). Possible explanations for a low NPQ signature in water lilies are: (1) some unknown physiological process found in water lilies that results in little energy being dissipated through NPQ, possibly because water lilies are adapted to growing in very bright light conditions; (2) the aquatic life style of water lilies means that

their tissues are always fully hydrated and surrounded by copious amounts of water. Potentially the availability of water is affecting the efficiency of PSII or NPQ. Clearly further studies are needed here to determine whether these atypically low levels of NPQ are characteristic of other aquatic species from different families which typically grow under high light intensities or whether these traits are restricted to Nymphaeaceae.

In water lilies, stomata only occur on the adaxial surface of the leaf, which is the surface that is most likely to be in contact with air. A significant and positive relationship was found between stomatal density and NPQ, a relationship that was the opposite to what might be expected. A negative relationship might be expected, because plants with a greater number of small stomata per unit leaf area are expected to have higher rates of gas exchange and electron transport, which might decrease NPQ, as seen in an experiment with *Arabidopsis* (Schlüter *et al.*, 2003).

Ideally gas exchange measures are sought for water lilies, however that is non trivial in their aquatic leaf for two reasons (1) the measurement itself is difficult because the plants are aquatic, and (2) even if plants are removed from the water for analysis, the leaves are thick and spongy, and the thickness of spongy tissues can influence gas flow in an IRGA system (Ritchie, 2012).

Conclusions

Data showing photosynthetic measures of fluorescence, as well as chloroplast and stomata numbers are given for the first time for water lilies species. Stomatal densities were high for most species. Ploidal level was found to have an influence on anatomy and physiology of *Nymphaea* leaves, as seen in the fluorescence measures. It remains unknown whether polyploid is advantageous or not for the efficiency of photosynthesis, however these results suggest a negative correlation between ploidy levels and rETR. There is a positive correlation between GS and guard cell size in *Nymphaea*. The density of guard cells is high and restricted to the adaxial surface of the leaf in these species. Potentially, the species with large stomatal sizes and high stomatal densities may be prone to much water loss, particularly because the stomata are on the adaxial surface. If so there may be selection against large GS, mediated via stomatal size, even in aquatics.

References

Beaulieu JM, Leitch IJ, Patel S, Pendharkar A, Knight CA. **2008**. Genome size is a strong

predictor of cell size and stomatal density in angiosperms. *New Phytologist* **179**: 975–986.

Camargo MAB, Marenco RA. **2011**. Density, size and distribution of stomata in 35 rainforest tree species in Central Amazonia. *Acta Amazonica* **41**: 205–212.

Chen ZJ. **2010**. Molecular mechanisms of polyploidy and hybrid vigor. *Trends in Plant Science* **15**: 57–71.

Coate JE, Luciano AK, Seralathan V, Minchew KJ, Owens TG, Doyle JJ. **2012**. Anatomical, biochemical, and photosynthetic responses to recent allopolyploidy in *Glycine dolichocarpa* (Fabaceae). *American Journal of Botany* **99**: 55–67.

DeMaggio AE, Wetmore RH, Hannaford JE, Stetler DA, Raghavan V. **1971**. Ferns as a model system for studying polyploidy and gene dosage effects. *BioScience* **21**: 313–316.

Demmig B, Björkman O. **1987**. Comparison of the effect of excessive light on chlorophyll fluorescence (77K) and photon yield of O_2 evolution in leaves of higher plants. *Planta* **171**: 171–184.

Dong B, Wang H, Liu T, Cheng P, Chen Y, Chen S, Guan Z, Fang W, Jiang J, Chen F. **2017**. Whole genome duplication enhances the photosynthetic capacity of *Chrysanthemum nankingense*. *Molecular Genetics and Genomics*: 1–10.

Dornhoff GM, Shibles R. **1976**. Leaf morphology and anatomy in relation to CO_2-exchange rate of soybean leaves. *Crop Science* **16**: 377.

Franks PJ, Beerling DJ. **2009**. Maximum leaf conductance driven by CO_2 effects on stomatal size and density over geologic time. *Proceedings of the National Academy of Sciences* **106**: 10343–10347.

Gao S, Yan Q, Chen L, Song Y, Li J, Fu C, Dong M. **2017**. Effects of ploidy level and haplotype on variation of photosynthetic traits: Novel evidence from two *Fragaria* species (J Yang, Ed.). *PLOS ONE* **12**: e0179899.

Greer BT, Still C, Cullinan GL, Brooks JR, Meinzer FC. **2017**. Polyploidy influences plant–environment interactions in quaking aspen (Populus tremuloides Michx.). *Tree Physiology*: 1–11.

Gregory TR. **2001**. Coincidence, coevolution, or causation? DNA content, cell size, and the C-value enigma. *Biological Reviews of the Cambridge Philosophical Society* **76**: 65–101.

Greilhuber J, Leitch I. **2013**. Genome size and the phenotype. In: Greilhuber, J., Dolezel, J., Wendel JF, ed. Plant Genome Diversity Volume 2. Springer Vienna, 323–344.

Hilu KW, Randall JL. **1984**. Convenient method for studying grass leaf epidermis. *Taxon* **33**: 413.

Jellings AJ, Leech RM. **1984**. Anatomical variation in first leaves of nine *Triticum* genotypes, and its relationship to photosynthetic capacity. *New Phytologist* **96**: 371–382.

Johnson MP, Davison PA, Ruban A V., Horton P. **2008**. The xanthophyll cycle pool size controls the kinetics of non-photochemical quenching in *Arabidopsis thaliana*. *FEBS Letters* **582**: 262–266.

Joseph MC, Randall DD, Nelson CJ. **1981**. Photosynthesis in polyploid tall fescue: II. photosynthesis and Ribulose-1,5-Bisphosphate Carboxylase of polyploid tall fescue. *Plant Physiology* **68**: 894–898.

Knight CA, Beaulieu JM. **2008**. Genome size scaling through phenotype space. *Annals of Botany* **101**: 759–766.

Murchie EH, Lawson T. **2013**. Chlorophyll fluorescence analysis: a guide to good practice and understanding some new applications. *Journal of Experimental Botany* **64**: 3983–3998.

Nasiri M, Navabpour S, Siavoshi M, Zandi P, Khodambashi M, A S oushmand H, Bilgrami SS, Sorkheh K, Tadayyon M, Amouei H. **2015**. Photosynthetic performance in ploidy levels and amphyploids of wheat during developmental stages. *The Journal of Animal & Plant Sciences* **25**: 1633–1643.

Negrón-Ortiz V. **2007**. Chromosome numbers, nuclear DNA content, and polyploidy in *Consolea* (Cactaceae), an endemic cactus of the Caribbean Islands. *American Journal of Botany* **94**: 1360–70.

Ohsumi A, Kanemura T, Homma K, Horie T, Shiraiwa T. **2007**. Genotypic variation of stomatal conductance in relation to stomatal density and length in rice (Oryza sativa L.). *Plant Production Science* **10**: 322–328.

Pellicer J, Kelly LJ, Magdalena C, Leitch IJ. **2013**. Insights into the dynamics of genome size and chromosome evolution in the early diverging angiosperm lineage Nymphaeales (water lilies). *Genome* **56**: 437–449.

Qiu Y-L, Li L, Wang B, Xue J-Y, Hendry TA, Li R-Q, Brown JW, Liu Y, Hudson GT, Chen Z-D. **2010**. Angiosperm phylogeny inferred from sequences of four mitochondrial genes. *Journal of Systematics and Evolution* **48**: 391–425.

Randall DD, Nelson CJ, Asay KH. **1977**. Ribulose bisphosphate carboxylase: altered genetic expression in tall fescue. *Plant Physiology* **59**: 38–41.

Ritchie RJ. **2012**. Photosynthesis in the blue water lily (*Nymphaea caerulea* Saligny) using pulse amplitude modulation fluorometry. *International Journal of Plant Sciences* **173**: 124–136.

Romero-Aranda R, Bondada BR, Syvertsen JP, Grosser JW. **1997**. Leaf characteristics and net gas exchange of diploid and autotetraploid citrus. *Annals of Botany* **79**: 153–160.

Ruban A. **2013**. *The photosynthetic membrane: molecular mechanisms and biophysics of light harvesting*. United Kingdom: Wiley.

Schlüter U, Muschak M, Berger D, Altmann T. **2003**. Photosynthetic performance of an *Arabidopsis* mutant with elevated stomatal density (sdd1-1) under different light regimes. *Journal of Experimental Botany* **54**: 867–874.

Soltis DE, Bell CD, Kim S, Soltis PS. **2008**. Origin and early evolution of angiosperms. *Annals of the New York Academy of Sciences* **1133**: 3–25.

The Angiosperm Phylogeny Group. **2016**. An update of the Angiosperm Phylogeny Group classification for the orders and families of flowering plants: APG IV. *Botanical Journal of the Linnean Society* **181**: 1–20.

Warner DA, Edwards GE. **1993**. Effects of polyploidy on photosynthesis. *Photosynthesis Research* **35**: 135–147.

Tables

Table 3.1. Plant material analysed in the current work

Species	Accession number	Family	1C-value (pg)	Ploidy level	Date of collection
Nymphaea* subgenus *Anecphya					
N. gigantea	1992-2007	Nymphaeaceae	2.77	16x	July 2016
N. immutabilis	2008-557	Nymphaeaceae	1.44	6x	July 2016
N. violaceae	2008-566	Nymphaeaceae	1.81	8x	December 2015
Nymphaea* subgenus *Brachyceras					
N. colorata	2004-1765	Nymphaeaceae	0.5	2x	July 2016
N. minuta	2010-539	Nymphaeaceae	0.46	2x	July 2016
N. thermarum	2010-535	Nymphaeaceae	0.51	2x	July 2016
Nymphaea* subgenus *Hydrocallis					
N. rudgeana	-	Nymphaeaceae	0.81	3x	November 2015
Nymphaea* subgenus *Lotos					
N. lotus var. *dentata*	1987-2035	Nymphaeaceae	1.82	4x	November 2015
Nymphaea* subgenus *Nymphaea					
N. mexicana	1973-12536	Nymphaeaceae	0.6	4x	November 2016
Victoria cruziana	2008-536	Nymphaeaceae	4.1	2x	July 2016
Brasenia schreberi	-	Cabombaceae	1.22	-	July 2016

Table 3.2. The number of specimens analysed (n) and average and standard deviation of stomatal lengths and densities of all species studied.

Species	n	Stomatal length (μm)	Stomatal density (stomata mm^{-2})
Nymphaea colorata	3	17.01±0.63	772±84
N. gigantea	2	28.03±1.26	544±37
N. immutabilis	2	18.72±1.09	772±81
N. lotus	3	19.5±1.98	636±132
N. mexicana	3	18.02±1.15	856±7
N. minuta	3	17.25±0.67	944±53
N. rudgeana	2	15.35±0.50	560±71
N. thermarum	3	20.25±0.58	339±23
N. violaceae	2	17.41±0.15	642±43
Victoria cruziana	3	23.33±1.09	562±168
Brasenia schreberi	1	25.10	393

Table 3.3. Linear models output showing relationships between stomatal characters (stomatal length and density), C-value and ploidy level between species of *Nymphaea*. (Significant values are highlighted in bold).

(a) stomatal density ~ stomatal length

	Estimate	Std. Error	t value	Pr(>|t|)
(Intercept)	1189.41	222.28	5.351	<0.0001
length	-26.85	11.58	-2.319	**0.0306**

(b) length ~ c-value

	Estimate	Std. Error	t value	Pr(>|t|)
(Intercept)	15.6898	0.9672	16.223	<0.0001
c-value	2.9304	0.7285	4.023	**0.0006**

(c) length ~ ploidy

	Estimate	Std. Error	t value	Pr(>|t|)
(Intercept)	15.9217	0.727	21.902	<0.0001
ploidy	0.6379	0.1187	5.372	**<0.0001**

(d) density ~ c-value

	Estimate	Std. Error	t value	Pr(>|t|)
(Intercept)	751.71	74.25	10.123	<0.0001
c-value	-63.69	55.93	-1.139	0.268

(e) density ~ ploidy

	Estimate	Std. Error	t value	Pr(>|t|)
(Intercept)	722.316	65.579	11.01	<0.0001

ploidy	-8.679	10.712	-0.81	0.427

(f) c-value ~ ploidy

	Estimate	Std. Error	t value	Pr(>|t|)
(Intercept)	0.2808	0.0818	3.432	0.00159
ploidy	0.1685	0.0134	12.556	<0.0001

Table 3.4. Phylogenetic independent contrasts estimates with the traits shown as functions of (a) genome size, (b) ploidy, (c) stomatal length and (d) stomatal density (significant values are highlighted in bold).

(a) Genome size

	F_v/F_m	qP	NPQ	rETR	E_k	Stomatal length	Stomatal density	Ploidy
Slope	0.0078	0.0227	-0.0027	-6.52	-36.15	4.393	-102.7	0.1304
R^2	0.14	-0.03	-0.111	0.17	0.1	0.58	0.04	0.59
p	0.135	0.413	0.978	0.11	0.18	**0.0038**	0.266	**0.0056**

(b) Ploidy

	F_v/F_m	qP	NPQ	rETR	E_k	Stomatal length	Stomatal density
Slope	0.002	0.0003	0.007	-1.846	-8.493	0.854	-18.05
R^2	0.45	-0.12	-0.1	0.68	0.32	0.77	0.035
p	**0.02**	0.948	0.695	**0.002**	0.052	**0.0005**	0.287

(c) Stomatal length

	F_v/F_m	qP	NPQ	rETR	E_k	Stomatal density
Slope	0.0041	0.0011	-0.0043	-1.5352	-9.084	-0.0112
R^2	0.45	-0.1	-0.1	0.38	0.22	0.24
p	**0.0138**	0.826	0.807	**0.0269**	0.0821	0.0697

(d) Stomatal density

	F_v/F_m	qP	NPQ	rETR	E_k
Slope	-6.8×10^{-5}	1.6×10^{-4}	0.0006	0.0145	0.17
R^2	0.29	0.22	0.34	-0.002	0.26
p	0.0504	0.082	**0.0342**	0.349	0.0629

Table 3.5. Linear models exploring relationships between stomatal length and chlorophyll fluorescence parameters (F_v/F_m, qP, NPQ, ETR_{max}, E_k) between species of *Nymphaea*. (Significant values are highlighted in bold).

(a) F_v/F_m ~ stomatal length

	Estimate	Std. Error	t value	Pr(>|t|)
(Intercept)	0.778	0.0147	52.977	<0.0001
length	0.0009	0.0008	1.185	0.249

(b) qP ~ stomatal length

	Estimate	Std. Error	t value	Pr(>|t|)
(Intercept)	0.3537	0.0936	3.779	0.001
length	0.01	0.0049	2.029	0.0553

(c) NPQ ~ stomatal length

	Estimate	Std. Error	t value	Pr(>|t|)
(Intercept)	0.9946	0.3743	2.657	0.0147
length	-0.0076	0.0195	-0.392	0.699

(d) rETR ~ stomatal length

	Estimate	Std. Error	t value	Pr(>|t|)
(Intercept)	56.62	13.4732	4.202	0.0004
length	-0.7468	0.7017	-1.064	0.2993

(e) log(E_k) ~ stomatal length

	Estimate	Std. Error	t value	Pr(>|t|)
(Intercept)	6.4211	0.2739	23.441	<0.0001

length	-0.0409	-0.0143	-2.867	**0.0092**

(f) F_v/F_m ~ stomatal density

	Estimate	Std. Error	t value	Pr(>|t|)
(Intercept)	0.808	0.009	89.677	<0.0001
density	$-1.8x10^{-5}$	$1.27x10^{-5}$	-1.414	0.172

(g) qP ~ stomatal density

	Estimate	Std. Error	t value	Pr(>|t|)
(Intercept)	0.4657	0.0612	7.604	<0.0001
density	0.0001	0.00009	1.275	0.216

(h) NPQ ~ stomatal density

	Estimate	Std. Error	t value	Pr(>|t|)
(Intercept)	0.493	0.2188	2.253	0.0351
density	0.0005	0.0003	1.697	0.1045

(i) rETR ~ stomatal density

	Estimate	Std. Error	t value	Pr(>|t|)
(Intercept)	33.66	8.3546	4.029	0.0006
density	0.013	0.0118	1.1	0.28

(j) $\log(E_k)$ ~ stomatal density

	Estimate	Std. Error	t value	Pr(>|t|)
(Intercept)	5.2	0.174	29.98	<0.0001

density	0.0006	0.0002	2.66	**0.0146**

Table 3.6. Average and standard deviation of chlorophyll fluorescence parameters of all species studied.

Species	n	F_v/F_m	qP	NPQ	rETR	E_k
Nymphaea colorata	5	0.785±0.008	0.553±0.025	0.837±0.057	53.2±9.1	407.9±53.7
N. gigantea	3	0.807±0.004	0.594±0.021	1.084±0.028	29.3±3.5	206.1±10.7
N. immutabilis	5	0.782±0.009	0.617±0.038	1.047±0.164	51.4±14.4	287.8±66.9
N. lotus	3	0.78±0.006	0.617±0.022	0.319±0.019	44.6±6.5	236±20
N. mexicana	4	0.805±0.005	0.505±0.049	0.828±0.105	39.9±10	373.2±47.4
N. minuta	5	0.782±0.009	0.582±0.021	1.211±0.102	42.5±4.5	308.5±46.2
N. rudgeana	3	0.802±0.006	0.351±0.024	1.011±0.12	30.7±10.2	246.1±16.1
N. thermarum	5	0.802±0.004	0.47±0.036	0.643±0.169	44.2±6.9	238.2±30.2
N. violaceae	3	0.799±0.002	0.521±0.048	0.959±0.192	39.4±6.7	249.2±85.2
Victoria cruziana	5	0.789±0.006	0.676±0.031	0.786±0.101	61.7±16.4	435.3±75.9
Brasenia schreberi	5	0.794±0.007	0.608±0.048	1.043±0.159	73.8±19.3	601.8±140.4

Table 3.7. Linear models exploring relationships between chlorophyll fluorescence parameters (F_v/F_m, qP, NPQ, ETR_{max}, E_k), C-value and ploidy level between species of *Nymphaea*. (Significant values are highlighted in bold).

(a) F_v/F_m ~ c-value

	Estimate	Std. Error	t value	Pr(>|t|)
(Intercept)	0.789	0.011	71.409	<0.0001
c-value	-0.0012	0.0008	-0.143	0.887

(b) F_v/F_m ~ ploidy

	Estimate	Std. Error	t value	Pr(>|t|)
(Intercept)	0.785	0.0097	81.221	<0.0001
ploidy	0.0006	0.0016	0.401	0.691

(c) qP~ c-value + season

	Estimate	Std. Error	t value	Pr(>|t|)
(Intercept)	0.0512	0.0222	23.046	<0.0001
c-value	0.491	0.0166	2.959	**0.0057**
winter	-0.072	0.025	-2.2884	**0.0069**

(d) qP ~ ploidy + season

	Estimate	Std. Error	t value	Pr(>|t|)
(Intercept)	0.5324	0.0221	24.058	<0.0001
ploidy	0.0059	0.0033	1.82	0.0778
winter	-0.0614	0.0265	-2.318	**0.0268**

(e) NPQ ~ c-value + season

	Estimate	Std. Error	t value	Pr(>|t|)
(Intercept)	0.9356	0.0843	11.101	<0.0001
c-value	0.0185	0.063	0.294	0.7708
winter	-0.1752	0.0948	-1.847	0.0737

(f) NPQ ~ ploidy + season

	Estimate	Std. Error	t value	Pr(>|t|)
(Intercept)	0.8788	0.0762	11.539	<0.0001
ploidy	0.016	0.0113	1.424	0.1638
winter	-0.1714	0.0912	-1.876	0.0695

(g) log(rETR) ~ c-value + season

	Estimate	Std. Error	t value	Pr(>|t|)
(Intercept)	3.8748	0.0815	47.528	<0.0001
c-value	-0.0898	0.0609	-1.474	0.15
winter	-0.1458	0.0918	-1.589	0.122

(h) log(rETR) ~ ploidy + season

	Estimate	Std. Error	t value	Pr(>|t|)
(Intercept)	3.9039	0.07239	53.929	<0.0001
ploidy	-0.0252	0.0107	-2.358	**0.0245**
winter	-0.1652	0.0867	-1.905	0.0655

(i) log(E_k) ~ c-value

	Estimate	Std. Error	t value	Pr(>|t|)

(Intercept)	5.8461	0.0746	78.331	<0.0001
c-value	-0.1938	0.0577	-3.357	**0.00195**

(j) $\log(E_k) \sim$ ploidy

	Estimate	Std. Error	t value	Pr(>|t|)
(Intercept)	5.775	0.0691	83.63	<0.0001
ploidy	-0.0291	0.01132	-2.57	**0.0147**

Table 3.8. Average and standard deviation of length of palisade cells (μm), number of chloroplasts in the palisade cells and length of chloroplasts (μm) in the palisade cells of all species analysed with transmission electron microscopy.

Species	Length of palisade cells	Number of chloroplasts	Length of chloroplasts
Nymphaea colorata	26.360±5.452	8.591±1.545	6.101±0.671
N. gigantea	42.247±7.807	12.853±2.765	6.209±1.093
N. immutabilis	37.671±11.800	10.833±1.877	5.540±1.197
N. lotus	37.562±9.927	9.147±2.245	6.453±1.619
N. mexicana	37.244±7.566	9.000±1.546	7.632±1.641
N. minuta	29.527±6.166	8.744±1.352	5.486±1.189
N. rudgeana	31.507±6.789	8.840±1.646	5.671±1.297
N. thermarum	30.743±7.640	7.200±1.705	5.945±1.121
N. violaceae	37.716±7.931	10.820±2.472	7.989±1.175
Victoria cruziana	27.339±5.189	6.500±1.482	9.651±2.003

Table 3.9. Linear models exploring relationships between palisade cells length, number of chloroplasts in the palisade cells and length of chloroplasts in the palisade cells and C-value, ploidy level and chlorophyll fluorescence parameters (ETR_{max}, E_k, F_v/F_m, qP, NPQ), between species of *Nymphaea*. (Significant values are highlighted in bold).

(a) Length of palisade cells ~ c-value

	Estimate	Std. Error	t value	Pr(>|t|)
(Intercept)	28.159	1.811	15.548	<0.0001
c-value	5.331	1.278	4.171	**0.0042**

(b) Number of chloroplasts ~ c-value

	Estimate	Std. Error	t value	Pr(>|t|)
(Intercept)	7.422	0.528	14.051	<0.0001
c-value	1.794	0.373	4.813	**0.0019**

(c) Length of chloroplasts ~ c-value

	Estimate	Std. Error	t value	Pr(>|t|)
(Intercept)	6.059	0.577	10.496	<0.0001
c-value	0.233	0.407	0.572	0.5850

(d) Length of palisade cells ~ ploidy

	Estimate	Std. Error	t value	Pr(>|t|)
(Intercept)	29.757	1.737	17.134	<0.0001
ploidy	0.910	0.258	3.532	**0.0096**

(e) Number of chloroplasts ~ ploidy

	Estimate	Std. Error	t value	Pr(>|t|)
(Intercept)	7.766	0.343	22.63	<0.0001
ploidy	0.343	0.051	6.74	**0.0003**

(f) Length of chloroplasts ~ ploidy

	Estimate	Std. Error	t value	Pr(>|t|)
(Intercept)	6.109	0.494	12.376	<0.0001
ploidy	0.043	0.073	0.594	0.5710

(g) log(ETR_{max}) ~ length of palisade cells

	Estimate	Std. Error	t value	Pr(>|t|)
(Intercept)	4.284	0.310	13.796	<0.0001
Length cells	-0.016	0.009	-1.817	0.0780

(h) log(ETR_{max}) ~ number of chloroplasts

	Estimate	Std. Error	t value	Pr(>|t|)
(Intercept)	4.128	0.281	14.69	<0.0001
Number of chloroplasts	-0.043	0.030	-1.45	0.156

(i) log(ETR_{max}) ~ length of chloroplasts

	Estimate	Std. Error	t value	Pr(>|t|)
(Intercept)	3.993	0.356	11.216	<0.0001
Length chloroplasts	-0.043	0.056	-0.757	0.4550

(j) $\log(E_k)$ ~ length of palisade cells

	Estimate	Std. Error	t value	Pr(>|t|)
(Intercept)	6.436	0.308	20.893	<0.0001
Length cells	-0.024	0.009	-2.617	**0.0131**

(k) $\log(E_k)$ ~ number of chloroplasts

	Estimate	Std. Error	t value	Pr(>|t|)
(Intercept)	6.085	0.291	20.943	<0.0001
Number of chloroplasts	-0.048	0.030	-1.557	0.129

(l) $\log(E_k)$ ~ length of chloroplasts

	Estimate	Std. Error	t value	Pr(>|t|)
(Intercept)	5.548	0.372	14.899	<0.0001
Length chloroplasts	0.014	0.059	0.246	0.8070

(m) F_v/F_m ~ length of palisade cells

	Estimate	Std. Error	t value	Pr(>|t|)
(Intercept)	0.766	0.0132	58.036	<0.0001
Length cells	0.001	0.0004	2.098	**0.0434**

(n) F_v/F_m ~ number of chloroplasts

	Estimate	Std. Error	t value	Pr(>|t|)
(Intercept)	0.783	0.012	63.34	<0.0001

Number of chloroplasts	0.001	0.001	0.84	0.4070

(o) F_v/F_m ~ length of chloroplasts

	Estimate	Std. Error	t value	Pr(>|t|)
(Intercept)	0.761	0.014	52.85	<0.0001
Length chloroplasts	0.005	0.002	2.32	0.0265

(p) qP ~ length of palisade cells

	Estimate	Std. Error	t value	Pr(>|t|)
(Intercept)	0.379	0.095	3.994	0.0003
Length cells	0.005	0.003	1.692	0.0998

(q) qP ~ number of chloroplasts

	Estimate	Std. Error	t value	Pr(>|t|)
(Intercept)	0.322	0.080	4.041	0.0003
Number of chloroplasts	0.023	0.008	2.756	**0.0093**

(r) qP ~ length of chloroplasts

	Estimate	Std. Error	t value	Pr(>|t|)
(Intercept)	0.607	0.108	5.595	<0.0001
Length chloroplasts	-0.011	0.017	-0.638	0.5280

(s) NPQ ~ length of palisade cells

	Estimate	Std. Error	t value	Pr(>|t|)
(Intercept)	0.911	0.327	2.785	0.0087
Length cells	-0.001	0.010	-0.058	0.9538

(t) NPQ ~ number of chloroplasts

	Estimate	Std. Error	t value	Pr(>|t|)
(Intercept)	0.258	0.2697	0.959	0.3445
Number of chloroplasts	0.068	0.0284	2.380	0.0231

(u) NPQ ~ length of chloroplasts

	Estimate	Std. Error	t value	Pr(>|t|)
(Intercept)	1.398	0.350	3.993	0.0003
Length chloroplasts	-0.081	0.056	-1.457	0.1542

Table 3.10. Phylogenetic independent contrasts estimates of palisade cells length, number of chloroplasts in the palisade cells and length of chloroplasts in the palisade cells as functions of (a) genome size and (b) ploidy; (c-g) chlorophyll fluorescence parameters (ETR_{max}, E_k, F_v/F_m, qP, NPQ) as functions of palisade cells length, number of chloroplasts in the palisade cells and length of chloroplasts in the palisade cells; and (h) number of chloroplasts as function of length of palisade cells (significant values are highlighted in bold).

(a) Genome size

	Length of palisade cells	Number of chloroplasts	Length of chloroplasts
Slope	2.957	1.034	0.502
R^2	0.294	0.291	0.136
p	0.061	0.062	0.159

(b) Ploidy

	Length of palisade cells	Number of chloroplasts	Length of chloroplasts
Slope	0.662	0.253	0.041
R^2	0.574	0.704	-0.066
p	**0.007**	**0.001**	0.524

(c) ETR_{max}

	Length of palisade cells	Number of chloroplasts	Length of chloroplasts
Slope	-1.671	-5.046	-1.792
R^2	0.338	0.395	-0.100
p	**0.046**	**0.030**	0.683

(d) E_k

	Length of palisade cells	Number of chloroplasts	Length of chloroplasts
Slope	-11.961	-18.280	-5.002

R^2	0.492	0.054	-0.120
p	**0.014**	0.254	0.854

(e) F_v/F_m

	Length of palisade cells	Number of chloroplasts	Length of chloroplasts
Slope	0.002	0.003	0.006
R^2	0.178	0.008	0.0412
p	0.125	0.331	0.273

(f) qP

	Length of palisade cells	Number of chloroplasts	Length of chloroplasts
Slope	0.001	0.012	-0.010
R^2	-0.118	-0.055	-0.107
p	0.834	0.487	0.729

(g) NPQ

	Length of palisade cells	Number of chloroplasts	Length of chloroplasts
Slope	-0.001	0.073	-0.075
R^2	-0.124	0.092	-0.040
p	0.955	0.204	0.442

(h) number of chloroplasts ~ length of palisade cells

Slope	0.267
R^2	0.527
p	**0.010**

Chapter 4. The effect of nitrogen and phosphate interactions on photosynthesis and the production of biomass in *Triticum aestivum* L. (wheat).

Summary

Introduction: Nitrogen (N) and/or phosphate (P) availability in the environment limits productivity across many ecosystems and agricultural settings. Because N and P frequently restrict plant growth, fertilizers are used in vast quantities to sustain and enhance crop yields. This is particularly true for wheat (*Triticum aestivum* L.), which is one of the world's most important crop species and used primarily for direct human consumption and livestock feed. Most breeding has been conducted in the presence of large quantities of fertilisers. However, the application of plentiful, even excess fertiliser is a problem, since run-off is polluting our soils, freshwater and coastal waters, leading to loss of biodiversity and eutrophication. N and P are required for plant growth (cell division, nucleic acids synthesis) and seed production (e.g. protein synthesis, which is demanding on N and P). This chapter investigates potential trade-offs between photosynthesis, growth and reproduction under N and P limitation using dwarf wheat (*Triticum aestivum* L. cv. USU-Apogee).

Methods: A total of 108 seeds of wheat were grown in 16 different combinations of N and P (4 different concentrations each). Biomass, seed production and C, N and phosphorus content in leaves and seeds were determined and compared with chlorophyll fluorescence (F_v/F_m, qP, NPQ, ETR_{max}, E_k) and rates of CO_2 uptake (A_{max}, V_{cmax}, J_{max}) measured. Statistical analyses were done using linear models in R.

Results: Linear modelling revealed significant ($p<0.05$) positive relationships between biomass and seed yield and increasing P, as well as significant ($p<0.05$) positive relationships arising through P and N interactions. Increase in P significantly affects qP and NPQ, while N and P interactions increase A_{max}, V_{cmax} and J_{max}.

Discussion: Crop plants are fertilised to make them more productive. This study finds evidence in wheat for strong N:P interactions in the production of biomass and seed yield. The co-limitation of these nutrients arises, in part, by differential effects of N and P on various components of photosynthesis. We suggest that deeper understanding of N:P interactions are needed to improve crop yields, and many more such studies are urgently needed, especially given that P is a finite resource.

Introduction

Nitrogen (N) and/or phosphate (P) availability in the environment limits productivity across many ecosystems and agricultural settings. Because N and P frequently restrict plant growth, fertilisers are used in vast quantities to sustain and enhance crop yields (Tilman *et al*., 2002). This is particularly true for wheat (*Triticum aestivum* L.), which is one of the world's most important crop species and used primarily for direct human consumption and livestock feed. Production of wheat has been steadily increasing, since the second world war, and global production in 2017/18 is expected to reach its highest ever at 757.6 million tonnes (FAO, 2018). Commensurate with yield increases is year on year rises in fertiliser use (N, P and potassium (K)) globally, with usage in agriculture generally expected to reach 200.5 million tonnes per annum by the end of 2018 (FAO, 2015).

Yield increases in wheat have also been achieved through intense breeding to produce elite lines. However, that breeding has almost entirely been in the presence of large (often in excess) quantities of fertilisers. High application of fertilisers causes problems, since run-off is polluting our soils, freshwater and coastal waters, leading to loss of biodiversity and eutrophication (i.e. when a body of water becomes greatly enriched with nutrients causing an over reproduction of microphytes and algae). In the US, eutrophication is estimated to cost $2.2 billion annually, through degradation of ecosystems (Dodds *et al.*, 2009). Furthermore, some researchers suggest that the long-term availability of P is potentially limiting because of finite high yield minable reserves (Cordell *et al.*, 2009). Despite these issues fertiliser supply must be sustainably met to accommodate the increasing demands of agriculture, associated with the need for increased yield for a growing human population and to enable land to be set aside for biofuels and nature conservation.

One potential solution to address all these problems is to breed wheat plants that are more efficient in their fertiliser usage. Yet, since wheat breeding has been conducted in the presence of abundant fertilisers, it is likely the plants have become N and P lazy, inefficiently utilising the fertiliser that is added. Such "laziness" may include inefficient transcription or cycling of RNA with gene expression, inefficient cycling of damaged or redundant proteins and pigments and inefficient harvesting of nutrients from the soil. In order to breed for high wheat yields with lower fertiliser input, it is therefore essential to gain a detailed understanding of the relationships between N and P availability and photosynthesis in the generation of plant biomass, the objective of this chapter.

Photosynthesis is demanding in N- and P-usage because of its requirement for the protein ribulose-1,5-bisphosphate carboxylase/oxygenase (RuBisCO) (Evans, 1989; Makino, 2003; Parry *et al.*, 2008), possibly the most abundant protein of the cell, and perhaps on earth (Ellis, 1979; Raven, 2013), requiring large numbers of N-rich amino acids. The Calvin cycle, where RuBisCO incorporates CO_2 into sugars in the dark reaction of photosynthesis, requires energy from the P containing chemicals ATP and NADPH. There is also a significant demand for N in synthesizing the light harvesting pigment-protein complexes, another major demand for N related to photosynthesis (Evans, 1989). Given all these competing demands, we investigate potential trade-offs between photosynthesis, growth and reproduction under nutrient limitation.

Crop biomass is the product of the cumulative action of photosynthesis during the growing period. Light harvesting in plants occurs in the chloroplasts by light harvesting complexes (LHCs) embedded in the photosynthetic membrane of the thylakoids. The light is absorbed as photons by chlorophylls (which is N-rich), which activates electron transport and proton translocation across the membranes, resulting in the synthesis of the molecules NADPH and ATP (P-rich), which are finally used in the Calvin cycle for CO_2 fixation (Hall & Rao, 1999).

Chlorophyll fluorescence is frequently used to assess the efficiency of the photosynthetic apparatus and how this is impacted by environmental stress (Sayed, 2003; Baker, 2008; Murchie & Lawson, 2013). It is based on the observation that only part of the absorbed sun's light energy is used for the photochemical energy conversion by photosystem II (PSII). The remaining light energy is emitted either as fluorescence or heat (Ruban, 2013). Photosynthetic efficiency can be measured from an analysis of Rapid Light Curves (RLC) and Induction Light Curves (ILC), which together provide details of the relative electron transfer rate (rETR), the amount of light energy that could be used (photochemical quenching – qP), or the amount of energy that cannot be used and is dissipated either as heat (= non-photochemical quenching (NPQ)) or as fluorescence (Maxwell & Johnson, 2000). Ruban (2017) highlights the importance of enhancing crop performance by optimization of light harvesting management, for example via modulation of NPQ.

The light energy needs to be transformed into chemical energy (ATP and NADPH) for the dark reaction of photosynthesis that involves CO_2 fixation via the Calvin cycle. The efficiency of the dark phase of photosynthesis can be measured by CO_2 uptake analysis (generating A/Ci curves), that measures maximum rate of CO_2 uptake (A_{max}), maximum RuBisCO activity (V_{cmax}) and maximum rate of electron transport used for the regeneration of ribulose-1,5-bisphosphate (RuBP) (J_{max}) (Farquhar *et al.*, 1980).

In previous chapters, we observed that plant GS influences photosynthesis, i.e. in *Fritillaria* A_{max}, V_{cmax}, J_{max}, g_s, F_v/F_m and rETR are all negatively correlated with GS, with similar results in *Nymphaea* for rETR, whilst in *Nymphaea* F_v/F_m and NPQ were positively related to ploidy. One reason why GS might influence photosynthesis could be that increasing GS leads to greater demands for N and P in the nucleus, leaving less of these nutrients available for photosynthesis. To test the hypothesis that N and P deficiency does indeed impair photosynthesis in a way predicted by this hypothesis, we grew wheat under different fertilizer input. We found similar responses to those predicted by the hypothesis, and we now need to repeat these observations in wheat at different ploidy levels (and hence GS), but that will be done in subsequent studies.

To investigate this, the chapter has studied the impact of N and P availability on a range of photosynthesis and growth parameters under limiting N and P in the dwarf wheat *Triticum aestivum* L. cv. USU-Apogee (Bugbee *et al.*, 1997). This cultivar was developed specifically for growth in the space station, because it is only 30cm high at flowering, it germinates easily without vernalisation, grows fast (seed to seed in 3 months) and is a polyploid (2n=6x=42) with a large genome size (GS, 1C=17.11pg), meaning that the plant should have high demands for N and P in the nucleus. It is thus an ideal model for these experiments. These characters contrast strikingly with those of the model plant *Arabidopsis thaliana* (1C= 0.16pg, 2n=2x=10) whose genome is c. 100x smaller and is functionally diploid. We reasoned that large GS will impact N and P metabolism, both through the direct N and P costs of building nucleic acids and their assembly into chromatin, which requires proteins.

Materials and methods

Plant material and growth conditions

A total of 108 seeds of the wheat cv. USU-Apogee were grown in 16 different combinations of nitrogen and phosphate (Table 4.1) in a synthetic soil mixture composed of perlite, vermiculite, fine sand and coir (3:2:1:1 by volume).

The seeds were sourced from two places, and subdivided into three categories: 1) 36 seeds from Utah University (USA) - US1G, 2) 36 from seeds obtained from University of Bristol (UK) - BS1G, and, 3) 36 seeds derived by selfing plants grown from the University of Bristol sourced material - BS2G. The seeds were divided equally into two different groups of experiments (A and B), thus there were 54 seeds for each group and six seeds per treatment, except the control (zero N/zero P – meaning no addition of N and P) which had the triple the number of seeds (i.e. 18).

The nutrient solutions were prepared with 4.33g/L MS medium (Murashige & Skoog, 1962) for high N/high P treatment; 0.61g/L MS modified medium (i.e. MS medium without NH_4NO_3, KNO_3 and KH_2PO_4), plus 1650 mg/L NH_4NO_3 and 1900 mg/L KNO_3 for high N/zero P treatment; 0.61g/L MS modified medium, plus 170 mg/L KH_2PO_4 and 710mg/L KCl for high P/zero N treatment, and 0.61g/L MS modified medium plus 710 mg/L KCl for the control treatment with no addition of N and P. The intermediary treatments were set up with 0.61g/L MS modified medium plus 0%, 25% and 50% of KCl, NH_4NO_3, KNO_3 and KH_2PO_4. For further detail of nutrients concentrations, please refer to Table 4.1.

Soil and nutrient solutions were mixed in a 4:1 volume ratio soil:solution, and the mixture was autoclaved to free the mixture of eventual fungi, pesticides and bacteria, then the mixture was left in the dark at 20ºC and turned over everyday for 8 days to allow complete homogenization of the nutrients with the soil.

All seeds were disinfected using a solution of 10% of sodium hypochlorite, 0.1% of Tween-20 and 89.9% distilled water. Ten seeds were placed into 2 mL tubes and 1 mL of the disinfection solution was added. The tubes were gently vortexed and left to stand for 10 minutes before being rinsed five times with distilled water. The seeds were then left to dry for one day before being sown in pots of dimensions 7.5 x 7.5 x 5 cm (= 200 ml volume) and watered with distilled water and left in a cold dark room for seven days to synchronize the germination of seeds. Finally, the pots were placed in a growth room with constant temperature (25ºC) and light (150-200 µmol photons m^{-2} s^{-1}) with intermittent light. There were three replicates of each treatment for experiment A and B, except the zero (=control) treatment, which had nine replicates because it is the experimental control which needs the greatest confidence in the distribution of the data (i.e. StDev, mean etc.) for comparisons with data from the different treatments.

For each N and P treatment, equal numbers of seeds from the three sources (BS1G, BS2G, US1G) were used. All seeds germinated on the third day after being transferred to the growth room and all the harvesting for experiment A was done between days 14 and 22 of growth (third week). Plants of experiment B which were used for the collection of photosynthesis data were analyzed at the same time as plants from experiment A were harvested. The plants were watered with distilled water three or four times a week as necessary. The pots were randomly arranged in groups of five on circular plates on the shelf and their positions were changed every second or third day by rotating the plates and changing the plate position on the shelf in a design that minimized potential position effects (e.g. edge effects) influencing the data.

Photosynthetic measurements

Chlorophyll fluorescence (i.e. F_o, F_m, F_v/F_m, qP, NPQ, ETR_{max}, E_k) and gas exchange (i.e. A_{max}, J_{max}, V_{cmax}) data were collected as described in Chapter 2. Measurements were made on fully emerged leaves of plants in experiment B (eight plants from the control and three plants from each of the treatments) two to three weeks after seed germination (age of plants was used as fixed effect in linear models) when they had only three to four leaves. The methods and equipment used for collecting the data are explained in Chapter 2.

Harvesting

Plants from experiment A were harvested on their third week of growth for C:N:P of green leaves, for biomass of above ground plant and roots, and for specific leaf area (SLA, leaf area/leaf dry mass). Plants from experiment B were measured also for photosynthesis at the third week of growth, but were harvested only after 3 months of growth, when they all had set seeds and dried. All plants had only one tiller (i.e. the main stem) and average of 5 leaves each. Measurements of above ground plant biomass, height, and biomass and number of seeds were obtained. Between one to three seeds were used per plant for C:N:P analysis while the remainder were set aside to enable further growth experiments to undertaken.

Specific Leaf Area (SLA) analysis

The SLA data were obtained by (i) measuring images of leaf pieces using ImageJ software to determine the leaf area, and (ii) after drying in a drying cabinet at 40˚C for three days, the leaves were weighed. Together these data were used to calculate SLA by dividing leaf area by leaf dry mass. These data were collected from all plants of experiment A.

Root biomass

Stems were cut off at their base. Roots were then taken from the soil, cleaned carefully with distilled water to remove the synthetic soil mixture. Rinsed roots were left to dry in the drying cabinet at 40˚C for 8 days and finally weighed.

C:N:P

The second leaf of each plant in experiment A were collected for carbon, nitrogen and phosphorus analyses. The fresh samples were weighed, and ~5 mg of material was placed in 2 mL tubes, put in a drying cabinet at 40°C for three days to allow them to dry completely, and weighed again. After that, they were ground in the TissueLyser LT

QIAGEN with one or two metal beads in each tube, then the beads were removed from the tubes.

Phosphorus determination: each sample was subjected to acid-peroxide digestion to allow the conversion of P-containing compounds to phosphate. Potassium persulfate (0.15 g) and 1N sulphuric acid (1mL) were added to each tube and homogenized, followed by autoclaving for 40 minutes at 120°C. The samples were left to cool and were then filtered using 0.2 µm filters. Finally, the samples were analysed in a Segment Flow Analyser (San^{++}, Skalar Analytical B.V., Breda, The Netherlands).

Carbon and nitrogen levels were determined by mass spectrometry in a stable isotope analyser (Integra 2, Sercon, United Kingdom). The leaf powder of samples for N and C determination was weighed in ultra-clean tin capsules using high precision weighing scales.

C, N and P measurements were also made using the seeds from plants in experiment B. One to three seeds per plant were ground and weighed for these determinations.

Second generation experiment

Seeds of each treatment from plants of experiment B were used to establish an additional growth experiment (refer to Table 4.5 for number of seeds sown) - this is referred to as the 'Second Generation Experiment'. They were grown in well-nourished soil in square pots of dimensions of 7.5 x 7.5 x 5 cm in the same growth room and conditions of light and temperature as the first experiments. The plants were watered with tap water twice a week to ensure they would uptake nutrients from water as well. After 3 months of growth the plants were harvested and the whole above ground plant biomass, seed number and seed biomass were recorded.

Statistical analyses

Data were analysed by linear models (LMs) using R version 3.3.1 (R Core Team, 2016). The best-fit models were found using the *drop1* function, comparing values of R^2 and observing the diagnostic plots. When appropriate, data were transformed using the $\log_e$ or square root functions. A generalized linear model (glm) was used for analyses with the number of seeds, the number of stems and the proportion of plant success (i.e. the number of plants that set seeds/number of plants planted). Interactions between N and P were always tested in the models, unless the command *drop1* showed that the interaction does not occur and the model performance is improved with its exclusion. Interaction between independent variables mean that the effect of one variable depends on the effects of another variable.

Results

Growth response curves in response to N and P limitation

Wheat plants were grown under sixteen treatments of N and P limitation (Table 4.1). The growth response curves in terms of above ground biomass over the range of N and P conditions tested are shown in Figure 4.1. They show that plants grown under increasing N in the presence of high P (Figure 4.1A), or under increasing P in the presence of high N (Figure 4.1B) increased in biomass over the range of concentrations of N and P used here, from about 0.6 g to 2 g per plant.

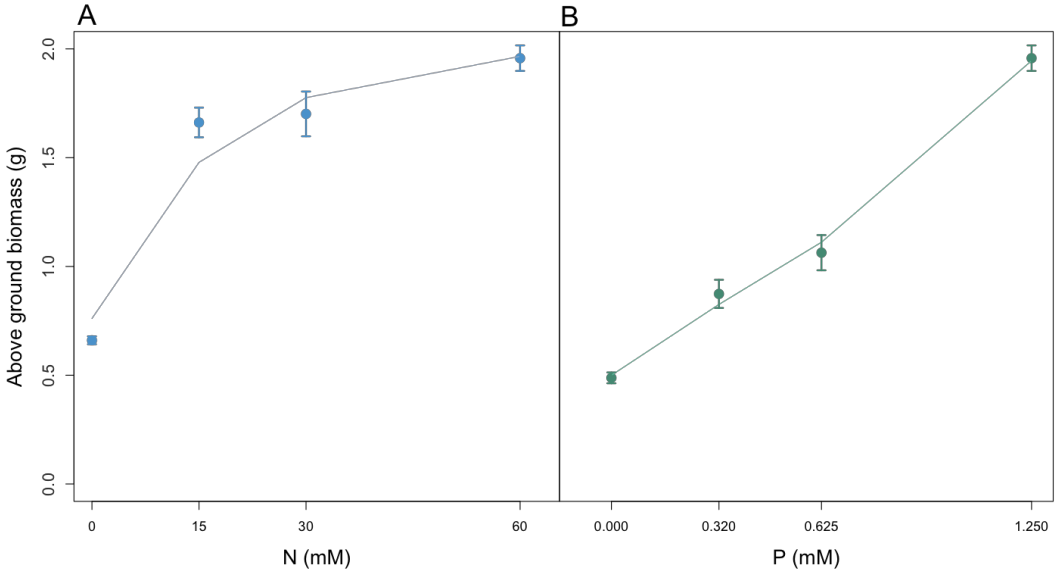

Figure 4.1. Response curves showing plant biomass with (a) addition of N and (b) addition of P. Each point is the average biomass for all plants in the treatment. Error bars = standard error.

For modelling, seed source and age of plants (at time of photosynthetic data collection) were considered as categorical and numerical variables in the models, respectively. Seed source had a significant effect on growth parameters (i.e. shoot:root biomass ratio (i.e. ratio between above ground biomass and root biomass), plant height, number of seeds produced), carbon in seeds, and the photosynthetic parameters (F_o, F_m), probably reflecting the condition of the seed (e.g. the C:N:P content) at the start of the experiment. In contrast the variable "age" of the plants over the period of photosynthetic data collecting had no significant effect. Nevertheless, even though these variables did not have significant effects on the response variable, they were retained in many of models because they improved the model performance (i.e. they were not excluded by *drop1* command in R).

The generation of biomass and number of seed under N and P limitation

In plants in their 3rd week of growth after germination (experiment A, Table 4.2 presents all the LMs results), LMs reveal that the application of N and P was not associated with any changes in root biomass. There was however a significant increase in above ground biomass ($p<0.001$, $R^2=0.28$) and in ratio of shoot to root biomass ($p<0.05$, $R^2=0.49$) caused with addition of P. There were also significant interactions between N and P associated with a decrease in specific leaf area (SLA, leaf area/leaf dry mass, $p<0.05$, $R^2=0.3$). Carbon content per gram of leaf dry weight increased significantly with addition of N and decreased with addition of P ($p<0.01$, respectively, $R^2=0.3$). In addition, there was a significant increase in leaf P content ($p<0.0001$, $R^2=0.76$) and leaf N content ($p<0.0001$, $R^2=0.54$) with added P and N respectively, but no evidence of interactions between available N and P and that found in the leaf. The nutrient ratios in green leaves were significantly affected by N and P input, N:P and C:P ratios increased with N and decreased with P ($p<0.0001$, $R^2>0.7$).

In wheat plants grown to seed set (i.e. experiment B, Table 4.3 shows all the LMs results), above ground biomass (excluding seeds) was estimated after seed set. Linear models showed significant positive effects on biomass with the addition of P and through N and P interactions ($p<0.05$, $R^2=0.72$, Figure 4.2a), N and P interactions also significantly influenced plant height ($p<0.01$, $R^2=0.55$, Figure 4.2b). The data from LM show that for each unit applied N there is an increase of 0.00012g in above ground biomass, and for each unit applied P the increase is of 0.0064g.

There was significant increase in total weight of seeds per plant with the addition of P and with N and P interactions ($p<0.05$, Table 4.3c, Figure 4.3a). Whilst there was an increase in number of seeds per plant with the addition of N and P, this was associated with a drop in individual seed weight ($p<0.05$, Table 4.3d). Depending on treatment used, the numbers of seeds ranged from zero to 30 per plant (high N, high P, Table 4.4, Figure 4.3c). Surprisingly, several plants made seeds even in soils with zero N and zero P added (i.e. the controls), probably reflecting high storage of these nutrients in the seed. There was a drop in individual seed weight when N was added and a rise with the addition of P ($p<0.05$, $R^2=0.35$), but no evidence of any interactions between N and P influencing individual seed weight. Curiously, P content in seeds did not differ between treatments, while N content in seeds increased with N and decreased with P ($p<0.001$, $R^2=0.53$). Yet, carbon content in seeds decreased significantly by the addition of P ($p<0.0001$, $R^2=0.49$), but it was also related to the seed's parental source ($p<0.05$). The N:P ratio

decreased significantly with the addition of N or P ($p<0.001$, $R^2=0.49$), and the C:P ratio decreased with the addition of P ($p<0.05$, $R^2=0.13$).

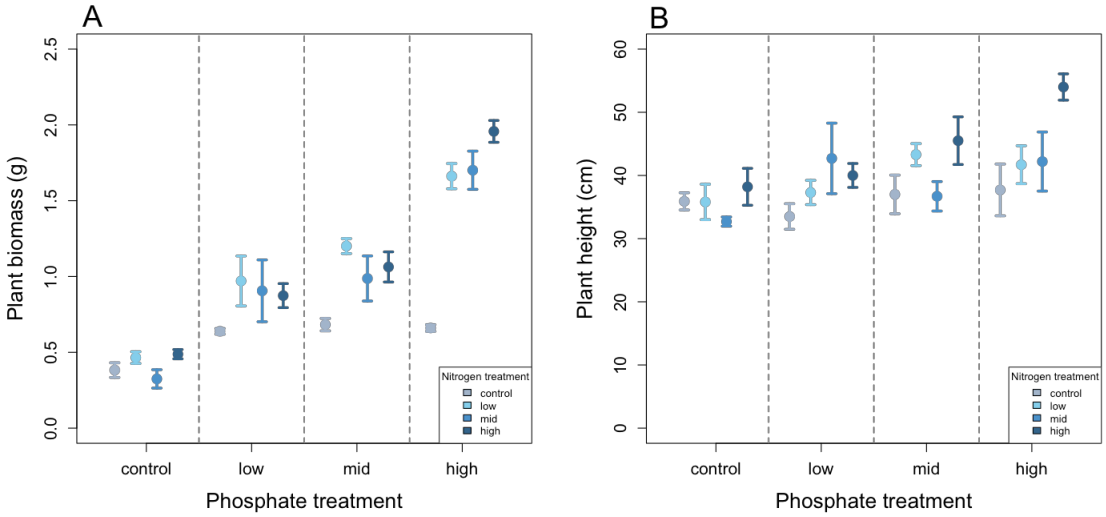

Figure 4.2. The effect of phosphate and nitrogen input on (a) above ground biomass and (b) height. Error bars = standard error.

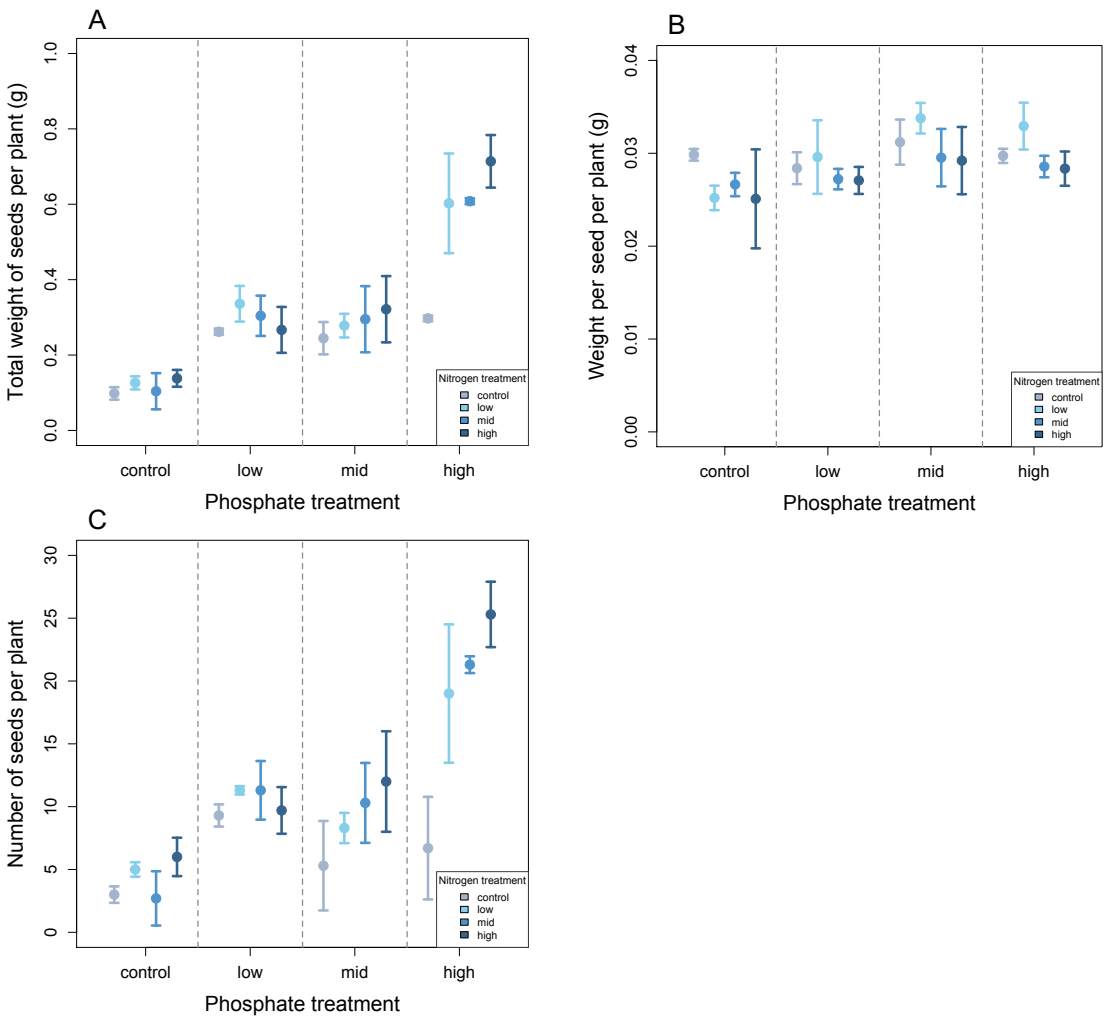

Figure 4.3. The effect of phosphate and nitrogen input on the production of seeds. (a) Number of seeds per plant; (b) total biomass of seeds per plant, (c) biomass per seed per plant. Error bars = standard error.

Second generation experiment

Most of the seeds produced from the 16 treatments of experiment B germinated, grew and set seeds themselves under high nutrient conditions (Tables 4.5 and 4.6). Neither the biomass of these plants, total seed weight, nor the proportion of number of plants which set seeds by number of seeds sown were significantly influenced by the N and P treatments of their parents (Table 4.7), while a significant decrease in the number of seeds and individual seed weight was significantly affected by the N and P input of the parents, respectively (Table 4.7d, f). A visual examination of the plants strongly indicated that the seeds derived from parents grown in zero N and zero P grew vigorously and put on more biomass than seeds from other treatments (Figure 4.4). However, this

observation was not borne out by the statistical tests (Table 4.7b). Nevertheless, it is of interest that the slope for biomass production is negative when the parents were grown on N and P. Although this trend was insignificant, for P it was close to significant (p=0.0619). It is possible that there was insufficient power in this second generation experiment for patterns to emerge, especially given that some categories of treatments had very few seeds (for example zero N zero P parents only produced 4 seeds for experimentation).

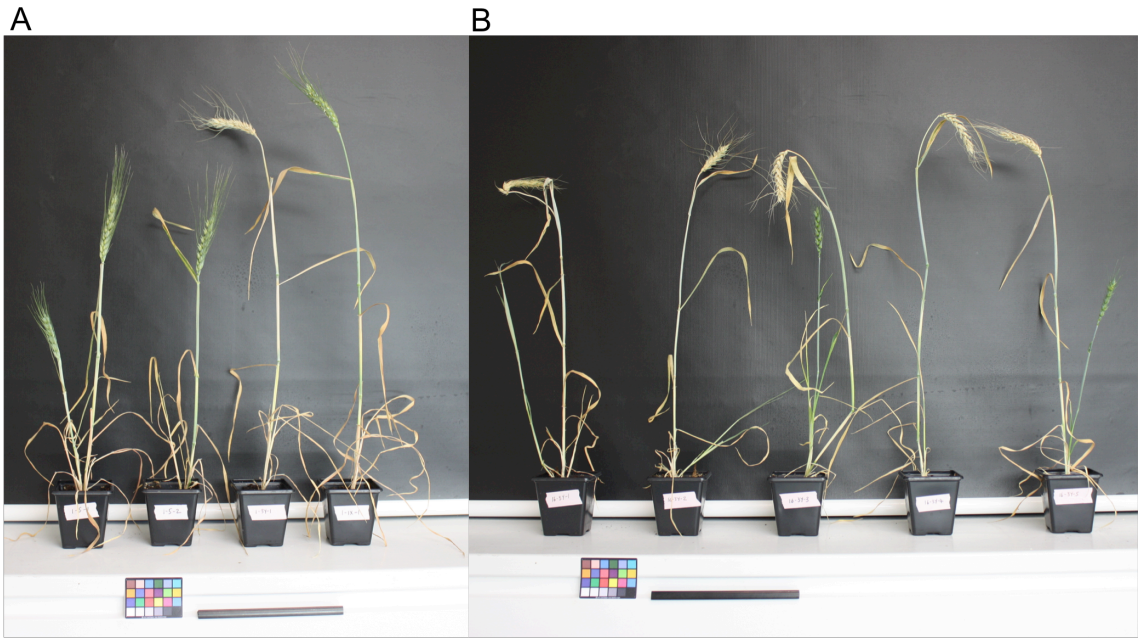

Figure 4.4. Plants from the second generation experiment. (a) Second generation of zero N and zero P treatment; (b) second generation of high N and high P treatment. Black ruler = 15 cm.

Photosynthesis efficiency

In young seedling plants (2 weeks post germination, experiment B), we obtained measures of the light reaction of photosynthesis under varying nutrient limitations. Readings of F_o, F_m and F_v/F_m were taken from both fluorescence rapid light curves (RLC) and induction light curves (ILC). The addition of P significantly decreased F_o (minimum fluorescence level, $p<0.05$, $R^2=0.11$, Table 4.8), however N and P had no significant effect on F_m or F_v/F_m. RLC revealed that N and P limitation had no significant effect on E_k, but N and P interactions increased rETR significantly ($p<0.05$, $R^2=0.11$, Table 4.8). ILC was used to obtain information on qP (photochemical fluorescence quenching) and NPQ (non-photochemical fluorescence quenching). The application of P significantly

increased qP ($p<0.001$, $R^2=0.23$, Table 4.8) and decreased NPQ ($p<0.01$, $R^2=0.38$, Table 4.8).

We also obtained readings of the dark reaction of photosynthesis from the same seedlings. A/Ci curves were used to get information on V_{cmax} (RuBisCO activity), J_{max} (maximum rate of electron transport used to regenerate RuBP, the substrate for RuBisCO) and A_{max} (maximum rate of CO_2 uptake). N and P interactions increased V_{cmax}, J_{max} and A_{max} ($p < 0.01$, $R^2=0.2$, Table 4.8).

Interactions between N, P and photosynthesis efficiency on production of seeds

Linear models were used to see how N, P plus photosynthesis efficiency influenced the production of seeds. The production of seeds and plant biomass were significantly and positively related with A_{max} (Table 4.9, Figure 4.5) when included in the models with N and P. Although A_{max} is positively related with total weight of seeds it did not influence significantly on that when included in the model together with N and P ($p=0.0522$, Table 4.9b, c).

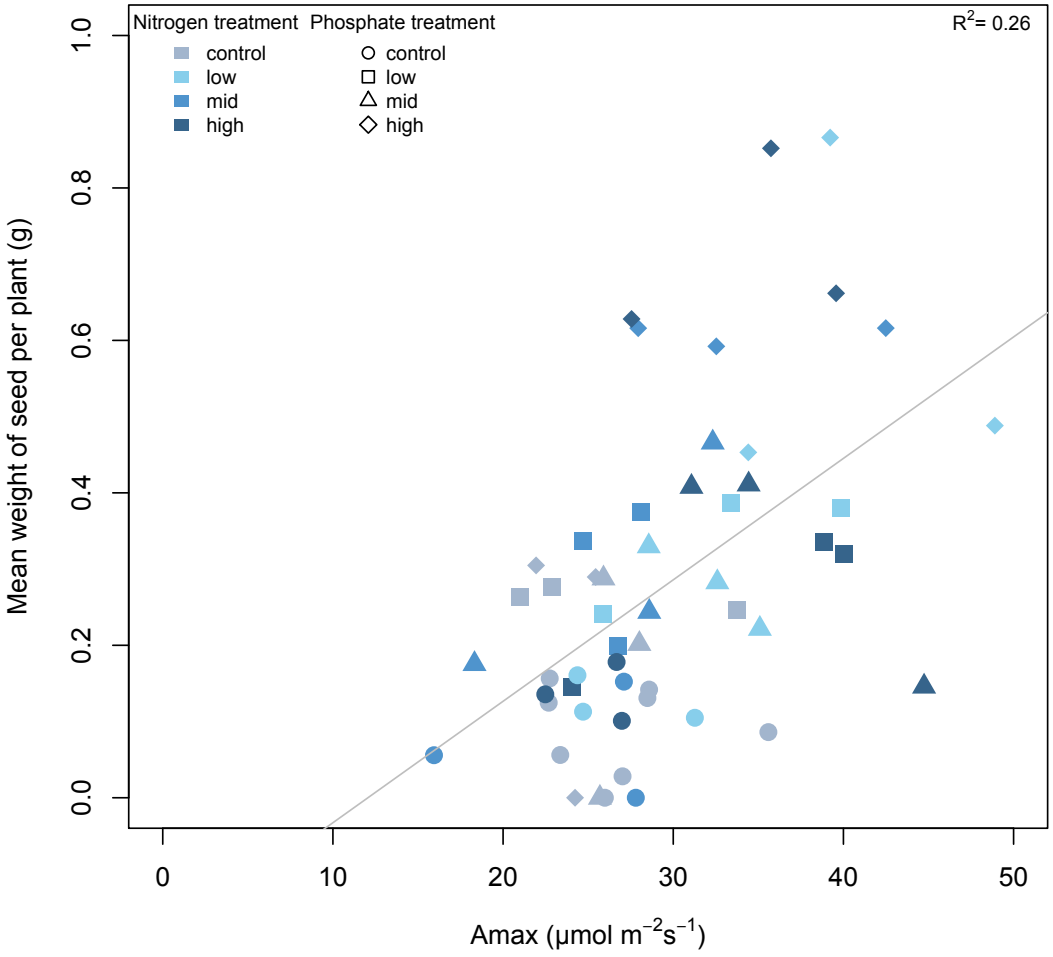

Figure 4.5. A_{max} in response to mean total weight of seeds per plant for all treatments.

Nitrogen and yield

The amount of nitrogen in seeds was significantly increased by addition of N, but decreased by addition of P, by number of seeds per plant and by interactions between N and P ($p<0.05$, $R^2=0.59$, Table 4.9e), while the amount of nitrogen in seeds was not explained by the individual weight of seeds.

Discussion

The generation of biomass and seeds under N and P limitation

This study shows that both nutrients N and P and their interaction are important for the production of vegetative biomass and grain yield (both numbers and biomass of grain, Table 4.3). Many studies have been performed in crops, including wheat, to look at optimal fertiliser input and type to improve yield, however most have only tested the effect of limiting N on crop yield (e.g. Evans (1983); Makino & Osmond (1991); Holford *et al.* (1992); Reeves *et al.* (1993); Shangguan *et al.* (2000); Wright *et al.* (2004); Gao *et al.* (2009); Basso *et al.* (2010); Cui *et al.* (2010)), while interactions between N and P were not the focus of these studies. Here, we show that the effects of P addition on the increase in shoot:root biomass ratio and on accumulation of biomass is already apparent in the 3 week old seedlings (experiment A), and highly significant by the end of their growth phase (experiment B).

Seed source and the interaction between N and P had a significant effect on plant height (Table 4.3b). Height is related to the ability of a plant to compete for light, however it is also a result of carbon sequestration through its relationship to biomass (Moles *et al.*, 2009). The tallest plants are the ones grown with high N and high P, and the interaction of these nutrients is important for height (i.e. individually they are not so important). The source of the seed also proved to be important, probably because they contained different levels of stored nutrients, especially N, given that the seeds were responsive to P. As seen in other studies, P stress and deficiency reduces shoot:root biomass ratio through reduction of shoot growth (Atkinson, 1973; Fredeen *et al.*, 1989), which directly reduces biomass. Stem emergence is slowed and reduced under P limitation, as seen previously in an experiment on wheat (Rodríguez *et al.*, 1999).

Nitrogen and P are required for plant growth (e.g. cell division, synthesis of nucleic acids) and seed production (protein synthesis, which is demanding on P). Above ground biomass was influenced by N and P interactions, and by P alone (Table 4.3a and Figures 4.1, 4.2a). The effect alone may be influenced by stored N in the seed and also by the

need for P for converting light into chemical energy, i.e. addition of P increases qP (i.e. energy transfer through PSII). Such a response is similar to that observed by Lauer *et al.* (1989) who showed that under P stress the photosynthetic efficiency of cells in soybean leaves were reduced through the lower availability of inorganic phosphate (Pi), used in ATP.

The study reported here also uncovered significant negative interactions between N and P and specific leaf area (SLA) (Table 4.2d) because the increase in nutrients resulted in thicker leaves and hence lower SLA. This could arise either through more cell layers or larger cells, or perhaps both. In some species the number of palisade layers can differ between individuals (Hanson, 1917), and increasing numbers of cell layers and/or larger cells could be associated with increased numbers of chloroplasts, photosynthetic proteins and chlorophyll pigments, all of which require large amounts of N (Doncheva *et al.*, 2008). Indeed chlorophyll content has been reported to decrease in leaves with N deficiency (Zhao *et al.*, 2005). However, the functioning of these proteins and pigments require P (e.g. for ATP, NADPH and protein phosphorylation), generating a co-limitation for both nutrients. Thus, whilst increasing abundance of chloroplasts and pigments may increase photosynthetic efficiency (Evans & Poorter, 2001), it is likely that such an increase (Table 4.8, 4.9) is dependent on interactions between both N and P, rather than each of these nutrients in isolation.

The production of seedling biomass in wheat was significantly influenced by P application alone (Table 4.2b), almost certainly because of high levels of stored N in the seed. In the mature plants and in seed yield, there were also interactions of N and P as well as P effects alone (Table 4.3a). We know the effects of stored N and P in the seeds are substantial, given that plants grown without any N or P applied were able to make seeds (Table 4.6), a situation where all biomass production must reflect that storage. Previous studies have measured the absolute levels of starch in plants of *Glycine max* grown under low and high P growing conditions in the presence of plentiful N. Starch levels were shown to be higher in plants grown under low P compared with those grown in high P, although the rates of starch accumulation and degradation were lower in low P growing plants (Fredeen *et al.*, 1989; Qiu & Israel, 1992). Potentially, here too, co-limitation of N and P impairs growth, and under low P the energy of photosynthesis is shunted towards starch production, perhaps the least N and P demanding process for that energy. These observations agree with those of Rao & Terry (1989) who showed that the levels of starch synthesis increased in plants of sugar beet (*Beta vulgaris*) grown under limited P, while Kindred *et al.* (2008) showed a decrease in starch content related to N fertiliser application. Potentially the plants in Kindred *et al.*'s experiment were

moving energy from storage to growth, but it is suspected that would not have happened unless sufficient P was also available.

Chlorophyll fluorescence

This study revealed that P limitation had a major, significant effect on the fluorescence parameters qP and NPQ (Table 4.8f and g). Potentially this arises in part because of ATP and NAPDH deficiencies in P limited plants which may therefore be less efficient/limited in their ability to convert light energy into chemical energy during the light reaction of photosynthesis (i.e. qP) and in dissipating excess light energy as heat (i.e. NPQ) (Campbell & Sage, 2006). In contrast, the parameter F_v/F_m did not significantly change between the different fertiliser treatments, perhaps through regulation in the number of chloroplasts, and number of PSII's and functional thylakoid membranes, commensurate with nutrient availability, to maintain optimal chloroplast functionality. In short, the wheat plants may be trading quality over quantity.

The significant effect of P addition on qP and NPQ may arise because the light energy for photosynthesis is used more effectively when there are sufficient levels of P. With the addition of P, NPQ drops and qP rises significantly. This means that more energy is being transferred for photochemistry and less dissipated as heat energy than in plants where P levels are limiting. Potentially, plants lacking P do not have sufficient ATP and NADPH to carry the energy needed in the Calvin cycle, where CO_2 is fixed. In addition, the activity of enzymes associated with P in the Calvin cycle could change under P limitation as previously shown by Rao & Terry (1989) who studied the impact of limiting levels of P on the activity of six of the Calvin cycle enzymes. Lu *et al.* (2001) examined the effects of N limitation on qP in maize (*Zea mays*) and wheat. They found an effect of N limitation, which differs from the results obtained here. However their experiment varied N (high and low) in constant P and without effect models the effects of N on its own or its interaction with P cannot be unpicked. This study also showed that a significant increase in ETR_{max} arose from interactions between N and P (Table 4.8e). This is probably because of an increase in chlorophyll content associated with the addition of N, which together with sufficient ATP and NADPH, enables an increased rate of electron transport through PSII.

Photosynthetic characters

In the wheat experiments presented here, interactions between N and P were shown to increase the photosynthetic rate parameters V_{cmax}, J_{max} and A_{max}. These results are consistent with previous research which has shown the importance of P for photosynthesis (Sivak & Walker, 1986; Terry & Rao, 1991; Xu *et al.*, 2007; Reich *et al.*,

2009). For example, in a large comparative analysis using data from 314 plant species, Reich *et al.* (2009), reported the impact of low P on A_{max} and its relationship with N. The study showed that there were interactions between N and P contents in leaves which contributed to increasing $A_{max,}$, and that the relationship between A_{max} and N content was constrained by P. Reich *et al.*'s broad scale analysis is consistent with experimental studies which have shown that P-deficiency limits ribulose-1,5-bisphosphate (RuBP) regeneration and that in the absence of adequate P availability, photosynthetic rates, activation of RuBisCO, and regeneration of (RuBP) decrease (Brooks, 1986; Brooks *et al.*, 1988; Campbell & Sage, 2006). A deficiency of N however may limit the production of pigments (Li *et al.*, 2008) and photosynthetic proteins are impaired. Overall it is clear that while some components of photosynthesis are impacted by N or P deficiency alone, other components are co-limited by both these nutrients. It is therefore to be expected that there is a strong co-limitation of these nutrients and that N and P interactions are central to plant growth and yield.

Seed production

Wheat generates seeds by reallocating nutrients from the plant to the seed. Thus seed production should be directly impacted by the amount of biomass produced, which are in turn influenced by N and P availability. In the absence of any N and P addition, plants were able to generate seeds, revealing that the parent seed must have had enough reserves of these nutrients for that to have happened. Nevertheless, we have shown that the total seed weight per plant is significantly affected by interactions between N and P limitation and further influenced by P alone (Table 4.3c), while number of seeds per plant is most strongly influenced by the presence of P (and close to significant for N) (Table 4.3d). A role for N (e.g. Cui *et al.*, 2010) and P (e.g. Grant *et al.*, 2001) separately have been shown previously. What is important to emphasise here is the importance of interactions between N and P in influencing seed yield.

The number of seeds is highly negatively correlated with the individual weight of seeds, i.e. plants with high numbers of seeds had lighter seeds (Table 4.3d). Yet, when looking at the amount of carbon (C), N and P in seeds, it was seen that while P increased individual seed weight (Table 4.3e), the addition of P decreased the proportion of C (Table 4.3h) and N (Table 4.3g) in the seeds, presumably through less stored starch and N. The decrease in individual seed weight in plants with a higher number of seeds can be explained by the decrease in C content (probably starch) in seeds grown under higher P treatments. Probably, under P limitation, plants selectively produce fewer larger seeds, with high starch content and in the presence of N, stored N as well.

Previous research has shown that N input as fertiliser is important for grain yield production in crops (Edmeades, 2003). However, the results shown here highlight that the importance of N addition is dependent on the availability of P (i.e. there are significant N:P interactions influencing total seed weight, Table 4.3c), or that only the addition of P increases individual seed weight (Table 4.3e). The later probably reflects plentiful stored N in the seeds. It is currently unclear why N input has a negative effect on individual seed weight (Table 4.3e).

Nitrogen content in seeds was significantly increased with the addition of N, but decreased with the addition of P and with N:P interactions (Table 4.9f). These negative effects probably arise through less stored N relative to biomass and a higher use efficiency of N by plants when P is present. It is also of interest that the seeds have high N, when N is applied without P. Clearly the plants do store excess N in seeds, providing further evidence that stored N in the seeds at the start of the experiment has influenced the data presented here. Many studies have been published on grain protein storage in wheat, for example gluten needed in bread making (Shewry & Halford, 2002; Goesaert *et al.*, 2005), but what has not been the focus is how these stored products can influence the future growth of seedlings under nutrient limitation.

The production of seeds (number and individual seed weight) was also correlated with A_{max}, that is probably because N and P are both important for increasing the rates of A_{max}, as discussed above. Figure 4.5 shows a positive relationship between total seed weight and A_{max}, however what drives that relation is the interaction between N and P.

Conclusion

Crop plants are fertilised to be more efficient in the production of vegetative or seed biomass, essential to sustain a growing human population (Tilman *et al.*, 2002). While there are many previous studies that have explored the optimal fertiliser treatment for different wheat cultivars/varieties (Memon *et al.*, 2011; Khan *et al.*, 2014; Abbas *et al.*, 2016), in general these studies were conducted in the field, where it is difficult to carefully control N and P availability to the plants (especially P). The experiments here attempted to overcome these issues by tightly controlling the levels of N and P, taking advantage of the wheat cultivar Apogee which is a cultivar with dwarfing genes that enables the plants to be easily grown under lab conditions. The results indicate a strong N and P co-limitation influencing the growth and yield of these wheat plants, an effect that may be partially masked by stored N in the seeds at the start of the experiment. The amount of

N probably reflects the condition of the parent plants, frequently generating significant seed source effects.

References

Abbas M, Shah JA, Irfan M, Yousuf Memon M. **2016**. Growth and yield performance of candidate wheat variety 'BWQ-4' under different nitrogen and phosphorus levels. *American-Eurasian Journal of Agricultural & Environmental Sciences* **16**: 952–959.

Atkinson D. **1973**. Some general effects of phosphorus deficiency on growth and development. *New Phytologist* **72**: 101–111.

Baker NR. **2008**. Chlorophyll fluorescence: a probe of photosynthesis in vivo. *Annual Review of Plant Biolology* **59**: 89–113.

Basso B, Cammarano D, Troccoli A, Chen D, Ritchie JT. **2010**. Long-term wheat response to nitrogen in a rainfed Mediterranean environment: Field data and simulation analysis. *European Journal of Agronomy* **33**: 132–138.

Brooks A. **1986**. Effects of phosphorus nutrition on Ribulose-1,5-Bisphosphate Carboxylase activation, photosynthetic quantum yield and amounts of some Calvin-cycle metabolites in spinach leaves. *Australian Journal of Plant Physiology* **13**: 221.

Brooks A, Woo KC, Wong SC. **1988**. Effects of phosphorus nutrition on the response of photosynthesis to CO_2 and O_2, activation of ribulose bisphosphate carboxylase and amounts of ribulose bisphosphate and 3-phosphoglycerate in spinach leaves. *Photosynthesis research* **15**: 133–41.

Bugbee B, Koerner G, Albrechtsen R, Dewey W, Clawson S. **1997**. Registration of cultivars: registration of 'USU-Apogee' wheat. *Crop science* **37**: 626.

Campbell CD, Sage RF. **2006**. Interactions between the effects of atmospheric CO_2 content and P nutrition on photosynthesis in white lupin (*Lupinus albus* L.). *Plant, Cell and Environment* **29**: 844–853.

Clarke JM, Campbell CA, Cutforth HW, DePauw RM, Winkleman GE. **1990**. Nitrogen and phosphorus uptake, translocation, and utilization efficiency of wheat in relation to environment and cultivar yield and protein levels. *Canadian Journal of Plant Science* **70**: 965–977.

Cordell D, Drangert J-O, White S. **2009**. The story of phosphorus: global food security and food for thought. *Global Environmental Change* **19**: 292–305.

Cordell D, White S. **2011**. Peak Phosphorus: clarifying the key issues of a vigorous debate about long-term phosphorus security. *Sustainability* **3**: 2027–2049.

Cui Z, Zhang F, Chen X, Dou Z, Li J. **2010**. In-season nitrogen management strategy for winter wheat: maximizing yields, minimizing environmental impact in an over-fertilization context. *Field Crops Research* **116**: 140–146.

Dodds WK, Bouska WW, Eitzmann JL, Pilger TJ, Pitts KL, Riley AJ, Schloesser JT, Thornbrugh DJ. **2009**. Eutrophication of U.S. freshwaters: analysis of potential economic damages. *Environmental Science & Technology* **43**: 12–19.

Doncheva S, Vassileva V, Ignatov G. **2008**. Influence of nitrogen deficiency on photosynthesis and chloroplast ultrastructure of pepper plants. *Agricultural and Food Science* **10**: 59–64.

Edmeades DC. **2003**. The long-term effects of manures and fertilisers on soil productivity and quality: a review. *Nutrient Cycling in Agroecosystems* **66**: 165–180.

Ellis RJ. **1979**. The most abundant protein in the world. *Trends in Biochemical Sciences* **4**: 241–244.

Evans JR. **1983**. Nitrogen and photosynthesis in the flag leaf of wheat (*Triticum aestivum* L.). *Plant Physiology* **72**: 297–302.

Evans JR. **1989**. Photosynthesis and nitrogen relationships in leaves of C_3 plants. *Oecologia* **78**: 9–19.

Evans JR, Poorter H. **2001**. Photosynthetic acclimation of plants to growth irradiance: the relative importance of specific leaf area and nitrogen partitioning in maximizing carbon gain. *Plant, Cell & Environment* **24**: 755–767.

FAO. **2015**. World fertilizer trends and outlook to 2018. Food and Agriculture Organization of the United Nations.

FAO. **2018**. Cereal Supply and Demand Brief | World Food Situation | Food and Agriculture Organization of the United Nations <http://www.fao.org/worldfoodsituation/csdb/en/>.

Farquhar GD, von Caemmerer S, Berry JA. **1980**. A biochemical model of photosynthetic CO_2 assimilation in leaves of C3 species. *Planta* **149**: 78–90.

Fredeen AL, Rao IM, Terry N. **1989**. Influence of phosphorus nutrition on growth and carbon partitioning in *Glycine max*. *Plant Physiology* **89**: 225–30.

Gao Y, Li Y, Zhang J, Liu W, Dang Z, Cao W, Qiang Q. **2009**. Effects of mulch, N fertilizer, and plant density on wheat yield, wheat nitrogen uptake, and residual soil nitrate in a dryland area of China. *Nutrient Cycling in Agroecosystems* **85**: 109–121.

Goesaert H, Brijs K, Veraverbeke WS, Courtin CM, Gebruers K, Delcour JA. **2005**. Wheat flour constituents: how they impact bread quality, and how to impact their functionality. *Trends in Food Science & Technology* **16**: 12–30.

Grant CA, Flaten DN, Tomasiewicz DJ, Sheppard SC. **2001**. The importance of early season phosphorus nutrition. *Canadian Journal of Plant Science* **81**: 211–224.

Hall DO, Rao KK. **1999**. *Photosynthesis*. Cambridge University Press.

Hanson HC. **1917**. Leaf-Structure as Related to Environment. *American Journal of Botany* **4**: 533–560.

Holford ICR, Doyle AD, Leckie CC. **1992**. Nitrogen response characteristics of wheat protein in relation to yield responses and their interactions with phosphorus. *Australian Journal of Agricultural Research* **43**: 969–986.

Khan P, Imtiaz M, Memon M, Aslam M, Depar N, Shah JA, Ali N. **2014**. Response of wheat genotype NIA-SUNDAR to varying levels of nitrogen and phosphorus. *Sarhad Journal of Agriculture* **30**: 325–331.

Kindred DR, Verhoeven TM., Weightman RM, Swanston JS, Agu RC, Brosnan JM, Sylvester-Bradley R. **2008**. Effects of variety and fertiliser nitrogen on alcohol yield, grain yield, starch and protein content, and protein composition of winter wheat. *Journal of Cereal Science* **48**: 46–57.

Lauer MJ, Blevins DG, Sierzputowska-Gracz H. **1989**. ^{31}P-nuclear magnetic resonance determination of phosphate compartmentation in leaves of reproductive soybeans (*Glycine max* L.) as affected by phosphate nutrition. *Plant Physiology* **89**: 1331–6.

Li Y, Horsman M, Wang B, Wu N, Lan CQ. **2008**. Effects of nitrogen sources on cell growth and lipid accumulation of green alga *Neochloris oleoabundans*. *Applied Microbiology and Biotechnology* **81**: 629–636.

Lu C, Zhang J, Zhang Q, Li L, Kuang T. **2001**. Modification of photosystem II photochemistry in nitrogen deficient maize and wheat plants. *Journal of Plant Physiology* **158**: 1423–1430.

Makino A. **2003**. Rubisco and nitrogen relationships in rice: leaf photosynthesis and plant growth. *Soil Science and Plant Nutrition* **49**: 319–327.

Makino A, Osmond B. **1991**. Effects of nitrogen nutrition on nitrogen partitioning between chloroplasts and mitochondria in pea and wheat. *Plant Physiology* **96**: 355–62.

Maxwell K, Johnson GN. **2000**. Chlorophyll fluorescence - a practical guide. *Journal of Experimental Botany* **51**: 659–668.

Memon MY, Khan P, Imtiaz M. **2011**. Response of candidate wheat variety 'NIA-8/7' to different levels/rations of nitrogen and phosphorus. *Pakistan Journal of Botany* **42**: 1959–1963.

Moles AT, Warton DI, Warman L, Swenson NG, Laffan SW, Zanne AE, Pitman A, Hemmings FA, Leishman MR. **2009**. Global patterns in plant height. *Journal of Ecology* **97**: 923–932.

Murashige T, Skoog F. **1962**. A revised medium for rapid growth and bio assays with tobacco tissue cultures. *Physiologia Plantarum* **15**: 473–497.

Murchie EH, Lawson T. **2013**. Chlorophyll fluorescence analysis: a guide to good practice and understanding some new applications. *Journal of Experimental Botany* **64**: 3983–3998.

Parry MAJ, Keys AJ, Madgwick PJ, Carmo-Silva AE, Andralojc PJ. **2008**. Rubisco regulation: a role for inhibitors. *Journal of Experimental Botany* **59**: 1569–1580.

Qiu J, Israel DW. **1992**. Diurnal starch accumulation and utilization in phosphorus-deficient soybean plants. *Plant Physiology* **98**: 316–23.

R Core Team. **2016**. R: A language and environment for statistical computing. R Foundation for Statistical Computing.

Rao IM, Terry N. **1989**. Leaf phosphate status, photosynthesis, and carbon partitioning in sugar beet: I. Changes in growth, gas exchange, and calvin cycle enzymes. *Plant Physiology* **90**: 814–9.

Raven JA. **2013**. Rubisco: still the most abundant protein of Earth? *New Phytologist* **198**: 1–3.

Reeves DW, Mask PL, Wood CW, Delaney DP. **1993**. Determination of wheat nitrogen status with a hand-held chlorophyll meter: influence of management practices. *Journal of Plant Nutrition* **16**: 781–796.

Reich PB, Oleksyn J, Wright IJ. **2009**. Leaf phosphorus influences the photosynthesis-nitrogen relation: a cross-biome analysis of 314 species. *Oecologia* **160**: 207–212.

Rodríguez D, Andrade FH, Goudriaan J. **1999**. Effects of phosphorus nutrition on tiller emergence in wheat. *Plant and Soil* **209**: 283–295.

Ruban A. **2013**. *The photosynthetic membrane: molecular mechanisms and biophysics of light harvesting*. United Kingdom: Wiley.

Ruban A V. **2017**. Plant science: crops on the fast track for light. *Nature* **541**: 36–37.

Sayed OH. **2003**. Chlorophyll fluorescence as a tool in cereal crop research. *Photosynthetica* **41**: 321–330.

Shangguan Z, Shao M, Dyckmans J. **2000**. Effects of nitrogen nutrition and water deficit on net photosynthetic rate and chlorophyll fluorescence in winter wheat. *Journal of Plant Physiology* **156**: 46–51.

Shewry PR, Halford NG. **2002**. Cereal seed storage proteins: structures, properties and role in grain utilization. *Journal of Experimental Botany* **53**: 947–958.

Sivak MN, Walker DA. **1986**. Photosynthesis *in vivo* can be limited by phosphate supply. *New Phytologist* **102**: 499–512.

Terry N, Rao IM. **1991**. Nutrient and photosynthesis: iron and phosphorus as case studies. In: Porter JR,, In: Lawlor DW, eds. Plant growth: interaction with nutrition and environment. Cambridge: Cambridge University Press, 55–79.

Tilman D, Cassman KG, Matson PA, Naylor R, Polasky S. **2002**. Agricultural sustainability and intensive production practices. *Nature* **418**: 671–677.

Wright DL, Rasmussen VP, Ramsey RD, Baker DJ, Ellsworth JW. **2004**. Canopy reflectance estimation of wheat nitrogen content for grain protein management. *GIScience & Remote Sensing* **41**: 287–300.

Xu HX, Weng XY, Yang Y. **2007**. Effect of phosphorus deficiency on the photosynthetic characteristics of rice plants. *Russian Journal of Plant Physiology* **54**: 741–748.

Zhao D, Reddy KR, Kakani VG, Reddy VR. **2005**. Nitrogen deficiency effects on plant growth, leaf photosynthesis, and hyperspectral reflectance properties of sorghum. *European Journal of Agronomy* **22**: 391–403.

Tables

Table 4.1. Concentrations for all treatments under which plants were grown.

	Zero N				**Low N**				**Mid N**				**High N**			
	N	**P**	**N**	**P**	**N**	**P**	**N**	**P**	**N**	**P**	**N**	**P**	**N**	**P**	**N**	**P**
	($mg.pot^{-1}$)		(mM)		($mg.pot^{-1}$)		(mM)		($mg.pot^{-1}$)		(mM)		($mg.pot^{-1}$)		(mM)	
Zero P	0	0	0	0	10.3	0	15	0	20.6	0	30	0	41.2	0	60	0
Low P	0	0.5	0	0.320	10.3	0.5	15	0.320	20.6	0.5	30	0.320	41.2	0.5	60	0.320
Mid P	0	1	0	0.625	10.3	1	15	0.625	20.6	1	30	0.625	41.2	1	60	0.625
High P	0	2	0	1.250	10.3	2	15	1.250	20.6	2	30	1.250	41.2	2	60	1.250

*Pot volume = 200ml = $200cm^3$
*Pot area = $44.18cm^2$
*Pot dimensions = 7.5x7.5x5cm

Table 4.2. Linear models showing the effects of N and P on wheat seedlings growth parameters.

(a) root biomass, R^2=-0.02				
	Estimate	Std. Error	t-value	Pr(>|t|)
(Intercept)	<0.0001	<0.0001	11.938	<0.0001
N	<0.0001	<0.0001	0.016	0.9880
P	<0.0001	<0.0001	0.932	0.3560

(b) sqrt(above ground biomass), R^2=0.28				
	Estimate	Std. Error	t-value	Pr(>|t|)
(Intercept)	0.3141	0.0141	22.210	<0.0001
N	0.0004	0.0002	1.923	0.0601
P	0.0009	0.0002	4.091	0.0002

(c) log(shoot to root ratio), R^2=0.49				
	Estimate	Std. Error	t-value	Pr(>|t|)
(Intercept)	0.5246	0.0714	7.346	<0.0001
N	0.001	0.0015	0.891	0.3773
P	0.0026	0.0015	2.274	0.0274
SX	0.2005	0.0728	2.753	0.0083
SY	0.2649	0.0728	3.636	0.0007
N:P	<0.0001	<0.0001	1.703	0.0951

(d) log(specific leaf area), R^2=0.3				
	Estimate	Std. Error	t-value	Pr(>|t|)
(Intercept)	3.4970	0.0600	58.233	<0.0001
N	-0.0020	0.0010	-1.982	0.0532
P	0.0015	0.0010	1.464	0.1497
SX	0.1253	0.0629	1.992	0.0520
SY	0.0555	0.0640	0.867	0.3902
N:P	<0.0001	<0.0001	1.024	0.0485

(e) carbon content in leaves, R^2=0.3

	Estimate	Std. Error	t-value	Pr(>|t|)
(Intercept)	412.286	4.0967	101.06	<0.0001
N	0.2895	0.0645	4.487	<0.0001
P	-0.1796	0.0645	-2.784	0.0075

(f) log(phosphate content in leaves), R^2=0.76

	Estimate	Std. Error	t-value	Pr(>|t|)
(Intercept)	0.4245	0.0793	5.349	<0.0001
N	-0.0016	0.0016	-1.027	0.3093
P	0.0162	0.0016	10.287	<0.0001
N:P	<0.0001	<0.0001	-1.866	0.0679

(g) nitrogen content in leaves, R^2=0.54

	Estimate	Std. Error	t-value	Pr(>|t|)
(Intercept)	43.6872	1.8454	23.673	<0.0001
N	0.2176	0.0292	7.456	<0.0001
P	0.0528	0.0292	1.811	0.0761

(h) sqrt(N:P ratio in leaves), R^2=0.72

	Estimate	Std. Error	t-value	Pr(>|t|)
(Intercept)	5.2869	0.1703	31.045	<0.0001
N	0.0173	0.0027	6.417	<0.0001
P	-0.0283	0.0027	-10.507	<0.0001

(i) log(C:P ratio in leaves), R^2=0.75

	Estimate	Std. Error	t-value	Pr(>|t|)
(Intercept)	5.5248	0.0738	74.829	<0.0001
N	0.0044	0.0012	3.801	<0.0001
P	-0.0146	0.0012	-12.478	<0.0001

Table 4.3. Linear models (a, b, d, e, f, g, h, I, j) or generalised linear model (c) to show the effects of N and P on wheat biomass and yield at point of harvest.

(a) sqrt(above ground biomass), R^2=0.72				
	Estimate	Std. Error	t-value	Pr(>|t|)
(Intercept)	0.6587	0.0372	17.721	<0.0001
N	0.0006	0.0007	0.834	0.4081
P	0.0039	0.0007	5.267	<0.0001
N:P	<0.0001	<0.0001	2.649	0.0108

(b) plant height, R^2=0.55				
	Estimate	Std. Error	t-value	Pr(>|t|)
(Intercept)	31.48	1.474	21.352	<0.0001
N	0.0228	0.0237	0.959	0.3423
P	0.0266	0.0237	1.12	0.2684
SX	5.25	1.504	3.491	0.001
SY	5.194	1.504	3.454	0.0012
N:P	0.0013	0.0004	2.908	0.0055

(c) total weight of seeds per plant, R^2=0.74				
	Estimate	Std. Error	t-value	Pr(>|t|)
(Intercept)	0.0964	0.0340	2.836	0.0069
N	-0.0002	0.0005	-0.306	0.7614
P	0.0032	0.0006	5.370	<0.0001
SX	0.0748	0.0357	2.093	0.0421
SY	0.0337	0.0344	0.980	0.3323
N:P	<0.0001	<0.0001	2.625	0.0119

Table 4.3. (continued)

(d) number of seeds per plant				
	Estimate	Std. Error	z-value	Pr(>|z|)
(Intercept)	2.2215	0.5522	4.023	<0.0001
N	0.0897	0.0456	1.967	0.0492
P	0.4780	0.045	10.635	<0.0001
SX	0.2104	0.1161	1.813	0.0698
SY	0.0332	0.1372	0.242	0.809
Weight per seed	-50.3385	16.9378	-2.972	0.003

(e) weight per seed, R^2=0.35				
	Estimate	Std. Error	t-value	Pr(>|t|)
(Intercept)	0.0308	0.001	31.79	<0.0001
N	<-0.0001	<0.0001	-2.847	0.0066
P	<0.0001	<0.0001	2.789	0.0077
SX	-0.0008	0.0011	-0.697	0.4893
SY	-0.0045	0.0011	-4.143	0.0001

(f) phosphate content in seeds, R^2=0.08				
	Estimate	Std. Error	t-value	Pr(>|t|)
(Intercept)	0.733	0.1072	6.839	<0.0001
N	-0.0034	0.0017	-2.025	0.0502
P	0.0024	0.0019	1.309	0.1985

(g) nitrogen content in seeds, R^2=0.0.53				
	Estimate	Std. Error	t-value	Pr(>|t|)
(Intercept)	33.7265	1.5516	21.736	<0.0001
N	0.1003	0.0239	4.2	0.0001
P	-0.1596	0.0239	-6.679	<0.0001

(h) carbon content in seeds, R^2=0.49				
	Estimate	Std. Error	t-value	Pr(>|t|)
(Intercept)	6.154	0.0221	278.137	<0.0001
N	<-0.0001	0.0003	-0.024	0.9812

P	-0.0016	0.0003	-5.917	<0.0001
SX	0.0911	0.0254	3.583	0.0009
SY	0.0696	0.0241	2.892	0.006

(i) log(N:P ratio in seeds), R^2=0.49

	Estimate	Std. Error	t-value	Pr(>|t|)
(Intercept)	2.7628	0.0994	27.795	<0.0001
N	-0.0066	0.0015	4.274	0.0001
P	-0.0079	0.0017	-4.727	<0.0001

(j) log(C:P ratio in seeds), R^2=0.13

	Estimate	Std. Error	t-value	Pr(>|t|)
(Intercept)	5.4699	0.1129	48.445	<0.0001
N	0.0034	0.0016	1.941	0.0603
P	-0.0041	0.0019	-2.156	0.0381

Table 4.4. Average number of seeds per plant for each treatment ± SD (standard deviation).

	Zero N	Low N	Mid N	High N
Zero P	2.9±1.8	5.0±1.0	2.7±3.1	6.0±2.6
Low P	9.3±1.5	11.3±0.6	11.3±4.0	9.7±3.2
Mid P	5.3±5.0	8.3±2.1	10.3±5.5	12.0±6.9
High P	6.7±5.8	19.0±9.5	21.3±1.2	25.3±4.5

Table 4.5. Second generation experiment. Number of seeds sown and germinated per treatment of the parent plants.

	Zero N		**Low N**		**Mid N**		**High N**	
	N° of seeds planted	N° of seeds germinated	N° of seeds planted	N° of seeds germinated	N° of seeds planted	N° of seeds germinated	N° of seeds planted	N° of seeds germinated
Zero P	4	4	4	4	2	2	7	7
Low P	14	14	15	15	13	12	12	12
Mid P	7	7	12	10	11	8	11	11
High P	10	10	15	12	15	13	15	14

Table 4.6. Second generation of wheat plants with the number of plants that set seeds and the production of seeds. Treat=treatment of the parent plants.

	Zero N			**Low N**			**Mid N**			**High N**		
	N° of plants with seeds	Total N° of seeds (per treat)	Mean weight per seed (g)	N° of plants with seeds	Total N° of seeds (per treat)	Mean weight per seed (g)	N° of plants with seeds	Total N° of seeds (per treat)	Mean weight per seed (g)	N° of plants with seeds	Total N° of seeds (per treat)	Mean weight per seed (g)
Zero P	4	51	0.029±0.014	3	19	0.034±0.027	2	23	0.014±0.014	6	73	0.024±0.012
Low P	10	213	0.014±0.008	11	140	0.025±0.015	9	175	0.015±0.008	11	100	0.024±0.013
Mid P	6	110	0.009±0.003	7	104	0.015±0.013	6	60	0.023±0.015	9	89	0.02±0.009
High P	7	167	0.018±0.008	7	110	0.013±0.008	8	80	0.011±0.009	11	148	0.015±0.011

Table 4.7. Linear models (b, e, f) or generalised linear models (a, c, d) to show the effects of N and P of the first generation on the second generation wheat plants production.

(a) ratio of plant success

	Estimate	Std. Error	z-value	Pr(>|z|)
(Intercept)	1.6152	1.2085	1.337	<0.181
N	0.0035	0.0162	0.219	0.827
P	-0.0145	0.0157	-0.921	0.357

(b) log(above ground biomass), R^2=0.14

	Estimate	Std. Error	t-value	Pr(>|t|)
(Intercept)	0.2316	0.0753	3.075	0.0025
N	-0.0006	0.0009	-0.706	0.4810
P	-0.0017	0.0009	-1.881	0.0619
N° of stems	0.1485	0.0306	4.831	<0.0001
N:P	<0.0001	<0.0001	1.015	0.3116

(c) number of stems per plant

	Estimate	Std. Error	z-value	Pr(>|z|)
(Intercept)	-0.1178	0.2782	-0.423	0.6721
N	0.0007	0.0017	0.430	0.667
P	-0.0002	0.0018	-1.092	0.927
Biomass	0.3759	0.1500	2.507	0.0122

(d) number of seeds per plant

	Estimate	Std. Error	z-value	Pr(>|z|)
(Intercept)	4.4758	3.546	1.262	0.2088
N	-0.0438	0.0206	-2.129	0.0349
P	0.0002	0.0217	0.008	0.9934
Biomass	5.2554	1.9932	2.637	0.0092

(e) total weight of seeds per plant, R^2=0.6

	Estimate	Std. Error	t-value	Pr(>|t|)
(Intercept)	-0.2946	0.0732	-4.027	0.0001
N	0.0009	0.0005	1.75	0.0827
P	<-0.0001	0.0005	-0.118	0.9066
Biomass	0.1816	0.0401	4.524	<0.0001
N° of seeds	0.0165	0.0014	11.798	<0.0001
N:P	<0.0001	<0.0001	-1.009	0.3150

(f) sqrt(weight per seed per plant), R^2=0.23

	Estimate	Std. Error	t-value	Pr(>|t|)
(Intercept)	0.0375	0.0213	1.759	0.0811
N	0.0001	<0.0001	1.108	0.2701
P	-0.0003	0.0001	-3.063	0.0027
Biomass	0.064	0.0124	5.18	<0.0001

Table 4.8. Linear models to show the effects of N and P on photosynthetic parameters in wheat seedlings.

(a) $\log(F_o)$, R^2=0.11				
	Estimate	Std. Error	t-value	Pr(>|t|)
(Intercept)	5.765	0.0364	158.559	<0.0001
N	<-0.0001	0.0004	-0.114	0.9099
P	-0.001	0.0004	-2.402	0.0202
SX	0.0447	0.039	1.147	0.2571
SY	0.0804	0.039	2.063	0.0445

(b) $\log(F_m)$, R^2=0.25				
	Estimate	Std. Error	t-value	Pr(>|t|)
(Intercept)	7.441	0.0847	87.877	<0.0001
N	<0.0001	0.0002	0.097	0.9229
P	-0.0004	0.0002	-1.636	0.1084
SX	0.0801	0.0223	3.598	0.0008
SY	0.0724	0.0223	3.255	0.0021
Age	-0.0071	0.0046	-1.566	0.124

(c) F_v/F_m, R^2=0.01				
	Estimate	Std. Error	t-value	Pr(>|t|)
(Intercept)	0.7864	0.0067	116.825	<0.0001
SX	0.01	0.0087	1.149	0.256
SY	-0.0015	0.0087	-0.168	0.868
N:P	<0.0001	<0.0001	1.21	0.232

(d) sqrt(E_k), R^2=0.3				
	Estimate	Std. Error	t-value	Pr(>|t|)
(Intercept)	21.9986	2.1374	10.292	<0.0001
N	0.0104	0.0066	1.584	0.12
P	0.0014	0.0063	0.224	0.824
Age	-0.208	0.1167	-1.782	0.081

(e) ETR_{max}, R^2=0.11

	Estimate	Std. Error	t-value	Pr(>|t|)
(Intercept)	25.06	11.41	2.196	0.0327
Age	0.7681	0.6094	1.261	0.2133
N:P	0.0012	0.0005	2.34	0.0233

(f) qP, R^2=0.23

	Estimate	Std. Error	t-value	Pr(>|t|)
(Intercept)	0.504	0.0162	31.061	<0.0001
N	-0.0001	0.0002	-0.551	0.5839
P	0.001	0.0002	4.188	0.0001

(g) NPQ, R^2=0.38

	Estimate	Std. Error	t-value	Pr(>|t|)
(Intercept)	1.934	0.0842	22.982	<0.0001
N	0.0015	0.0013	1.171	0.2475
P	-0.0039	0.0013	-3.029	0.004
SX	0.0506	0.0824	0.615	0.5416
SY	-0.1368	0.0824	-1.66	0.1035
N:P	<0.0001	<0.0001	-1.042	0.3027

(h) V_{cmax}, R^2=0.2

	Estimate	Std. Error	t-value	Pr(>|t|)
(Intercept)	103.5579	6.4591	16.033	<0.0001
SX	-4.7576	8.3841	-0.567	0.573
SY	-15.5853	8.3841	-1.859	0.069
N:P	0.0046	0.0013	3.471	0.0011

(i) J_{max}, R^2=0.21

	Estimate	Std. Error	t-value	Pr(>|t|)
(Intercept)	164.3413	8.6624	18.972	<0.0001
SX	-17.6389	11.2439	-1.569	0.1231
SY	-21.8839	11.2439	-1.946	0.0574
N:P	0.0062	0.0018	3.529	0.0009

(j) A_{max}, R^2=0.2

	Estimate	Std. Error	t-value	Pr(>|t|)
(Intercept)	29.5208	1.5834	18.643	<0.0001
SX	-2.6945	2.0554	-1.311	0.196
SY	-3.2	2.0554	-1.557	0.1259
N:P	0.0012	0.0003	3.651	0.0006

Table 4.9. Linear models and generalised linear model (c) to show the associations between N, P, yield and photosynthesis.

(a) weight per seed ~ N + P + seed source + A_{max}, R^2=0.41

	Estimate	Std. Error	t-value	Pr(>|t|)
(Intercept)	0.0261	0.0022	11.792	<0.0001
N	<-0.0001	<0.0001	-3.394	0.0015
P	<0.0001	<0.0001	1.629	0.1107
SX	-0.0006	0.0011	-0.419	0.6771
SY	-0.0039	0.0011	-3.656	0.0007
A_{max}	0.0002	<0.0001	2.39	0.0213

(b) total weight of seeds per plant seed + A_{max}, R^2=0.26

	Estimate	Std. Error	t-value	Pr(>|t|)
(Intercept)	-0.2229	0.1224	-1.821	0.0752
SX	0.0156	0.0036	4.292	<0.0001
SY	0.0970	0.0616	1.574	0.1225
A_{max}	0.0834	0.0604	1.380	0.1743

(c) total weight of seeds per plant seed ~ N * P + seed source + A_{max}, R^2=0.75

	Estimate	Std. Error	t-value	Pr(>|t|)
(Intercept)	-0.0330	0.0757	-0.435	0.6655
N	-0.0003	0.0005	-0.498	0.6210
P	0.0029	0.0006	4.818	<0.0001
SX	0.0826	0.0357	2.312	0.0258
SY	0.0470	0.0350	1.345	0.1859
A_{max}	0.0048	0.0239	1.998	0.0522
N:P	<0.0001	<0.0001	2.431	0.0194

(d) number of seeds per plant ~ N + P + A_{max} + weight per seed

	Estimate	Std. Error	z-value	Pr(>|z|)
(Intercept)	2.7700	0.3772	7.344	<0.0001
N	0.0016	0.0013	1.211	0.2260
P	0.0123	0.0012	9.832	<0.0001
A_{max}	0.0226	0.0079	2.845	0.0044

Weight per seed	-62.2204	14.5680	-4.271	<0.0001

(e) above ground biomass ~ N * P + A_{max}, R^2=0.8

	Estimate	Std. Error	t-value	Pr(>|t|)
(Intercept)	0.0726	0.1503	0.483	0.631
N	-0.0002	0.0012	-0.179	0.8583
P	0.0058	0.0012	4.725	<0.0001
A_{max}	0.0149	0.0052	2.862	0.0062
N:P	<0.0001	<0.0001	3.833	0.0004

(f) nitrogen content in seeds ~ N * P + number of seeds, R^2=0.59

	Estimate	Std. Error	t-value	Pr(>|t|)
(Intercept)	37.5449	1.9270	19.484	<0.0001
N	0.0669	0.0313	2.139	0.0382
P	-0.1478	0.0393	-3.758	0.0005
N° of seeds	-0.5467	0.2150	-2.543	0.0147
N:P	0.0015	0.0006	2.403	0.0206

(g) nitrogen content in seeds ~ N * P + weight per seed, R^2=0.55

	Estimate	Std. Error	t-value	Pr(>|t|)
(Intercept)	25.6	7.056	3.628	0.0008
N	0.075	0.0336	2.228	0.0311
P	-0.2098	0.059	-5.843	<0.0001
Weight per seeds	326.3	236.9	1.377	0.1755
N:P	0.0009	0.0006	1.503	0.14

Discussion

The experiments with *Fritillaria* (Chapter 2) and *Nymphaea* (Chapter 3) show that GS or ploidy do have an impact on photosynthesis and that stomatal size and/or density influence photosynthetic rates. These data support the hypothesis that photosynthesis may act as a selection pressure against the evolution of large GSs. There are two possible explanations as to why GS might be inversely correlated with photosynthesis efficiency:

(1) The nutrient, metabolite and energy requirements for enabling the photosynthesis pathway to function efficiently compete with those for building and maintaining the genome (DNA and associated proteins). However, there is no additional evidence available to support this theory, and that could be the subject of future research (see below).
(2) Because of scaling effects of GS and cell size, larger GSs may result in larger guard cells and intracellular spaces, which might negatively impact photosynthesis (Franks & Beerling, 2009). However, this hypothesis is not supported in *Fritillaria* data, where GS does not correlate with guard cell size, despite the big range in GS of the species included in the analysis (31.1 pg/1C-to 90.71pg/1C-value). It is however supported for a global analysis of GS and guard cell size across angiosperms (Beaulieu *et al.*, 2008) and for the *Nymphaea* species reported here in Chapter 3.

This work proposes that there is an N and P resource competition between the demands of photosynthesis and the demands of nucleic acids (especially in the nucleus) in the production of biomass and growth. If so, this represents a new dynamic between the plastid and the nucleus, building on from the well established transfer of organellar genes to the nucleus over evolution (Martin & Herrmann, 1998). At the level of the gene, an analysis of 13 plant species varying in photosynthetic N-use efficiency showed that the least N-use efficient species had the strongest selection against codons that code for amino acids that are most N demanding (Kelly, 2018). For example, in the production of RuBisCO, given its abundance, a single A to T substitution could save 15,000 N atoms per cell (Kelly 2018). Whilst much is written on the allocation of resources between for example, nucleic acids, proteins and pigments, there are no data on the effects of GS or ploidy level in that allocation. Such data are now urgently needed.

Despite the absence of a correlation between GS and guard cell size in *Fritillaria*, there is a negative relationship between GS and photosynthesis efficiency (A_{max}, V_{cmax}, J_{max}, g_s, ETR_{max} and F_v/F_m), an observation that could be supported by either, or a mixture of, the hypotheses outlined above. For *Fritillaria*, these data suggest that stomatal size/density is controlled by physiologically and developmental processes and not by GS alone, although it remains likely

that GS provides a minimum constraint on stomatal size and density. Whilst this response may be a peculiarity of *Fritillaria*, it is also possible that the relationship between GS and guard cell size breaks down amongst plants with very large GSs, given that the smallest GS studied amongst the *Fritillaria* species used here (*F. davidii*, 1C=31.1 pg/1C-value) is still large compared with the mean and modal GS of angiosperms (1C=0.6 pg and 1C=5.9 pg, respectively). Assuming so it would be interesting to know at what GS the GS-guard cell size relationship breaks down. Further generic-level studies representing different ranges in GSs are needed for such experiments.

More research is also needed to compare measures of photosynthesis and guard cell size across more families and genera. In particular, we need more understanding of ranges in variation between species of the same genus (with similar physiologies), especially those that cover the range of GSs found in land plants. As examples of potential target groups that might be interesting to compare are : (i) Fabaceae, where the presence of N fixation may be expected to result in plants that are less constrained by available N. (ii) CAM and C4 plant genera (all the analyses in this thesis were conducted on C3 plants). Potentially mechanisms that allow for CO_2 to be stored prior it being fed into the Calvin cycle, acting to improve water-use efficiency in the plants, could come at an N and P metabolic cost. (iii) Species with mycorrhizal associations, which may impact these relationships through the nutrient exchange that occurs. (iv) Insectivorous plants that have evolved to live in extremely low N and P nutrient conditions. (v) Plants that live in extremely low light conditions, where the costs of photosynthesis as opposed to growth may be severe.

The wheat experiments conducted here support the hypothesis that N and P limitation does constrain photosynthesis efficiency and the production of seeds and biomass. The most important conclusion from these experiments is that there are significant interactions between N and P in the production of biomass and seeds through their roles in facilitating photosynthesis. What is now needed is to consider nutrient limitation in relation to GS and ploidy level. Wheat USU-Apogee is a hexaploid (GS = 17.11pg/1C), which is large compared with rice (*Oryza sativa*, 0.5pg/1C). Therefore, it is possible that a larger amount of N and P is needed to build and maintain the nucleus of wheat than species with smaller GS, leaving less available to perform photosynthesis under nutrient limitation. We are now in a position to test that hypothesis by repeating the same experimental design in wheat and wheat relatives at different ploidy levels (diploid to octaploid). Possibly such an experiment will reveal a competition between DNA (and RNA) and photosynthesis for N and P. Such a finding may generate key data establishing if there is selection for small GS in evolution, because in many soils of the world N and/or P are limiting. From the analyses, we found evidence that such a response may arise from the specific effects of N and P on particular components of the

photosynthesis pathways. For example a linear relationship was shown between seed biomass and A_{max} (maximum CO_2 uptake), a relationship that seems to be driven by N and P addition.

It has been shown in previous studies that enhancing photosynthetic efficiency via increased CO_2 fixation, under optimal nutrients and environmental conditions (water, climate), does improve crop yield (Ainsworth & Long, 2005; Zhu *et al.*, 2010; Parry *et al.*, 2011). Studies with high concentration of CO_2 have also found an increase in yield in major food crops using both C3 and C4 photosynthesis (Long *et al.*, 2006; Raines, 2011). Parry *et al.* (2011) discuss several strategies that have been developed to enhance photosynthesis to increase biomass and grain yield in wheat, but in most cases these strategies involve growing wheat in conditions where N and P are not limited. What is now needed is to conduct such trials under limiting nutrients, to reduce the costs of fertilizers to farmers and to reduce excess fertilizer run-off to the environment. That research will need to establish what N and P-use trade-offs occur in the cell. It is in that context that GS may be significant.

Under limiting nutrients the relationship between photosynthesis and CO_2 levels may be different, since here other factors are probably limiting. More attention needs to be paid as well to consider exactly yield means, since, for example, increased carbohydrates in seeds, are probably much more cheaply made by the plant (in terms of N and P) than proteins and pigments (requiring predominantly N), which are in turn cheaper than nucleic acids (requiring N and P). Körner (2015) argues that photosynthetic CO_2 uptake is not the primarily driver for plant growth, instead it is just one of the drivers, and it is not even the most critical one, the latter being environmental control (temperature, water and nutrients). For Körner, in studies of wild plants, carbon assimilation is more a “slave” than the “master”, where carbon is converted into biomass via “permission” of other chemical elements. Such a scenario is pertinent since soil nutrients, particularly N and P, are frequently limiting in nature, and yet they are essential requirements for carbon assimilation processes.

There is a need to increase understanding of the relationship between N and P availability, GS and yield. The role of GS in this potential relationship has yet to be determined, however the experiment on wheat could be expanded to other crops and their wild relatives that differ in GS and ploidy levels. Such research on crops may lead to new understanding that can be exploited in breeding for growth and yield. Potential projects might be: (i) to determine in multiple wheat species (in *Triticum* and *Aegilops*) with differing GSs (three ploidy levels), how trade-offs in resources between growth and photosynthesis is influenced by varying N and P; (ii) to determine in wheat (*Triticum aestivum*), if domestication and elite varieties, developed under a plentiful supply of N and P fertilizers, has led to inefficient use of N and P; (iii) to

determine if there has been a general relaxation of N and P efficiency through the long-term application of N and P fertilizers across a diversity of crops with a range of GS and ploidy levels. Any new insights might enable us to engineer plants that will maintain or increase yield with lower fertilizer inputs; reduce costs and application of fertilizers, which is especially important given that P reserves are expected to become limiting within 50 years, and; reduce agricultural run-off for improved ecosystem services, since run-off degrades ecosystems and biodiversity.

Potentially improvements in growth, yield and photosynthesis can only be met if sufficient environmental resources (minerals, temperature and water) are available. The challenge will be to keep, or enhance, yield whilst reducing N and P inputs. That goal is made even more pertinent by the need to reduce agricultural run-offs to the environment, which reduces biodiversity and degrades ecosystem services.

References

Ainsworth EA, Long SP. **2005**. What have we learned from 15 years of free-air CO_2 enrichment (FACE)? A meta-analytic review of the responses of photosynthesis, canopy properties and plant production to rising CO_2. *New Phytologist* **165**: 351–372.

Beaulieu JM, Leitch IJ, Patel S, Pendharkar A, Knight CA. **2008**. Genome size is a strong predictor of cell size and stomatal density in angiosperms. *New Phytologist* **179**: 975–986.

Franks PJ, Beerling DJ. **2009**. Maximum leaf conductance driven by CO_2 effects on stomatal size and density over geologic time. *Proceedings of the National Academy of Sciences* **106**: 10343–10347.

Kelly S. **2018**. The amount of nitrogen used for photosynthesis modulates molecular evolution in plants (M Purugganan, Ed.). *Molecular Biology and Evolution* **35**: 1616–1625.

Körner C. **2015**. Paradigm shift in plant growth control. *Current Opinion in Plant Biology* **25**: 107–114.

Long SP, Ainsworth EA, Leakey ADB, Nösberger J, Ort DR. **2006**. Food for thought: lower-than-expected crop yield stimulation with rising CO_2 concentrations. *Science* **312**: 1918–1921.

Martin W, Herrmann RG. **1998**. Gene transfer from organelles to the nucleus: how much, what happens, and Why? *Plant Physiology* **118**: 9–17.

Parry MAJ, Reynolds M, Salvucci ME, Raines C, Andralojc PJ, Zhu X-G, Price GD, Condon AG, Furbank RT. **2011**. Raising yield potential of wheat. II. Increasing photosynthetic capacity and efficiency. *Journal of Experimental Botany* **62**: 453–67.

Raines CA. **2011**. Increasing photosynthetic carbon assimilation in C3 plants to improve crop yield: current and future strategies. *Plant Physiology* **155**: 36–42.

Zhu X-G, Long SP, Ort DR. **2010**. Improving photosynthetic efficiency for greater yield. *Annual Review of Plant Biology* **61**: 235–261.

Supplementary data

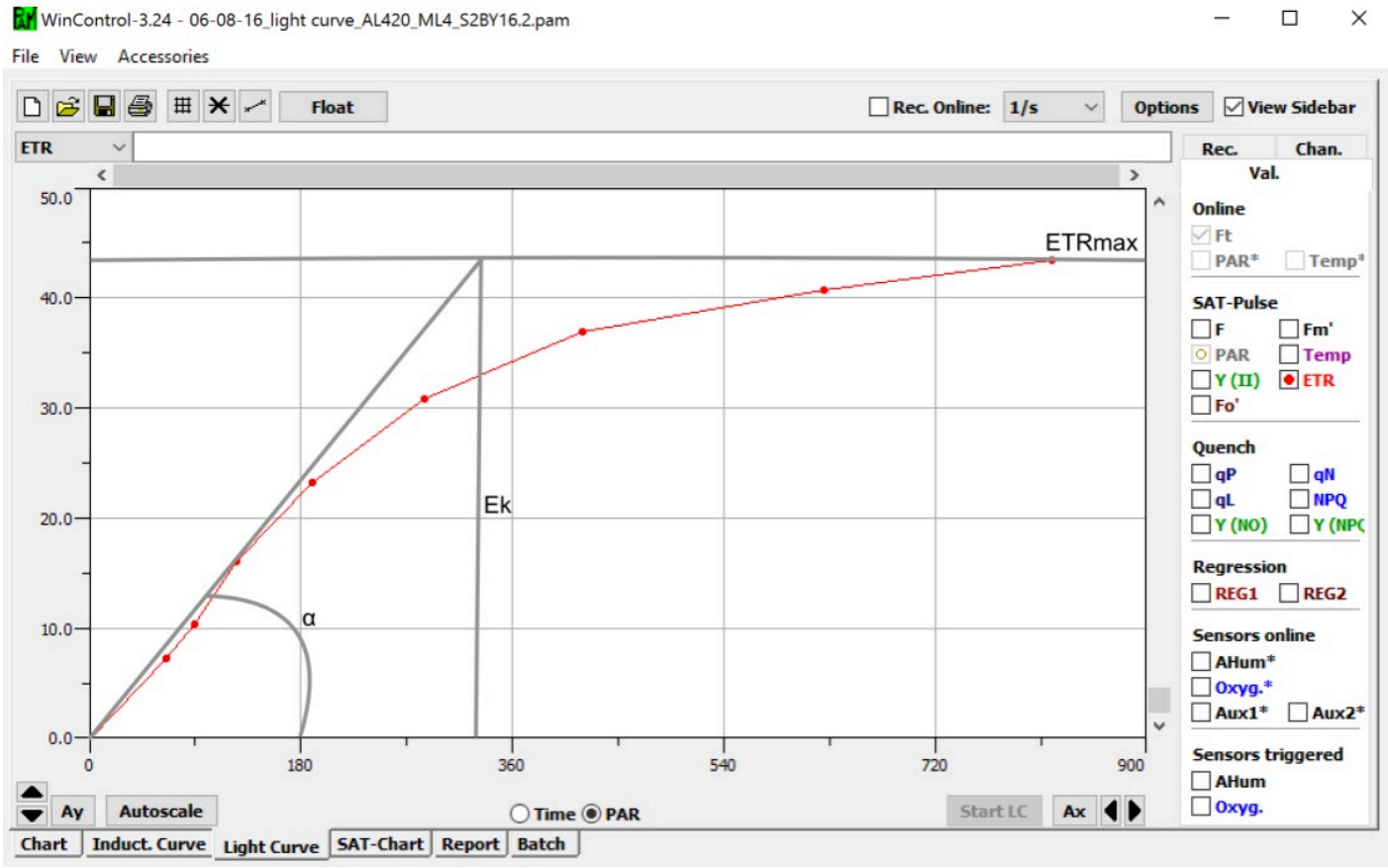

Figure 1S. Screenshot modified of an RLC from a measurement of wheat under high N and high P nutrient condition, where α is the initial slope (photon/electron); Ek (µmol m^{-2} s^{-1}) is the minimum saturating irradiance; rETR (µmol electrons m^{-2} s^{-1}) is the relative electron transport rate. PAR is the photosynthetic active radiation (µmol photons m^{-2} s^{-1}). Axis x is PAR and axis y is ETR.

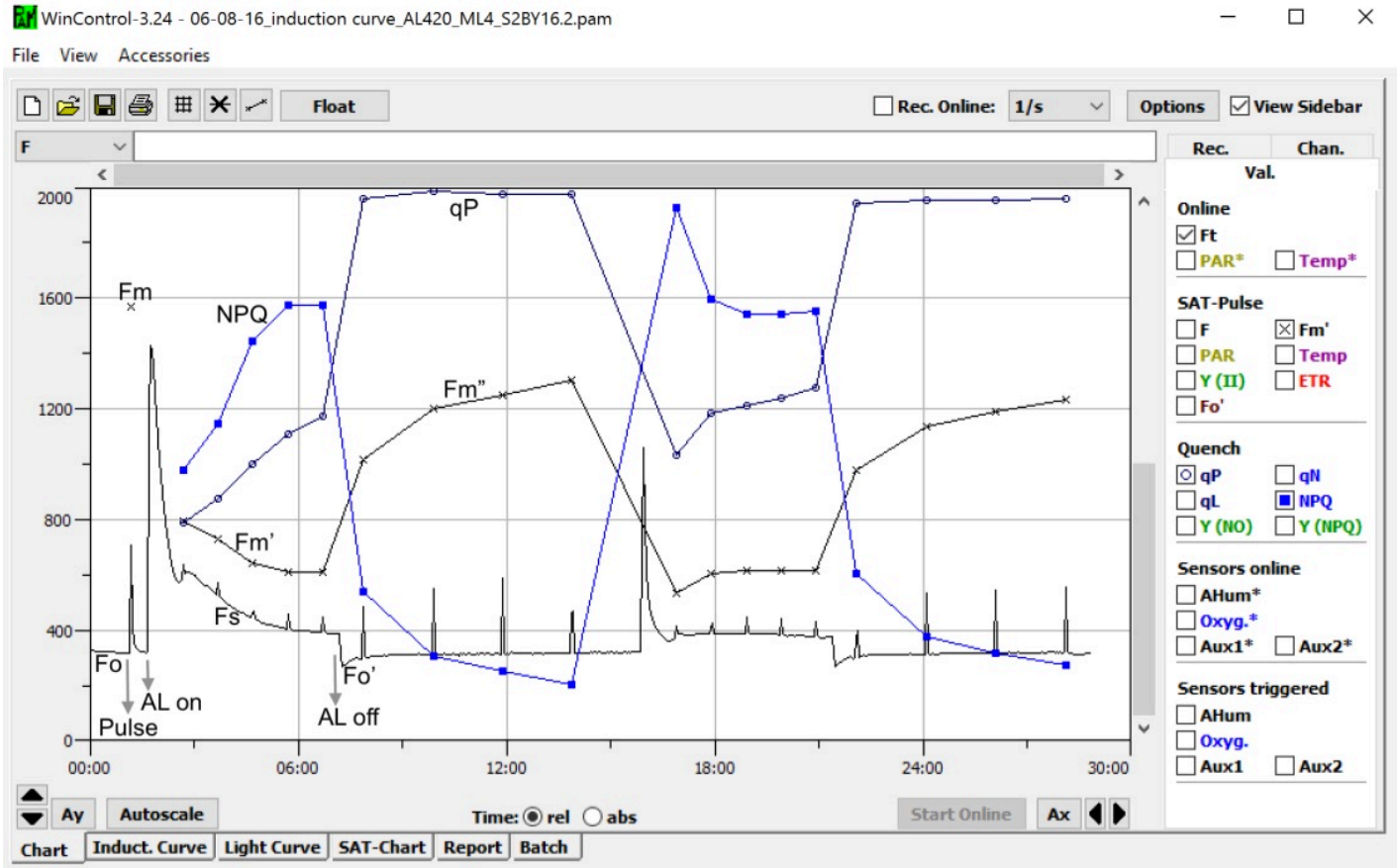

Figure 2S. Screenshot of an ILC from a measurement of wheat under high N and high P nutrient condition, where the y axis is Fluorescence and the x axis is time (minutes). AL, actinic light, is an imitated sunlight to allow the electron transport through the reaction centres; F_m, maximum fluorescence after 30 minutes of dark adaptation; F_m', maximum fluorescence under AL; F_m'' is the maximum fluorescence without AL; F_o, minimum fluorescence in dark-adapted tissues; F_o', minimum fluorescence without AL; F_s, minimum fluorescence under AL; NPQ, non-photochemical quenching; qP, photochemical quenching.

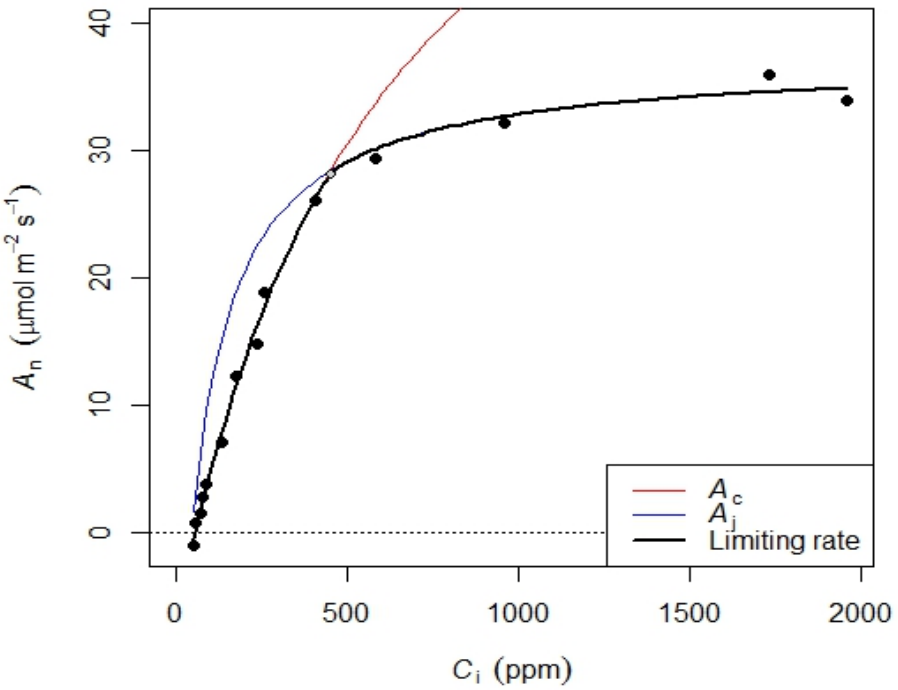

Figure 3S. A/Ci curve of *Stenanthium gramineum* derived using the package Plantecophys (Duursma, 2015) showing the two main phases in which photosynthesis is limited: the RuBisCO-limited state, it is the linear phase, which is RuBisCO activity in the leaf (V_{cmax}); and the RuBP-regeneration-limited, where the curvature begins, which is the maximum rate of electron transport used for regeneration of RuBisCO substrate (J_{max}). Legend: Ac, when A (net CO_2 assimilation) is limited by V_{cmax}; Aj, when A is limited by J_{max}; limiting rate, the fitted curve given the points at C_i (internal CO_2) and A.